



POLITECNICO MILANO 1863

MASTERS ON MANAGEMENT ENGINEERING

Master Thesis

Design of a pulley-driven centrifugal compressor for a car.

Author: Guillermo López Sánchez

Student ID: 10836636

Advisor: Sergio Terzi

Co-advisor: Juan de Norverto Moriñigo

Milan

September 2023

Author's Signature

Date

30th of September of 2023

Table of Contents

INTRODUCTION	3
ACKNOWLEDGMENT	4
STATE OF THE ART	5
MOTIVATION	6
WORK METHODOLOGY	7
PROJECT PURPOSE	8
ENGINE MODEL	9
COMPRESSOR MODEL THEORY	12
FUNDAMENTALS (CHAPTER 1)	12
SELECTION (CHAPTER 2)	13
RADIAL COMPRESSOR (CHAPTER 6)	14
CASE STUDY (CHAPTER 8)	15
COMPRESSOR-ENGINE MODEL	16
INPUTS AND BOUNDARY CONDITIONS DIRECT CALCULATIONS	18
KINEMATIC CALCULATIONS	21
THERMODYNAMIC CALCULATIONS	23
GEOMETRIC CALCULATIONS	27
LOSSES CALCULATIONS.....	36
MODEL CONVERGENCE	41
COUPLING TO THE ENGINE MODEL.....	44
MODEL SIMULATIONS.....	45
RESULTS	46
SELECTION AND DESIGN RESULTS	46
MIDDLE RESULTS	50
DESIGN	52
IMPELLER DESIGN.....	53
CASE DESIGN	54
VOLUTE.....	55
COVER	56
GEARBOX	57
CONNECTING ELEMENTS.....	60
ASSEMBLY	62
ECONOMIC FEASIBILITY	64
CONCLUSIONS	65
ANNEX I: ALIGNMENT WITH SDGS	68
WORK CITED AND TOOLS NEEDED	68
ANNEX II: DRAWINGS	71

Table of Figures

FIGURE 1: DIFFERENT TURBOMACHINERY EXAMPLES	5
FIGURE 2: CAR TARGET OF DESIGN	6
FIGURE 3: ENGINE MODEL ILLUSTRATIVE DIAGRAM	11
FIGURE 4: DOCUMENTATION STRUCTURE	12
FIGURE 5: TURBOMACHINERY SELECTION OPTIONS	13
FIGURE 6: THEORETICAL PROPOSED MODEL ILLUSTRATIVE DIAGRAM	14
FIGURE 7: EXECUTION DIAGRAM OF THE THEORETICAL PROPOSED MODEL	15
FIGURE 8: DEVELOPED MODEL ILLUSTRATIVE DIAGRAM	16
FIGURE 9: THEORETICAL VELOCITY TRIANGLES	22
FIGURE 10: THEORETICAL THERMODYNAMICAL CYCLE	25
FIGURE 11: THEORETICAL GEOMETRY AND DIMENSIONS	27
FIGURE 12: THERMODYNAMIC CYCLE OF THE SELECTED SOLUTION	50
FIGURE 13: TRIANGLES OF VELOCITIES OF THE SELECTED SOLUTION	51
FIGURE 14: IMPELLER (1)	53
FIGURE 15: IMPELLER (2)	53
FIGURE 16: CASE (1)	54
FIGURE 17: CASE (2)	54
FIGURE 18: VOLUTE (1)	55
FIGURE 19: VOLUTE (2)	55
FIGURE 20: COVER (1)	56
FIGURE 21: COVER (2)	56
FIGURE 22: GEARBOX (1)	58
FIGURE 23: GEARBOX (2)	58
FIGURE 24: GEARBOX (3)	59
FIGURE 25: BEARING	60
FIGURE 26: INNER GASKET	60
FIGURE 27: OUTER GASKET	60
FIGURE 28: CASE SCREW	61
FIGURE 29: VOLUTE SNAP-FIT	61
FIGURE 30: OUTER SNAP-RING	61
FIGURE 31: INNER SNAP-RING	61
FIGURE 32: IMPELLER NUT	61
FIGURE 33: COMPRESSOR ASSEMBLY (1)	62
FIGURE 34: COMPRESSOR ASSEMBLY (2)	63
FIGURE 35: POWER THEORETICAL INCREASE	66
FIGURE 36: TORQUE THEORETICAL INCREASE	66
FIGURE 37: RENDER OF THE EXPECTED MVP	67
FIGURE 38: GLOBAL EFFICIENCY THEORETICAL INCREASE	69
FIGURE 39: SPECIFIC FUEL CONSUMPTION THEORETICAL DECREASE	70

Introduction

This project intends to develop a calculation model capable of parameterizing the design of a centrifugal compressor for a car according to the power supply needs of its combustion engine.

It will start from the analysis of the theoretical operation of the engine, in order to identify its characteristics and main limitations. With this, a first simplified model of the engine in atmospheric operating conditions (standard) will be made, adjusted to the values found within its data sheet.

Subsequently, the calculation model for the design of the turbomachine will be built over the first model. This second version will be able, once the fixed operating parameters have been entered, to vary other input parameters to provide different design solutions.

For each simulation, the model output values will be saved and analyzed to find the most suitable design based on different criteria. Once the optimal scenario has been chosen, the geometric parameters obtained will be used and the design phase will proceed. The final development of which will be a three-dimensional model generated with design tools.

The three-dimensional model will be made for the whole assembled set. However, greater importance will be given in the design and analysis phases to the parts that make contact with the fluid, since these will be the protagonists of the project.

To establish the modeling equations of the compressor, the theory of turbo machines described in the book by Marco Gambini and Michela Vellini entitled [1] "Turbomachinery Fundamentals: selection and preliminary design" will be applied.

As a design object, the reference vehicle will be the 2006 Mini Cooper r50, which is powered by a 1.6-liter naturally aspirated engine developed by Chrysler.

The main objective of the compressor will be to increase the peak power and torque values of the engine, with additional objectives being considered in the design process when the performance and efficiency values of the engine improve in a generic way throughout the engine's operating speed range.

It is important to mention that centrifugal compressors driven by pulley (drive shaft) are uncommon in the automotive sector, so it will be a design case of interest, especially because it will make use of the advantages of additive manufacturing throughout the design process.

Acknowledgment

This project would not have been possible without the impeccable direction of Juan de Norverto Moriño. His way of inspiring the author and guiding his work has been fundamental and appropriate to the creative nature of this master's thesis.

The author would also like to thank Eva María Arenas Pinilla for her support at the beginning of the project. For motivating him and transmitting him the necessary knowledge about turbomachines to devise the development proposal.

He also wishes to thank his academic institutions, the Universidad Pontificia de Comillas and the Politecnico di Milano, for giving him the opportunity and the challenge to venture into the development of this Master's thesis that he has been so passionate about.

Finally, the author would like to thank his family and friends for their support during the months of work. Without this support, the motivation for this project would not have been the same.

State of the art

As mentioned, the centrifugal compressor will be driven by pulley, connected to the vehicle's drive shaft through a gearbox with planetary gears.

Normally, supercharged engines use two different technologies:

Volumetric (screw or helicoidal) compressor: this is a positive displacement compressor which, like the design of this project, is driven mechanically by the motor shaft. The pressure increase in the comburent is achieved by reducing the specific volume of the gas. The supercharged engine allows the addition of power and torque in the whole range of revolutions, adding a proportional and lower drag load, generally assuming the worsening of the vehicle's energy efficiency in comparison with the atmospheric simile. A positive point to highlight of these compressors is how quickly the compression variation is reflected in the engine operation, being the engine response practically direct.

Centrifugal compressor (Turbo compressor): these are dynamic flow compressors, in which the air pressure increases thanks to the acceleration applied by the blades to the fluid and the deceleration in the volute or casing. The compression method of the machine designed in this project will be similar. The difference lies in the impeller drive. In turbo compressors, the shaft of the compressor is solid with the shaft on which the turbine is mounted. This turbine receives kinetic energy from the engine exhaust gases, which are decelerated. The most relevant characteristics of this type of turbo machines are, generally, the increase of power and peak torque in a certain range of revolutions and the improvement of the engine's energy efficiency. In addition, in volumetric compressors it was mentioned their fast response, in the case of turbo compressors there is the so-called "turbo lag", which generates a slight delay in the engine response with respect to the actuation of the intake pedal.

The design proposed for this project allows to choose some of the characteristics of the other schemes to find an intermediate solution in many aspects:

Centrifugal compressor driven by pulley: the "cold gases" part of a turbo compressor will modify the pressure of the inlet gases in a similar way to the machine it replicates, thanks to the acceleration and deceleration of these. On the other hand, the shaft drive will be done through direct mechanical linkage with the motor shaft. This will involve a linear and direct relationship with the engine speed in real time, whose conversion ratio will have to be of great magnitude, since the compressor impeller must work in ranges of revolutions per minute significantly higher than those of the engine.

Examples of the three configurations can be seen in *Figure 1* below:

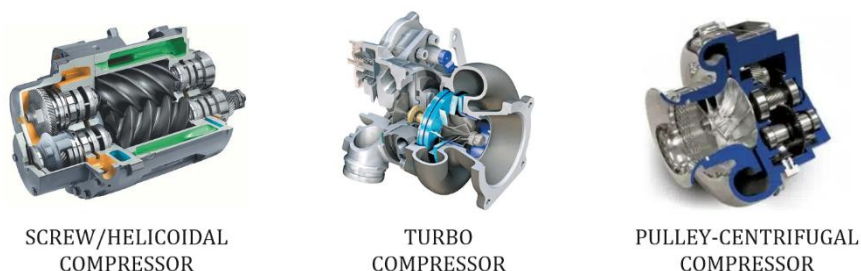


Figure 1: Different Turbomachinery Examples

Motivation

The motivation of the project stems from the desire to increase the maximum power of the car used as an example, which is the vehicle of the author of the document.

The car model of the Mini brand was manufactured and put on sale in two similar versions. One with a naturally aspirated engine (case study) and the other with a volumetric compressor as mentioned in the previous chapter (case to be replicated). Similarly, there are examples in the enthusiast community of this model of car that have been modified by adding a turbocharger, which has also been described above, to the lower power version.

Figure 2 shows an illustrative image of the vehicle mentioned above:



Figure 2: Car Target of Design

Given the proven robustness of the aforementioned engine, which is the same for all models, the possibility of developing an unusual device in the automotive world to replicate the performance improvement achieved with the other options was considered.

In addition, technical expertise will be employed to take advantage of additive manufacturing design technologies that seek to improve machine efficiency, using all the rigorous documentation that can be found to facilitate the modeling process and introduce realistic boundary conditions, taking into account the constraints set by the automotive community.

Work Methodology

At the beginning of the project, the following action plan was established to achieve the development of the project:

Date	Principal Actions
September	Settle the bases, objectives, tools and plan to tackle the project
October	Documentation selection and analysis
November	Documentation selection and analysis
December	Documentation selection and analysis
January	Input parameters and limitations collection
February	Preliminary design
March	Geometry modelling according to the designing process
April	Geometry modelling according to the designing process
May	Design and hypothesis building
June	Design and hypothesis building
July	Design and hypothesis building
August	Project documentation

Project purpose

The project can be divided into four distinct parts or phases, each of which pursues different objectives. The breakdown of the project is as follows:

1. Documentation process: the objective is to acquire a high degree of knowledge in the subject, trying to understand in detail the modeling procedure proposed by the book, [1] "Turbomachinery Fundamentals: selection and preliminary design". The main goal here will be to understand in depth the relationship between the design parameters and the final product generated.

2. Modeling process: the aim is to develop a dynamic model that allows the replication of the design process for other operating conditions. The idea is that the model will allow the input parameters to be introduced for another combustion engine configuration and that the dimensional values can be obtained to adjust the machine geometry to the new conditions. The tools employed for this part are [A] Excel by Microsoft and the property calculator plugin for Excel called [B] Coolprop.

3. 3D design process: once the parameters that allow to capture the geometry of the assembly have been obtained, the designing part may proceed, using an advanced level in the software to be used, that is [C] Solid Edge by Siemens. In addition, at this point, the potential manufacturing process will be considered, making a proposal of the materials that will make up the final product. The design of all the constituent parts of the machine will be carried out, although some of them may be rethought in future projects or replaced by standardized parts, since they are not the focus of interest of this engineering project.

4. Economic analysis: this last part will focus on the study of the economic feasibility of the product, first conceived as a prototype and then considering mass production. This will be useful to evaluate the future steps to be taken in case the results are positive for this project.

Once the four phases have been completed, the aim is to obtain a technical document of a valid level to consider the manufacture of a prototype.

And more in the long term, as a final utopian goal, if this manufactured prototype turns out to be viable, it could become the basis that justifies the manufacture of others. For which it would be necessary to rethink the project and raise it to a higher level that would allow the commercial development of the proposed idea.

Engine Model

The template used to model the vehicle's engine was provided and worked on with the Director of this project. Although it has undergone slight modifications, its operation remains similar.

A simplified model is used to approach the combustion engine performance. This approach loses details with respect to the real operation of the engine, but since it is not the main objective of the project, it will be more than enough to give context to the results of the study. It will serve as a decision-making tool, since it will provide a more visual image of the effect that the machine can have on the vehicle's engine.

This first model, which will later be coupled with another, uses parameters taken from the [2] Vehicle's Data Sheet and other reliable sources to simulate engine operation as a function of the engine speed, the amount of fuel and the amount of comburent passing through the engine intake.

The fixed parameters of the model that are engine dependent are as follows:

CR_{eng} – Compression Ratio

D_{cyl} – Cylinder Diameter

S_{cyl} – Cylinder Stroke

N_{cyl} – Number of Cylinders

E_{95} – 95 Octane Gasoline Specific Energy

AF_r – Air Fuel ratio

η_V – Volumetric Efficiency

η_I – Indicated/Thermodynamic efficiency

With these data known, you can proceed to model others directly, using the correct relationships.

For the volume of the cylinder:

$$V_{cyl} = \frac{D_{cyl}^2 \cdot \pi}{4} \cdot S_{cyl}$$

To calculate the engine displacement:

$$V_{eng} = V_{cyl} \cdot N_{cyl}$$

And to calculate combustion chamber capacity:

$$V_{cc} = \frac{V_{cyl}}{CR_{cyl} - 1}$$

To proceed with the remaining formulas that are necessary to extract the results, it will be necessary to know the value of the comburent and fuel mass flow rates, given a working regime.

A linear relationship will be assumed between both mass flows, which will be determined by the ratio of air and gasoline presented above.

$$\dot{m} = \frac{\dot{f}}{AFr}$$

It is important to mention now that actually the input parameter will be the air flow rate, so it will be necessary to know the air density, which will be calculated with the model that will be presented below. In any case, it is anticipated that:

$$\dot{m} = V_{\text{need}} \cdot \rho_{\text{air}} = V_3 \cdot \rho_3$$

The motor capacity is calculated using this same density, according to the equation:

$$\dot{m}_{\text{max}} = \frac{\rho_{\text{air}} \cdot V_{\text{eng}} \cdot n_{\text{eng}}}{2}$$

The indicated power and pressure can then be calculated, which are respectively:

$$IP_{\text{eng}} = \dot{f} \cdot E_{95} \cdot \eta_I$$

$$Ip_{\text{eng}} = \frac{IP_{\text{eng}}}{V_{\text{eng}} \cdot n_{\text{eng}}}$$

The average mechanical loss pressure can be approximated by:

$$ML_{\text{mp}} = 0,97 + 0,15 \cdot \frac{n_{\text{eng}}}{1000} + 0,05 \cdot \left(\frac{n_{\text{eng}}}{1000}\right)^2$$

And the power of mechanical losses thanks to:

$$MLP = \frac{ML_{\text{mp}} \cdot V_{\text{eng}} \cdot n_{\text{eng}}}{2}$$

Similarly, the mechanical loss torque is approximated by the formula:

$$MLT = \frac{MLP}{n_{\text{eng}}}$$

With these approximate values, the mechanical efficiency of the engine can be calculated:

$$\eta_{\text{mec}} = 1 - \frac{MLP}{IP_{\text{eng}}}$$

And combining this with the indicated performance, the overall engine performance is obtained:

$$\eta_G = \eta_I \cdot \eta_{\text{mec}}$$

The average velocity of the cylinders is approximated using the equation:

$$MPS = n_{\text{eng}} \cdot S_{\text{cyl}} \cdot 2$$

And with these values, the most interesting results can be obtained once both models have been coupled.

The power delivered by the engine (referred to as Horse Power), knowing the engine speed and intake data at that time:

$$HP = \dot{f} \cdot E_{95} \cdot \eta_G$$

The Torque delivered by the engine to the vehicle under the same conditions:

$$T = \frac{HP}{n_{eng}}$$

The Specific Fuel Consumption:

$$SFC = \frac{\dot{f}}{HP}$$

And the Brake Mean Effective Pressure, which indicates the pressure exerted on the piston face at the moment of maximum explosion:

$$BMP = \frac{HP}{n_{eng} \cdot V_{eng}}$$

This concludes the first model that will be part of the final tool generated in this project.

Although it is a tool that has great simplifications and is of low complexity, it will be very useful when evaluating the results once it is coupled to the final tool that will model the turbomachine that will be explained in the following two chapters.

As a summary and in order to simplify the operation of this first model, an illustrative diagram is presented in *Figure 3* below:

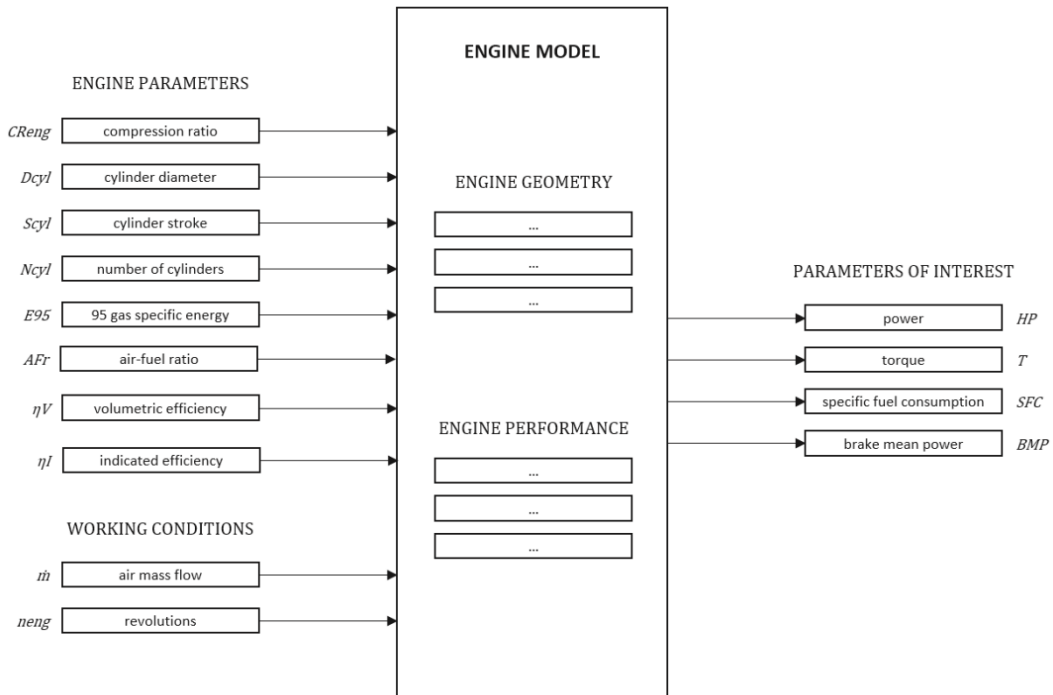


Figure 3: Engine Model Illustrative Diagram

Compressor Model Theory

For the development of the model to calculate the optimal geometries for the preliminary design of the compressor, the book [1] "Turbomachinery Fundamentals: selection and preliminary design" by Marco Gambini and Michela Vellini was used as the main documentation.

In this documentation, the main concepts that are necessary for the design process are reviewed at the beginning, followed by the selection of the turbomachinery according to the needs of the project and then 5 chapters dedicated to each configuration can be found. These 5 chapters are structured in parallel, the one of interest for this project being chapter 6, which documents the method to define the geometry that allows the optimal operation of the centrifugal compressor. Finally, in Chapter 8 case studies can be found to illustrate the theory presented in some of the previous chapters.

The structure of the documentation is illustrated in *Figure 4* below:

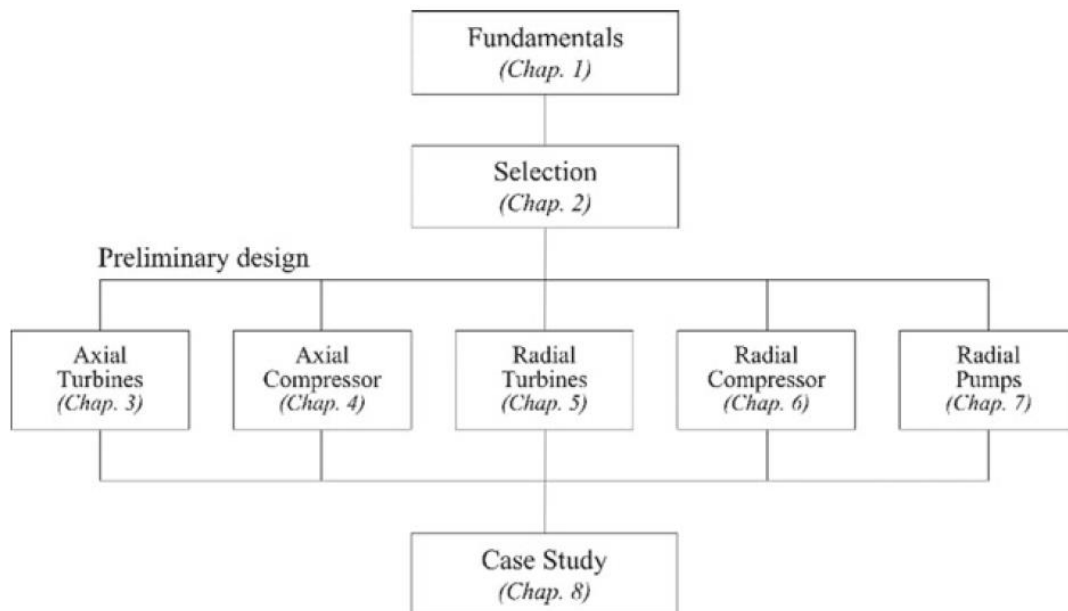


Figure 4: Documentation Structure

In order to facilitate the explanation of the model construction process, a similar structure will be followed, trying to go only through the points considered essential for the project.

Fundamentals (chapter 1)

This chapter introduces concepts mainly from the field of thermodynamics. The main differences between a closed system and an open system are explained, as well as how a fluid can exchange energy in the form of work and heat within these systems. Turbomachines are open systems that exchange energy through both channels with the environment, and depending on their type and configuration, they will do so to a greater or lesser extent through one or the other.

For the explanation and support of all the subsequent formulation, the Three Principles of Thermodynamics and Euler's equation, which are the scientific basis on which the whole technique is based, are recalled.

Similarly, concepts such as the thermodynamic properties of fluids that can define their states are refreshed. And depending on these and the ways in which they vary, how they can be classified. A distinction is made between perfect gases, perfect liquids and real fluids, the latter being the ones of interest for the process and especially for this project, since atmospheric air will be used as the gas of interest.

Since it is necessary to know the properties of air at different working points and since its behavior is different from that of an ideal gas for these applications in which precision is required, it is not possible to model its state with the ideal gas equation:

$$P \cdot v = n \cdot R \cdot T$$

And it will be necessary to use empirical tables or thermodynamic software. This will be explained later, but it is anticipated now that it was decided to use [B] Coolprop as a property calculator for air in this project.

To close the chapter, the processes of expansion and compression are explained, and how in real cases of application, the energy transfer from the environment to the fluid or vice versa is different from the ideal or adiabatic. The concept of isentropic efficiency is introduced, which measures the difference between the real enthalpy exchange versus the isentropic exchange, this difference being generated by the irreversibilities that the fluid undergoes when changing state.

Selection (chapter 2)

This chapter introduces the methods for selecting the optimum type of turbomachinery for the working conditions required for the fluid. The methods used are based on dimensionless numbers and will allow to choose between axial or centrifugal configurations for compressors and between axial or radial configurations for pumps.

For the case of interest of this project the selection method is of little relevance, since it was already established that the design object is a centrifugal compressor. However, it is interesting and could be useful for other projects.

The typology was pre-established since in the automotive world this is the indicated solution given the conditions of high flow rate and reduced pressure increase compared to other applications. The dimensionless numbers proposed in the methodology mainly use these two magnitudes for the selection process.

Figure 5 below shows some examples seen in the documentation:

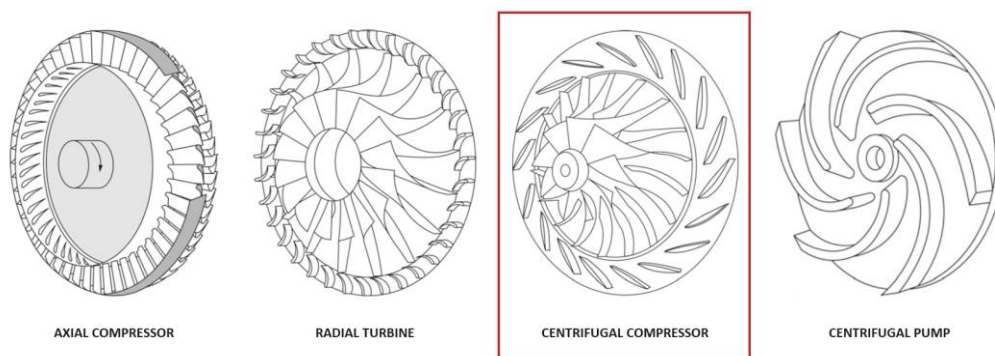


Figure 5: Turbomachinery Selection Options

Radial Compressor (chapter 6)

Having the machine typology selected, the book allows to jump to the chapter of interest directly, since as mentioned, for each configuration there is a dedicated chapter that is similarly explained in parallel.

This chapter will be the main documentary basis for the construction of the compressor model.

It begins by explaining certain kinematic parameters that were already introduced in the previous chapter, such as flow coefficient, work coefficient, rotor meridional velocity ratio, rotor tip diameter ration and degree of reaction. These will be important parameters in the search for the optimal design.

The book's method, seen as a black box, allows obtaining all the necessary dimensions for the design of the rotor and stator, as well as other outputs, starting from boundary conditions and input data.

Figure 6 below shows a symbolic scheme of the model that could be built following the method proposed in the literature:

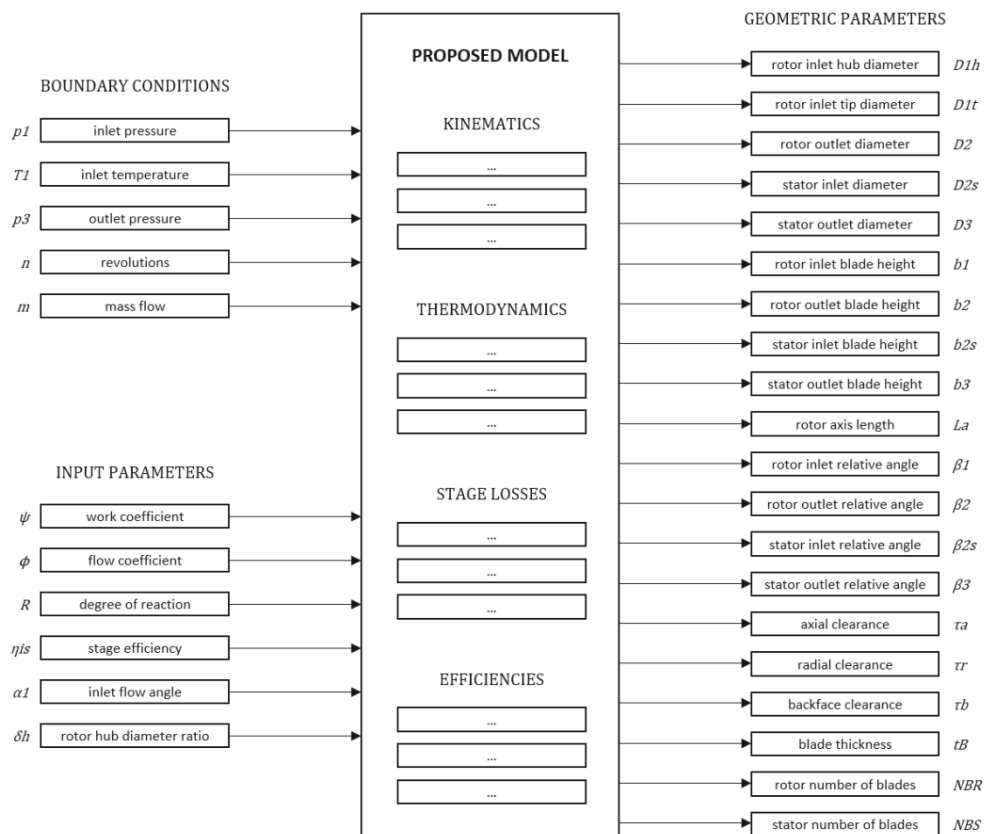


Figure 6: Theoretical Proposed Model Illustrative Diagram

The model, if one looks inside this "black box", is an iterative model. That is, in order to reach the solution with given boundary conditions and input parameters, the values of the theoretical impeller efficiency and isentropic efficiency must converge with those calculated from the losses.

Figure 7 below shows the iteration process followed by the model in the form of a symbolic scheme:

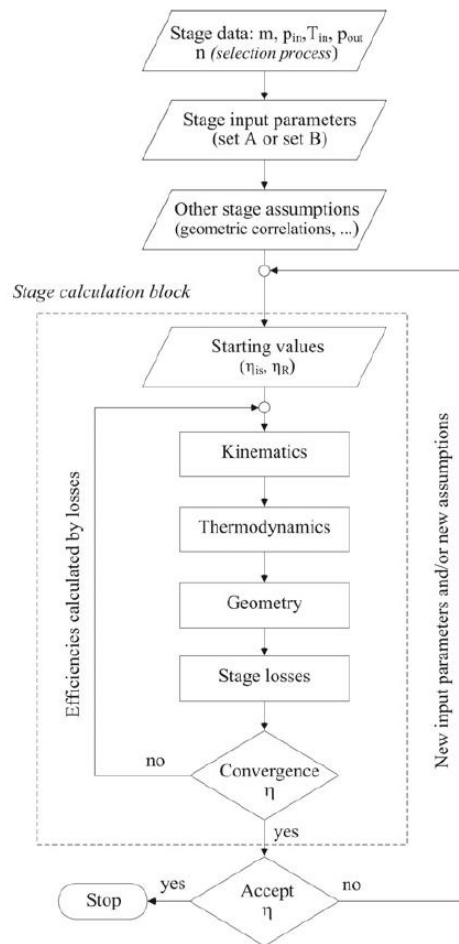


Figure 7: Execution Diagram of the Theoretical Proposed Model

The model of this project differs from the theoretical one that has just been exposed, this is because the boundary conditions of this project must be different and because the final functional model combines the two models that have just been explained, the one of the simple modeling of the combustion engine and the one of the book [1] "Turbomachinery Fundamentals: selection and preliminary design".

This is why the structure and the equations that justify the construction of the model will be explained in the next section, where the detail of each part that composes the final model will be given.

Case Study (chapter 8)

As previously stated, in this chapter some examples of application of the theory of the previous chapters are collected. As there are no use cases of centrifugal compressor design in this chapter, it is not relevant to the project and will not be developed in this section.

Compressor-Engine Model

The final model used for the calculation of the optimum compressor geometries is, as already mentioned, composed of the other two models explained above. In addition, it has some of its own developments to allow the adjustment to the project objectives.

The combustion engine model is used in the first instance to size the flow rate required by the engine at the revolutions that define the design point, which is 4000 RPM. This design point was selected because it is the highest torque regime in the case of operating with atmospheric fuel supply, according to the [2] Vehicle's Technical Data Sheet. It is desired that at this point the losses in the compressor are minimal and the increase in power and torque is remarkable compared to the base case. It is also a point of high engine revolution, within what is considered a healthy permanent regime.

To calculate this flow rate, it is needed to use the equation that relates the total engine displacement, the volumetric efficiency of the engine and the speed of rotation of this, which is as follows:

$$V_{\text{need}} = V3 = V_{\text{eng}} \cdot \eta_{\text{eng}} \cdot n_{\text{eng}}$$

With this, it is possible to begin to develop the adaptation that has been made of the theoretical compressor design model for this particular project.

In the method found in the documentation, one of the boundary conditions is not valid for the design case of this project, since we will not know the mass flow at the inlet of the engine (and compressor outlet) accurately to know another variable state of the fluid at this point other than the required pressure, which has been imposed. Therefore, replicating the scheme presented in the previous section, the model is presented below, with this variation in the boundary conditions in the following *Figure 8*:

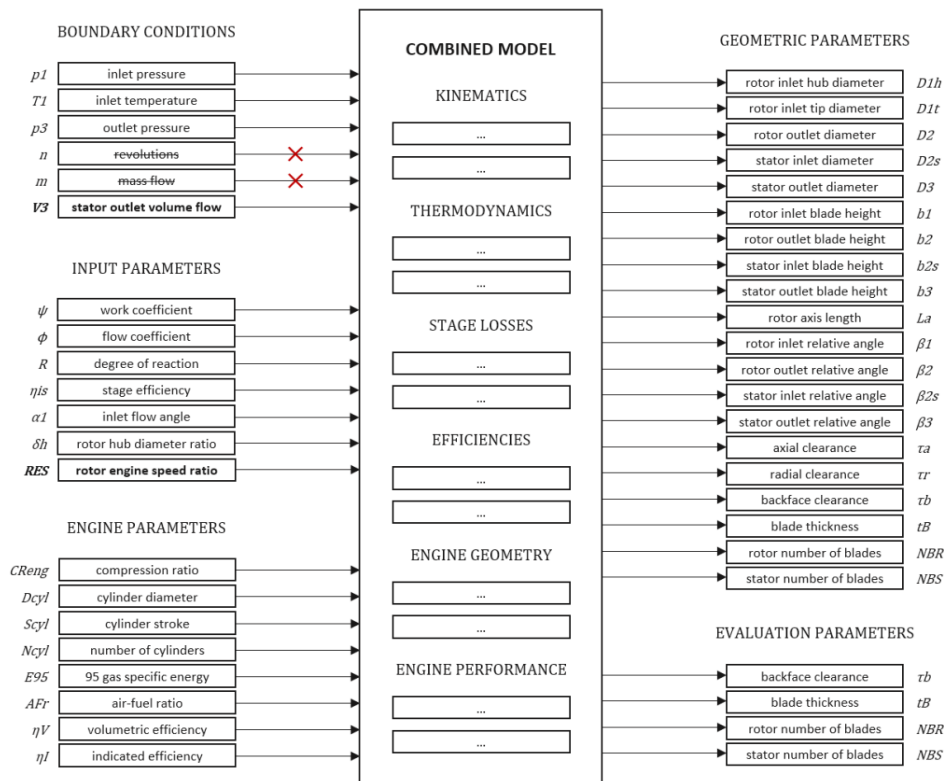


Figure 8: Developed Model Illustrative Diagram

This change with respect to the theoretical model means that we must relate the mass flow rate of the machine to this volume at the outlet. This is done using a state variable such as air density.

The density of the air is not known a priori, so it must be related to another state variable, such as the enthalpy of the fluid. Again, this enthalpy at point 3 (machine outlet) is not known, so it must be expressed as a function of the isentropic enthalpy thanks to the isentropic efficiency, which is input to the model. This makes it possible to use a similar model for the variables mentioned above.

Similarly, note that the rotor speed is not known a priori, so it has been decided to make it a variable instead of a boundary condition. For this purpose, it has been formulated as a function of the engine revolutions, leaving the gearbox conversion ratio as an input parameter.

With these first modifications on the theoretical model, we can proceed to the explanation of the developed model. Although it is important to mention that for the construction of this model it was decided to use [A] Microsoft Excel calculation software. And on this the thermodynamic calculation resolution software of [B] Coolprop was installed as a plugin. This last software is Open Source and allows to know any variable of a fluid once two other different variables that define its state are known. Needless to say, that the chosen fluid is air under standard conditions.

The model, as can be seen in the previously presented *Figure 8*, has 4 boundary conditions, 8 engine parameters and 7 input parameters. Some of the latter will vary their values within the ranges recommended by the book [1] "Turbomachinery Fundamentals: selection and preliminary design", so that several simulations will be obtained with different geometries that will allow selecting the input values that offer the most optimal result.

Furthermore, the isentropic yield, although it has been presented as an input parameter, will actually be the iteration parameter for solving the model. As mentioned above, this parameter will allow firstly to calculate the geometry of the turbomachine and with this obtained, the theoretical losses can be formulated. These losses will allow the calculation of a new efficiency that must converge with the efficiency inserted as input parameter for the model to reach a valid solution.

The model will be explained following the same order in which it was built, which is similar to the order of execution of the model. By doing this it will be easy to understand how it works and the scientific basis on which it is based.

The ordered sections that make up this chapter are as follows:

1. Inputs and Boundary Conditions Direct Calculations
2. Kinematic Calculations
3. Thermodynamic Calculations
4. Geometric Calculations (design output of the model)
5. Losses Calculations
6. Model Convergence
7. Coupling to the Engine Model

Inputs and Boundary Conditions Direct Calculations

These are the boundary conditions of the model:

p_1 – inlet pressure

T_1 – inlet temperature

p_3 – outlet pressure

V_3 – outlet volume flow

And these are the input parameters of the same:

Ψ – work coefficient

φ – flow coefficient

R – degree of reaction

η_{is} – stage efficiency

α_1 – rotor inlet flow angle

δ_h – rotor hub diameter ratio

RES – rotor engine speed ratio

Thanks to the [B] Coolprop plugin, the air conditions at the compressor inlet can be known immediately. This, for the rest of the document, will be denoted as follows:

$$\rho_1 = f[\rho](p_1, T_1)$$

$$v_1 = f[v](p_1, T_1)$$

$$s_1 = f[s](p_1, T_1)$$

$$h_1 = f[h](p_1, T_1)$$

The density, specific volume and enthalpy at the impeller inlet will be useful later. The entropy at point 1 can then be used to obtain the isentropic enthalpy at the turbomachine outlet:

$$h_{3_{is}} = f[h](p_3, s_1)$$

Thanks to the isentropic efficiency, introduced as input parameter (and iteration parameter), the enthalpy at the stator output can be calculated, according to its definition:

$$\eta_{is} = \frac{h_{3_{is}} - h_1}{h_3 - h_1} \rightarrow h_3 = h_1 + \frac{h_{3_{is}} - h_1}{\eta_{is}}$$

Again, by knowing two state variables in point 3, we can know others of interest:

$$\rho_3 = f[\rho](p_3, h_3)$$

$$v_3 = f[v](p_3, h_3)$$

$$s_3 = f[s](p_3, h_3)$$

$$T_3 = f[T](p_3, h_3)$$

The adiabatic enthalpy increase can be calculated as:

$$\Delta h_{ad} = h_3 - h_1$$

Now, to simplify the model, it will be assumed that the absolute fluid velocity at the inlet and outlet of the assembly is similar. Also, remembering that this is a real application case, by keeping the impeller inlet velocity similar to the stator outlet velocity, we will be able to ensure that air filters similar to the original ones of the vehicle can be used. However, the most relevant will perhaps be to save an iteration of another parameter to the model. The equation defining the adiabatic work is simplified as follows:

$$\left. \begin{aligned} W = \Delta h_{t,ad} = \Delta h_{ad} + \frac{c_3^2 - c_1^2}{2} \\ c_3 = c_1 \end{aligned} \right\} \rightarrow W = \Delta h_{t,ad} = \Delta h_{ad}$$

The definition of the work coefficient (assuming the speed $c_1 = c_3$) now allows to calculate the impeller speed at its outlet end, according to the equation:

$$\Psi = \frac{\Delta h_{t,ad}}{u_2^2} \rightarrow u_2 = \sqrt{\frac{\Delta h_{t,ad}}{\Psi}}$$

If the equality of absolute velocities is not assumed, the equation would remain as follows:

$$\Psi = \frac{\Delta h_{t,ad}}{u_2^2} + \frac{c_3^2 - c_1^2}{u_2^2}$$

Knowing the impeller speed at point 2 and the revolutions at which the impeller rotates, we can obtain the impeller outlet diameter directly:

$$D_2 = \frac{n}{u_2}$$

The speed is obtained by applying the gearbox conversion ratio to the speed that has been selected as the design point as follows:

$$n = RES \cdot n_{eng}$$

On the other hand, knowing the specific volumes (or densities) of the fluid at the inlet and outlet of the machine and the volumetric flow rate at the outlet, we can obtain the value of the volumetric flow rate at the impeller inlet:

$$V_1 = V_3 \cdot \frac{v_1}{v_3}$$

The rotor tip diameter ratio can be related to the values obtained above according to the following formula:

$$\delta_t = \sqrt{\delta_h^2 + \frac{4 \cdot V_1}{\pi \cdot \varphi \cdot u_2 \cdot D_2^2}}$$

And with this, the meridional velocity ratio can be calculated, which is defined as:

$$\xi = \sqrt{1 - \frac{2 \cdot \psi}{\varphi^2} \cdot \left(R + \frac{\psi}{2} - 1\right) + \tan^2(\alpha_1) \cdot (1 - \delta_t^2) - \frac{2 \cdot \psi \cdot \delta_t}{\varphi} \cdot \tan(\alpha_1)}$$

This last relationship will be of great importance for obtaining the first objective block of results, which are the kinematic results. With them it will be possible to plot the velocity triangles of the impeller, as well as to begin to know the first geometrical results, such as those defined by the relative angles that make up the triangle.

Kinematic Calculations

The absolute angle of the fluid at the impeller inlet is introduced as an input, as mentioned at the beginning of this chapter. As usual in the field of turbomachinery, this parameter is proposed to have a zero value at the design point, to eliminate incidence losses at this speed of revolution.

Thanks to certain relationships and the availability of the inlet parameters and other calculated values, the values of the absolute runner outlet angle, as well as the relative angles at the inlet and outlet, can then be obtained by means of the following equations:

$$\tan \alpha_2 = \frac{\psi}{\xi \cdot \varphi} + \frac{\delta_t}{\xi} \cdot \tan \alpha_1$$

$$\tan \beta_1 = \frac{\delta_t}{\varphi} - \tan \alpha_1$$

$$\tan \beta_2 = \frac{\psi}{\xi \cdot \varphi} \cdot (1 - \psi) - \frac{\delta_t}{\xi} \cdot \tan \alpha_1$$

With this, all the values necessary to calculate the modules of the vectors that compose the triangles of velocities at the inlet and outlet of the impeller are now available. The equations used are as follows:

$$c_{1m} = u_2 \cdot \varphi$$

$$c_{1u} = u_2 \cdot \varphi \cdot \tan(\alpha_1)$$

$$c_{2m} = u_2 \cdot \xi \cdot \varphi$$

$$c_{2u} = u_2 \cdot \xi \cdot \varphi \cdot \tan(\alpha_2)$$

$$w_{1u} = u_2 \cdot \varphi \cdot \tan \beta_1$$

$$w_{2u} = u_2 \cdot \xi \cdot \varphi \cdot \tan(\beta_2)$$

$$c_1 = u_2 \cdot \varphi \cdot \sqrt{1 + \tan^2(\alpha_1)}$$

$$c_2 = u_2 \cdot \xi \cdot \varphi \cdot \sqrt{1 + \tan^2(\alpha_2)}$$

$$w_1 = u_2 \cdot \varphi \cdot \sqrt{1 + \tan^2(\beta_1)}$$

$$w_2 = u_2 \cdot \xi \cdot \varphi \cdot \sqrt{1 + \tan^2(\beta_2)}$$

$$c_{1m} = u_2 \cdot \delta_t$$

In addition, it is recalled that it has been previously imposed that the absolute velocities at points 1 and 3 are equal, so we also know the value of the velocity at the exit of the stator:

$$c_3 = c_1$$

The calculation of the kinematic parameters allows to draw the triangles of velocities at the impeller inlet and outlet. It is not yet possible to paint the triangles at the inlet and outlet of the stator finned zone, which, although less relevant, will be presented once they can be calculated (after knowing the geometrical parameters).

The triangles known so far are illustrated in *Figure 9* below:

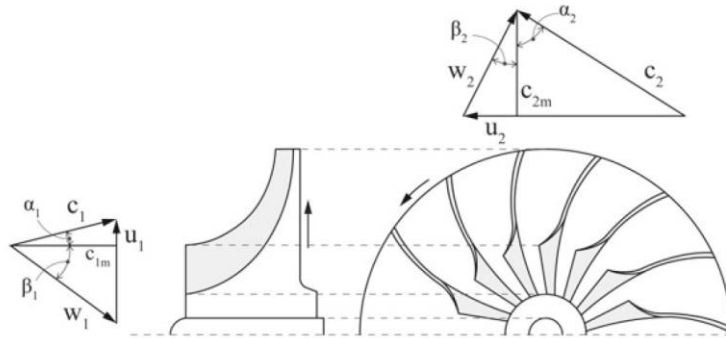


Figure 9: Theoretical Velocity Triangles

This concludes the first stage of the formulation to obtain the kinematic values. The pending kinematic values (2s and 3) will be calculated once the geometrical values of the machine have been formulated.

It is now possible to calculate the thermodynamic values at some points of the machine, as can be seen in the next section.

Thermodynamic Calculations

Thanks to the boundary conditions, point 1 has been completely described thermodynamically. Similarly, thanks to the target pressure boundary condition, which is that of point 3, and to the input parameter and isentropic performance iteration that allowed us to obtain the enthalpy at this point, it is also completely defined at the stator output.

Starting from these points and knowing the kinematics and other calculated values, others can begin to be deduced.

Point 1 when the total quantities are considered, including the absolute velocity at this point, is denoted as 1t. This point has the same entropy as point 1 and its enthalpy is obtained by applying the following formula:

$$h_{1t} = h_1 + \frac{c_1^2}{2}$$

This makes it possible to define it completely, thanks to the [B] Coolprop tool:

$$T_{1t} = f[T](h_{1t}, s_1)$$

$$p_{1t} = f[p](h_{1t}, s_1)$$

$$\rho_{1t} = f[\rho](h_{1t}, s_1)$$

$$v_{1t} = f[v](h_{1t}, s_1)$$

The next point to be defined will be point 1 by counting the relative total quantities, which is denoted as 1tr. Again, this is an isentropic point, for which the enthalpic relationship to the original point is known, shown in the following formula:

$$h_{1tr} = h_1 + \frac{w_1^2}{2}$$

Having again the same entropy value as the impeller entry point (point 1), the rest of the thermodynamic properties of interest can be calculated in a similar way thanks to the [B] property calculator:

$$T_{1tr} = f[T](h_{1tr}, s_1)$$

$$p_{1tr} = f[p](h_{1tr}, s_1)$$

$$\rho_{1tr} = f[\rho](h_{1tr}, s_1)$$

$$v_{1tr} = f[v](h_{1tr}, s_1)$$

Next, it is necessary to define and calculate the rothalpy of point 1, as follows:

$$I_1 = h_1 + w_1^2 - u_1^2 = h_{1tr} - u_1^2$$

In centrifugal compressors, the rothalpy value is maintained between the rotor inlet and rotor outlet. If the rotor efficiency value is also known, the calculation of the thermodynamic properties at the rotor outlet is immediate.

As mentioned above, the value of the rotor efficiency, as well as that of the isentropic efficiency of the turbomachine, are introduced with an initial (and similar) value to the model to be subsequently iterated accordingly to calculate the losses. Then at the first iteration, it can be stated that:

$$\eta_R = \eta_{is}$$

Therefore, one can proceed to the thermodynamic formulation of point 2, which is as follows:

$$I1 = I2$$

$$h2 = I2 - w2^2 + u2^2$$

And with the definition of isentropic performance:

$$\eta_R = \frac{h2_{is} - h1}{h2 - h1}$$

$$h2_{is} = \eta_R \cdot (h2 - h1) + h1$$

Thanks to the value of the enthalpy at the isentropic point at the outlet, we can know the value of the pressure at point 2, using the value of the entropy at the inlet:

$$p2 = f[p](h2_{is}, s1)$$

And again, with the property calculator, the rest of the properties for the point of interest (point 2) are obtained:

$$s2 = f[s](h2, p2)$$

$$T2 = f[T](h2, s2)$$

$$\rho2 = f[\rho](h2, s2)$$

$$v2 = f[v](h2, s2)$$

The thermodynamic properties for this item considering the total quantities and relative total quantities are calculated in a similar way as how it was done for point 1:

$$h2_t = h2 + \frac{w2^2}{2}$$

$$T2_t = f[T](h2_t, s2)$$

$$p2_t = f[p](h2_t, s2)$$

$$\rho2_t = f[\rho](h2_t, s2)$$

$$v2_t = f[v](h2_t, s2)$$

$$h2_{tr} = h2 + \frac{c2^2}{2}$$

$$T2_{tr} = f[T](h2_{tr}, s2)$$

$$p2_{tr} = f[p](h2_{tr}, s2)$$

$$\rho2_{tr} = f[\rho](h2_{tr}, s2)$$

$$v2_{tr} = f[v](h2_{tr}, s2)$$

Now, thanks to the conservation of the total enthalpy in the stator (between points 2t and 3t), the properties for this point can be calculated considering the total quantities. Although it will be necessary to know the entropy at point 3, which was already obtained at the beginning of this chapter. Applying a formulation similar to that applied above for the total quantities at points 1 and 2, the relationships remain:

$$h_{3t} = h_{2t}$$

$$T_{3t} = f[T](h_{3t}, s_3)$$

$$p_{3t} = f[p](h_{3t}, s_3)$$

$$\rho_{3t} = f[\rho](h_{3t}, s_3)$$

$$v_{3t} = f[v](h_{3t}, s_3)$$

And with these values, the calculation of the thermodynamic values is completed, being able to draw the diagram of the compression process in the s and h axes for all the points of interest. The result obtained will be similar to the one shown in *Figure 10* below:

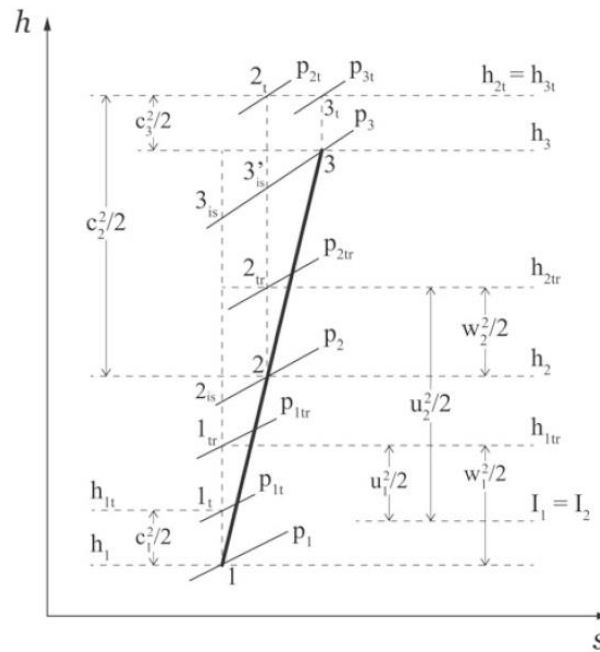


Figure 10: Theoretical Thermodynamical Cycle

Before closing this chapter, the calculation of other parameters of interest for points 1, 2 and 3 is still pending. Which are, as mentioned: the rotor inlet, the rotor outlet (or stator inlet) and the stator outlet respectively.

First, the sound velocities for these points are calculated thanks to the property calculation software:

$$c_{s1} = f[c_s](p_1, T_1)$$

$$c_{s2} = f[c_s](p_2, T_2)$$

$$c_{s3} = f[c_s](p_3, T_3)$$

The Mach numbers can then be calculated, using the relative speeds at the rotor and the absolute speeds at the stator for these points:

$$\text{Ma}_1 = \frac{w_1}{c_{s1}}$$

$$\text{Ma}_{2_R} = \frac{w_2}{c_{s2}}$$

$$\text{Ma}_{2_S} = \frac{c_2}{c_{s2}}$$

$$\text{Ma}_3 = \frac{c_3}{c_{s3}}$$

Note that point 2 is defined at two points, one at the rotor outlet and stator inlet (2_R) and the other at the inlet of what will be the stator vaned zone (2_S).

Again, [B] Coolprop software is used to calculate the fluid viscosities at these points:

$$\mu_1 = f[\mu](p_1, T_1)$$

$$\mu_2 = f[\mu](p_2, T_2)$$

$$\mu_3 = f[\mu](p_3, T_3)$$

These viscosities will be used for the calculation of Reynolds numbers later in the section on the calculation of losses.

With these last equations, the calculation of the thermodynamic values can be concluded and we can proceed with the calculation of the geometrical parameters.

Geometric Calculations

The result of this section will be the output of the model, since with the geometrical values it should be possible to define the geometry of the rotor and the stator that allow to start the design phase using the [C] Solid Edge tool.

However, the model does not end here. As it has been explained, it is an iterative process of obtaining results, so when this section is finished, others will follow to understand the operation of the model as a whole, including the convergence of the model result and the functionality added that allows to achieve the optimum design among many different viable results.

The list of geometric parameters defining the dimensions of interest has already been presented in *Figure 8* at the beginning of this chapter. In order to give a more visual explanation, *Figure 11* below shows most of them:

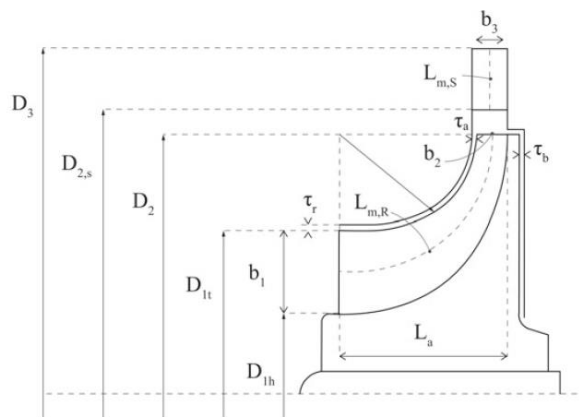


Figure 11: Theoretical Geometry and Dimensions

Certain parameters are not represented, but are described below:

β_1 : physical angle of entry to the impeller measured between a plane containing the shaft of the turbomachine and any of its blades and the plane at the entry end of the involved blade.

β_{2B} : physical impeller exit angle measured between a plane containing the shaft of the turbomachine and any of its blades and the plane at the exit end of the blade in question. It is distinct from the kinematic rotor exit angle as will be discussed later.

β_{2S} : physical stator inlet angle measured between a plane containing the turbomachine shaft and any of its guide vanes and the plane at the inlet end of the guide vane in question.

β_3 : physical stator exit angle measured between a plane containing the turbomachine shaft and any of its guide vanes and the plane at the exit end of the guide vane of interest.

t_B : thickness of the turbomachine blades and vanes.

b_{2S} : height of the vane at the stator inlet measured in the shaft direction.

b_3 : height of the vane at the stator outlet measured in the shaft direction.

Next, the equations that allow the calculation of the mentioned dimensions are presented according to their order of execution in the model.

First of all, the area of the inlet section of the machine will be calculated. For this, it is necessary to use the volumetric flow rate at the inlet and the absolute meridional velocity of the fluid at this point, which have already been calculated at the beginning of the model:

$$A1 = \frac{V1}{c1_m}$$

In the same way, the section at the outlet can be calculated:

$$A2 = \frac{V2}{c2_m}$$

As already mentioned, but presented again, the equation defining the rotor outlet diameter D2 is as follows:

$$D2 = \frac{n}{u2}$$

With these values calculated, the dimensions defining the cross-section geometries can be calculated. At the inlet, the inner and outer diameters of the rotor must be obtained. For this purpose, their ratios to the diameter in point 2, which have already been defined above, can be used:

$$D1_h = D2 \cdot \delta_h$$

$$D1_t = D2 \cdot \delta_t$$

The parameter b1 is therefore immediately defined as the semi-difference of diameters:

$$b1 = \frac{D1_t - D1_h}{2}$$

And at the outlet, it is necessary to calculate the height of the blade. This is achieved by dividing the section obtained by the circumference determined by the diameter as follows:

$$b2 = \frac{A2}{D2 \cdot \pi}$$

In the kinematic part, the tip of the blade furthest from the axis was considered as the point of interest; in this section the kinematic parameters can be obtained at the midpoint between the two extremes, which is more representative.

The mean inlet diameter is defined, where it is considered that the fluid has the representative properties of all the flow along the radius:

$$D1_M = \frac{D1_t + D1_h}{2}$$

The relative and absolute angles at this point are:

$$\tan(\alpha1_M) = \tan(\alpha1) \cdot \frac{D1_t}{D1_M} \qquad \tan(\beta1_M) = \frac{\delta_t}{\varphi} \cdot \frac{D1_t}{D1_M} - \tan(\alpha1_M)$$

And the relative velocity at this point is therefore:

$$w_{1M} = \frac{c_{1m}}{\cos(\beta_{1M})}$$

Another important parameter for the calculation of the geometry is the number of blades. To obtain this it is necessary to remember that in this type of machines the fluid guidance by the moving part is not completely parallel to the outlet of the vane, but there is a certain deviation (slip).

This causes the angle of the blade to differ slightly from the relative angle of the fluid seen at the exit of the impeller. To calculate it is necessary to know the slip factor which is defined as the ratio between the real absolute velocity and the absolute velocity in case of having an infinite number of vanes (with perfect guidance):

$$SF = \frac{c_{2u}}{c_{2u,\infty}}$$

In the bibliography used, book [1] "Turbomachinery Fundamentals: selection and preliminary design", a complex system of equations is presented to obtain this factor. Since [A] Excel was used as a calculation tool, it was decided to use an iterative method for the calculation of the parameter.

First, the geometric angle of the blade outlet is inserted as input. And with this, the mean angle is calculated using the mean relative angle in the input that has just been formulated is calculated. Its formula can be seen here:

$$\beta_M = \frac{\beta_{2B} + \beta_{1M}}{2}$$

In addition, it is necessary to introduce a value for the parameter proposed by Eckert and Schnell, represented by the symbol ζ , which the literature recommends that it should fall in the interval between 0.35-0.45.

Once the model was built, it was observed that the optimal values that minimized the number of blades were at the upper limit, so it was decided to use 0.45.

The number of blades can now be calculated using the equation proposed by Osnaghi:

$$NBR = \text{integer} \left(\frac{2 \cdot \pi \cdot \cos(\beta_M)}{\zeta \cdot \log \left(\frac{1}{\delta_t} \right)} \right)$$

With the proposed optimum number of blades for these values, the slip factor described by Wiesner can be calculated:

$$SF = 1 - \frac{\sqrt{\cos(\beta_{2B})}}{NBR^{0.7}}$$

And using the relation to the actual geometric angle of the blade:

$$\tan(\beta_{2B}) = \frac{1}{\xi \cdot \varphi} - \frac{\tan(\alpha_2)}{SF}$$

The iteration can be performed to obtain the value of β_{2B} that satisfies the above equations.

Finally, in relation to the number of blades, there is a correction for the case in which split blades are used, but it will be obviated with the objective of achieving simplicity in the model and in the design. In addition, these are useful only when the compressor ratio in the machine is high (greater than 2), and this is not the case.

The ratio between blade thickness and rotor outlet diameter is suggested to be higher than certain values depending on whether you want to model a covered or uncovered rotor. In order to make use of additive technologies and to avoid axial stresses on the machine shaft it was decided that the impeller would be of the covered type, so the limit imposed according to the book and imposed in the model is as follows:

$$\frac{t_B}{D2} \approx 0,01 \rightarrow t_B = 0,01 \cdot D2$$

Similarly, the documentation suggests ratios for calculating the clearances between the rotor and the rest of the parts. In addition, it adds lower limits that should not be exceeded:

$$\tau_a > 0,05 \cdot b2 \quad \text{and} \quad \tau_a > 0,3 \text{ mm}$$

$$\tau_b > 0,05 \cdot b2 \quad \text{and} \quad \tau_b > 0,3 \text{ mm}$$

$$\tau_r > 0,05 \cdot b2 \quad \text{and} \quad \tau_r > 0,3 \text{ mm}$$

The length of the rotor shaft significantly influences the value of the meridional length and therefore the rotor losses. It can be calculated using Aungier's definition which optimizes the rotor efficiency:

$$L_a = D2 \cdot \left[0,014 + \frac{0,023}{\delta_h} + 1,58 \cdot (\delta_t^2 - \delta_h^2) \cdot \varphi \right]$$

Geometric parameters are then calculated which, although not directly used in the design software, will be of vital importance for the final section of this chapter, where losses will be calculated to achieve model convergence.

For the calculation of the rotor mean hydraulic diameter, it will be necessary to previously calculate, for the inlet and outlet; the distances between blades, the distances to the leading edge, the wetted areas, the wetted perimeters and the hydraulic diameters. The formulation is as follows:

$$S1_R = \frac{\pi \cdot D1_M}{NBR}$$

$$S2_R = \frac{\pi \cdot D2}{NBR}$$

$$O1 = S1_R \cdot \cos(\beta1_M)$$

$$O2 = S2_R \cdot \cos(\beta2_B)$$

$$A_w1 = O1 \cdot b1$$

$$A_w2 = O2 \cdot b2$$

$$P_w1 = 2 \cdot (O1 + b1)$$

$$P_w2 = 2 \cdot (O2 + b2)$$

$$D_{hyd1} = 2 \cdot \frac{O1 \cdot b1}{O1 + b1}$$

$$D_{hyd2} = 2 \cdot \frac{O2 \cdot b2}{O2 + b2}$$

The average hydraulic diameter of the rotor, as the name suggests, is the average of the hydraulic diameters at the rotor inlet and outlet:

$$D_{\text{hyd,R}} = \frac{D_{\text{hyd}1} + D_{\text{hyd}2}}{2}$$

For the calculation of the hydraulic length it will be necessary, for simplicity, to define two intermediate parameters:

$$a = L_a - \frac{b^2}{2}$$

$$b = \frac{D_2 - D_{1M}}{2}$$

And subsequently, use these to formulate the meridional length:

$$L_{\text{m,R}} = \pi \cdot \frac{a + b}{4}$$

Finally, the hydraulic length is calculated as:

$$L_{\text{hyd,R}} = \frac{L_{\text{m,R}}}{\cos(\beta_M)}$$

With this, the rotor geometry is completely defined and the geometrical parameters defining the stator can be proceeded with.

The diameter at the stator inlet can be formulated following the relation proposed by Aungier and Kim:

$$D_{2S} = D_2 \cdot \left(1 + \frac{\frac{\pi}{2} - \alpha_{2S}}{2 \cdot \pi} + \frac{Ma_2^2}{15} \right)$$

With α_{2S} defined in radians.

Where:

$$\alpha_{2S} = \frac{4 \cdot \pi}{5} + \frac{\alpha_2 - \frac{4 \cdot \pi}{5}}{4} \quad \text{if } \alpha_2 \geq \frac{4 \cdot \pi}{5}$$

$$\alpha_{2S} = \frac{4 \cdot \pi}{5} \quad \text{if } \alpha_2 < \frac{4 \cdot \pi}{5}$$

With α_2 was also formulated in radians.

And:

$$Ma_2 = \frac{c_2}{c_{2S}}$$

With:

$$c2_s = \sqrt{c2_{s,u}^2 + c2_{s,m}^2}$$

$$c2_{s,u} = c2_u \cdot \frac{D2}{D2_s}$$

$$c2_{s,m} = \frac{c2_{s,u}}{\tan(\alpha2_s)}$$

For the sake of simplicity, despite the existence of a method in the documentation for calculating the height of the guide vanes, the proposed alternative is to match this height to that of the rotor blade outlet:

$$b2_s = b2$$

The hydraulic length in the area of the stator without vanes as well as the meridional length in the same section are calculated in a simple way, using the formula:

$$L_{hyd,vaneless} = L_{m,vaneless} = \frac{D2_s - D2}{2}$$

And to calculate the hydraulic diameter in this section, the simplified formula is used:

$$D_{hyd,vaneless} = b2 + b2_s$$

It is important to emphasize that the stator zone considered as the vaneless zone is the one comprised between diameters $D2$ y $D2_s$.

Moving on to the vaned zone, Aungier suggests the following formula for the calculation of the stator outer diameter:

$$D3 = D2 \cdot (1,55 + (\delta_t^2 + \delta_h^2) \cdot \varphi)$$

Again, the blade height is assumed to be constant, so:

$$b3 = b2_s = b2$$

And the meridional velocity of the fluid can be calculated, using:

$$c3_m = \frac{V3}{\pi \cdot D3 \cdot b3}$$

In addition, as imposed in the design conditions:

$$c3 = c1$$

This allows immediate calculation:

$$\alpha3 = \arccos\left(\frac{c3_m}{c3}\right)$$

And:

$$c_{3m} = c_{3u} \cdot \tan(\alpha_3)$$

This concludes the section on kinematic parameters which had not yet been completed in this chapter because the values at the outlet of the machine could not be known until the geometrical values of the machine were determined, as mentioned at the beginning of the chapter.

For the calculation of the number of flux guide vanes in the stator, the limits are used:

$$NBS = NBR - 1 \quad \text{if } 10 < NBR < 20$$

$$|NBS - NBR| \geq 8 \quad \text{if } NBR \leq 10 \text{ or } NBR \geq 20$$

The meridional length in the vaned zone is calculated using:

$$L_{m,vaned} = \frac{D_3 - D_{2s}}{2}$$

And the hydraulic length (which coincides with the vane chord) in the same section:

$$L_{hyd,vaned} = C_s = \frac{D_3 - D_{2s}}{2 \cdot \cos\left(\frac{\alpha_{2s} + \alpha_3}{2}\right)}$$

The vane spacing for the inlet and outlet is calculated:

$$S_{2s} = \frac{\pi \cdot D_{2s}}{NBS}$$

$$S_3 = \frac{\pi \cdot D_3}{NBS}$$

The distance from the vane to the axis of attack for the outlet and inlet, as well as the wetted areas and perimeters are:

$$A_{w2s} = O_{2s} \cdot b_{2s}$$

$$A_{w3} = O_3 \cdot b_3$$

$$P_{w2s} = 2 \cdot (O_{2s} + b_{2s})$$

$$P_{w3} = 2 \cdot (O_3 + b_3)$$

Therefore, the hydraulic diameters at both points can be calculated:

$$D_{hyd2s} = 2 \cdot \frac{O_{2s} \cdot b_{2s}}{O_{2s} + b_{2s}}$$

$$D_{hyd3} = 2 \cdot \frac{O_3 \cdot b_3}{O_3 + b_3}$$

And with them, the average hydraulic diameter for the vaned area:

$$D_{hyd,vaned} = \frac{D_{hyd2s} + D_{hyd3}}{2}$$

There are three parameters proposed by Aungier that relate different geometric and kinematic values to check the validity of the model when the values calculated for these parameters fall within certain ranges. For simplicity, they will not be analyzed in this chapter which tries to explain the functioning of the constructed tool.

However, the formulas and ranges of values that guarantee the optimization of the machine are presented below.

The divergence angle:

$$\tan(\theta_C) = \frac{\pi \cdot (D3 \cdot \cos(\alpha3) - D2_S \cdot \cos(\alpha2_S))}{2 \cdot NBS \cdot L_{hyd,vaned}} \quad 7^\circ < 2 \cdot \theta_C < 11^\circ$$

The vane loading parameter:

$$BL = \frac{\pi \cdot (D2_S \cdot c2_{S,u} - D3 \cdot c3_u)}{NBS \cdot L_{hyd,vaned} \cdot (c2_S - c3)} \quad 0 < BL < \frac{1}{3}$$

The ratio of areas:

$$A_R = \frac{D3 \cdot b3 \cdot \cos(\alpha3)}{D2_S \cdot b2_S \cdot \cos(\alpha2_S)} \quad 1,4 < A_R < 2,4$$

Note that the easiest way to vary these values without modifying the values defined as input will be to vary the number of blades and vanes, which, although they are formulated, can be varied freely even if other dependent parameters vary. Since, as explained in the book [1] "Turbomachinery Fundamentals: selection and preliminary design", the number of blades and the number of vanes are free parameters that, despite having to meet certain conditions, can be slightly modified, and they will be.

Finally, in the section on geometrical parameters, the roughness of the parts is modeled. To do this, first the Reynolds numbers are calculated for the main points of interest:

$$Re1 = \frac{\rho1 \cdot w1 \cdot D_{hyd,R}}{\mu1}$$

$$Re2 = \frac{\rho2 \cdot w2 \cdot D_{hyd,R}}{\mu2}$$

$$Re2_S = \frac{\rho2_S \cdot c2_S \cdot D_{hyd,vaned}}{\mu2_S}$$

$$Re3 = \frac{\rho3 \cdot c3 \cdot D_{hyd,vaned}}{\mu3}$$

And then, with these, the maximum allowable manufacturing roughness for the rotor and stator can be obtained:

$$K_{Sadm,R} = 100 \cdot \frac{D_{hyd,R}}{Re1}$$

$$K_{Sadm,vaned} = 100 \cdot \frac{D_{hyd,vaned}}{Re2_S}$$

These values serve as upper limits and other actual values will be inserted into the model. It is important to note that the upper bounds are loose and that in no simulation did the limit values approach the manually entered values.

For the calculation of the losses, as will be seen below, the roughness values inserted in the model are used, and not the limit values, as is logical.

The geometrical section is concluded and can be continued with the section explaining the calculation of the different losses occurring in the machine.

Losses Calculations

Two loss models are proposed in the literature [1] "Turbomachinery Fundamentals: selection and preliminary design", one based on pressure losses and the other based on energy (enthalpy) losses. Both models are equally valid, and the result is similar, the difference lies in the type of physical units to be used for the calculation.

For simplicity, we will opt for the load loss method for the resolution of the model, although both are represented in the tool.

Only the formulation of the method chosen for the resolution will be explained in detail below. Taking into account that the pressure drops in centrifugal compressors are calculated for each part of interest (rotor and stator).

It begins with the rotor, similarly to the execution of the model. Being their losses of different nature, as indicated by the following equation:

$$Y_R = Y_{inc} + Y_{sf} + Y_{BL} + Y_{HS} + Y_{mix} + Y_{CL}$$

Next, each of the terms that make up the losses in the rotor are calculated according to the values obtained in the previous sections.

The incidence losses (Y_{inc}) represent the load losses that the fluid suffers when impinging on the machine, it has two terms. The first represents the losses when the angle of incidence differs from the relative angle at design point ($\beta_{1M,nom} = \beta_{1M,B}$). While the second represents the losses due to the section obstructed by the thickness of the blades. The formula is:

$$Y_{inc} = 0,8 \cdot \left(1 - \frac{c_{1m}}{w_{1m} \cdot \cos(\beta_{1M,B})}\right)^2 + \left(\frac{NBR \cdot t_B}{\pi \cdot D_{1M} \cdot \cos(\beta_{1M,B})}\right)^2$$

Skin friction losses (Y_{sf}) are those due to friction between the fluid and the rotor surface, and are calculated as follows:

$$Y_{sf} = 4 \cdot f_{sf} \cdot \frac{L_{hyd,R}}{D_{hyd,R}} \cdot \left(\frac{\bar{w}}{w_{1M}}\right)^2$$

Where:

$$\bar{w} = \sqrt{\frac{w_{1M}^2 + w_2^2}{2}}$$

The calculation of the skin friction factor is complex and can be noted in the formulation of the tool in case of doubt. The complexity is given by the need to declare several Reynolds numbers (Re_D and Re_e) which are used to select the optimal formula according to the result of these. As it does not add much value to this document, it has been decided to omit this explanation, however, it can be consulted on pages 280 and 281 of the [1] book (Edition: ©Springer Nature/Switzerland AG 2021).

It is important to note that the factor used is dependent on the roughness chosen for the manufacture of the part, which must always be lower than the upper limit value calculated above. Since this is a part manufactured by high-precision additive technologies (dental prosthetic technology) it has been estimated to be 5 μm .

The blade loading losses (Y_{BL}) are simpler to calculate than the previous ones and are related to the difference of velocities in the fluid between the inlet and outlet of the rotor:

$$Y_{BL} = \frac{1}{24} \cdot \left(\frac{\Delta w}{w_{1M}} \right)^2$$

With:

$$\Delta w = \frac{2 \cdot \pi \cdot D2 \cdot u2 \cdot \Psi}{NBR \cdot L_{hyd,R}}$$

The hub to shroud losses (Y_{HS}) are related to the change in direction of the fluid inside the rotor, which enters axially and exits radially. Its simplified equation under these conditions is:

$$Y_{HS} = \frac{1}{6} \cdot \left(\frac{\bar{K}_m \cdot \bar{b} \cdot \bar{w}}{w_{1m}} \right)^2$$

Where:

$$\bar{K}_m = \frac{\pi}{2 \cdot L_{m,R}}$$

The mixing losses (Y_{mix}) are slightly more complex to calculate than the previous ones:

$$Y_{mix} = \left(\frac{c2_{m,wake} - c2_{m,mix}}{w_{1m}} \right)^2$$

Where it is defined that:

$$c2_{m,mix} = c2_m \cdot \left(1 - \frac{NBR \cdot t_B}{\pi \cdot D2} \right)$$

$$c2_{m,wake} = \sqrt{w_{sep}^2 - w_{2u}^2}$$

To formulate w_{sep} , it is necessary to define the optimum diffusion factor, using the formula:

$$DF_{eq} = \frac{w_{max}}{w2} = \frac{w_{1M} + w2 + \Delta w}{2 \cdot w2}$$

And with this we can select the appropriate formula for the calculation of w_{sep} :

$$w_{sep} = w2 \quad \text{if } DF_{eq} \leq 2$$

$$w_{sep} = w2 \cdot \frac{DF_{eq}}{2} \quad \text{if } DF_{eq} > 2$$

Finally, to finish with the rotor losses, there are the clearance losses, which only apply when the rotor is of open type and, as mentioned above, in this project a covered rotor will be used to avoid the axial stresses that are generated when the part is of open type. However, to give context, its calculation is formulated below:

$$Y_{CL} = \frac{2 \cdot m_{CL} \cdot \Delta p_{CL}}{m \cdot \rho_1 \cdot w_1^2 M}$$

Where:

$$\Delta p_{CL} = \frac{m \cdot \Psi \cdot u^2}{NBR \cdot L_{hyd,R} \cdot w \cdot \left(\frac{D1_M + D2}{4}\right) \cdot \left(\frac{b1 + b2}{2}\right)}$$

$$m_{CL} = \rho_2 \cdot NBR \cdot \tau_a \cdot L_{hyd,R} \cdot u_{CL}$$

$$u_{CL} = 0,816 \cdot \sqrt{\frac{2 \cdot \Delta p_{CL}}{\rho_2}}$$

Next, the losses occurring in the stator can be calculated, which will be divided into two types:

$$Y_S = Y_{vaneless} + Y_{vaned}$$

In the vaneless part of the stator, we found a new composition of different losses:

$$Y_{vaneless} = Y_{sf} + Y_{diff}$$

The first are the skin friction losses (Y_{sf}), and similar to those calculated for the rotor, they can be formulated as follows:

$$Y_{sf} = 4 \cdot f_{sf} \cdot \frac{L_{hyd,vaneless}}{D_{hyd,vaneless}} \cdot \left(\frac{\bar{c}}{c_2}\right)^2$$

With:

$$\bar{c} = \sqrt{\frac{c_{2S}^2 + c_2^2}{2}}$$

And where the skin friction factor is the same as the one calculated for the rotor, since as mentioned, the roughness for both parts will be identical and equal to 5 μ m.

The second term for the vaneless part is the diffusion losses (Y_{diff}):

$$Y_{diff} = -2 \cdot (1 - E) \cdot \frac{c_{2S, is} - c_2}{c_2}$$

In its equation we find the E term that represents the diffusion efficiency, for its determination it is necessary to evaluate the divergence and reference parameters:

$$D_v = \frac{b_2 \cdot \left(\frac{D_{2S}}{D_2} - 1\right)}{L_{hyd,vaneless}}$$

$$D_{rif} = 0,4 \cdot \left(\frac{b_2}{L_{hyd,vaneless}}\right)^{0,35}$$

And with them:

$$E = 1 \quad \text{when } D_v \leq 0$$

$$E = 1 - 0,2 \cdot \left(\frac{D_v}{D_{rif}}\right)^2 \quad \text{when } 0 < D_v < D_{rif}$$

$$E = 0,8 \cdot \sqrt{\frac{D_{rif}}{D_v}} \quad \text{when } D_v \geq D_{rif}$$

Losses in the vaned part are due to three causes:

$$Y_{vaned} = Y_{inc} + Y_{sf} + Y_{mix}$$

As can be seen, the loss terms that compose them have already been calculated for the other parties of interest. Their formulation is as follows.

The incidence losses (Y_{inc}):

$$Y_{inc} = 0,8 \cdot \left(1 - \frac{c_{2s,m}}{c_{2s} \cdot \cos(\alpha_{2s})}\right)^2 + \left(\frac{NBS \cdot t_B}{\pi \cdot D_{2s}}\right)^2$$

The skin friction losses (Y_{sf}):

$$Y_{sf} = 4 \cdot \frac{f_{sf}}{A} \cdot \frac{L_{hyd,vaned}}{D_{hyd,vaned}} \cdot \left(\frac{\bar{c}}{c_{2s}}\right)^2$$

Where the f_{sf} is again the same as previously calculated, and:

$$\bar{c} = \sqrt{\frac{c_{2s}^2 + c^2}{2}}$$

$$A = \left(5,142 \cdot f_{sf} \cdot \frac{L_{hyd,vaned}}{D_{hyd,vaned}}\right)^{0,25}$$

Finally, mixing losses (Y_{mix}) in the vaned part have the following equation:

$$Y_{mix} = \left(\frac{c_{3m,wake} - c_{3m,mix}}{c_{2s}}\right)^2$$

Where:

$$c_{3m,mix} = c_{3m} \cdot \left(1 - \frac{NBS \cdot t_B}{\pi \cdot D_2}\right)$$

$$c_{3m,wake} = \sqrt{c_{3sep}^2 - c_u^2}$$

Considering that in order to determine $c_{3_{sep}}$ it is necessary to calculate the equivalent diffusion factor:

$$DF_{eq} = \frac{c_{2s}}{c_3}$$

That when assessed:

$$c_{3_{sep}} = c_3 \quad \text{if } DF_{eq} \leq 2$$

$$c_{3_{sep}} = c_3 \cdot \frac{DF_{eq}}{2} \quad \text{if } DF_{eq} > 2$$

The losses have been formulated for all the zones of interest according to the pressure loss coefficient calculation method. These coefficients relate the actual pressure values in each zone to the theoretical pressure values calculated in the thermodynamic parameters section and will be useful to recalculate the actual enthalpy situation at different points of the machine. The values of the rotor efficiency and total isentropic efficiency are then iterated until convergence is achieved.

Model Convergence

The relationship between the calculated loss coefficients and the actual pressure situations on the parts is shown below.

For the rotor:

$$Y_R = \frac{p_{2_{tr,is}} - p_{2_{tr}}}{\frac{p_{2_{tr}}}{p_{1_{tr}}} \cdot (p_{1_{tr}} - p_1)}$$

And for the stator, differentiating between the vaned and vaneless parts:

$$Y_{\text{vaneless}} = \frac{p_{2_t} - p_{2_{S,t}}}{p_{2_t} - p_2}$$

$$Y_{\text{vaned}} = \frac{p_{2_{S,t}} - p_{3_t}}{p_{2_{S,t}} - p_{2_S}}$$

$$Y_S = Y_{\text{vaneless}} + Y_{\text{vaned}}$$

The model requires two convergence conditions. It will start with the convergence at the rotor.

It is necessary to recalculate the enthalpy at point 2, which will allow to know the rotor efficiency, taking the isentropic enthalpy calculated in the thermodynamic parameters section.

We start by recalculating the pressure by counting the relative total quantities. This will allow to obtain the enthalpy under the same conditions. And once calculated, it will be possible to obtain, thanks to the thermodynamic properties calculation software [B] Coolprop, the real enthalpy and entropy conditions depending on the losses in point 2, as shown below:

$$p_{2_{tr}} = \frac{p_{2_{tr,is}}}{1 + Y_R \cdot \left(1 - \frac{p_1}{p_{1_{tr}}}\right)}$$

$$h_{2_{tr}} = h_{1_{tr}} + \frac{u_{2_{tr}}^2 - u_{1_{tr}}^2}{2}$$

$$s_2 = f[s](p_{2_{tr}}, h_{2_{tr}})$$

$$h_2 = f[h](p_2, s_2)$$

The actual loss dependent rotor efficiency is then easily obtained and can be used to iterate the model until convergence is achieved between this value and the same value entered as input:

$$\bar{\eta}_R = \frac{h_{2_{is}} - h_1}{h_2 - h_1}$$

The second convergence condition, as mentioned above, is the convergence between the isentropic efficiency result calculated from the losses and the total isentropic efficiency inserted as input to the model.

To relate these parameters, it will be necessary to recalculate the enthalpy value at point 3 and obtain the new isentropic efficiency value of the machine relating to the conditions at point 1

and the isentropic enthalpy at point 3 calculated in the third section of this chapter (Thermodynamic Calculations).

As shown at the beginning of this section, the relationship between the pressure loss coefficient in the vaneless part of the stator relates the pressures at point 2, at point 2 by accounting for the total quantities and at point 2s (output of the vaneless zone). However, since the properties at point 2 (first convergence) have been recalculated, it is necessary to recalculate point 2 by accounting for the total quantities, since it is dependent on the previous one according to the equations:

$$h_{2t} = h_2 + \frac{c_2^2}{2}$$

$$p_{2t} = f[p](s_2, h_{2t})$$

It will now be possible to calculate the pressure situation at the inlet point to the vaned zone (and outlet of the vaneless zone) of the stator, using the loss coefficient calculated above:

$$p_{2s,t} = p_{2t} - Y_{\text{vaneless}} \cdot (p_{2t} - p_2)$$

And likewise, knowing this pressure situation, it can be related to the pressure at point 3, applying the loss coefficient for the zone with vanes:

$$p_{3t} = p_{2s,t} - Y_{\text{vaned}} \cdot (p_{2s,t} - p_2)$$

In addition, there is the relationship already presented in the Thermodynamic Calculations section:

$$h_{2t} = h_{3t}$$

This allows [B] Coolprop to be used to determine the thermodynamic conditions at the outlet of the machine following the loss dependent method:

$$s_3 = f[s](p_{3t}, h_{3t})$$

$$h_3 = f[h](s_3, p_3)$$

The explanation of the model is therefore completed for the turbomachine part once the iteration is performed on the input isentropic efficiency, which must coincide with the isentropic efficiency calculated from the losses:

$$\eta_{is} = \frac{h_{3is} - h_1}{h_3 - h_1}$$

In addition, the total to total yield, which relates the isentropic enthalpy jump by counting the total quantities at inlet and outlet to the enthalpy jump under similar conditions; and the total to static yield, which relates the isentropic enthalpy jump from point 1 by counting the total quantities up to point 3 and the enthalpy jump between inlet and outlet by counting the total quantities at both points, can be known. Their calculation equations are as follows, respectively:

$$\eta_{TT} = \frac{h_{3t,is} - h_{1t}}{h_{3t} - h_{1t}}$$

$$\eta_{TS} = \frac{h_{3is} - h_{1t}}{h_{3t} - h_{1t}}$$

It is important to mention that in addition to the two convergence conditions in the yields there are two others that have already been mentioned in their sections (β_{2B} in the section on geometric parameters and f_{sf} which, although it was not described, requires iteration for the resolution in Excel of the system of complex equations). This assumes that the iteration process is performed sequentially until the convergence of the four values is reached, following an order similar to the explanation given in this chapter.

Coupling to the Engine Model

The model for the combustion engine was explained in its own chapter, entitled Engine Model.

In this section the adaptation with the model developed for the turbomachine is explained.

The objective will be to know the values of power, torque and fuel mass flow, as well as other less relevant results, for the engine speed at the design point. And to make a simplified approximation for other engine revolutions.

As mentioned in the chapter describing the Engine Model, for a given engine, given the parameters that describe its geometry and operation, the variables that will modify the results will be the engine speed and the mass flow of comburent and fuel in it. Since the mixture is an approximately fixed value under ideal conditions, the comburent and fuel will always have a linear mass ratio in the model.

Thus, the coupling of both models will be done through two variables: engine revolutions and air mass flow rate.

For the design point, the model results are immediate, since the engine speed (4000 RPM) and the mass air flow rate are known.

In order to know the approximate effect of the designed assembly over the entire engine speed range, it was decided to make a simplification of the previous model in which the mass flow rate would be calculated for the engine speed from 1000 RPM to 6000 RPM in 1000 RPM steps.

Therefore, the air mass flow rate for revolutions other than those imposed for the design point involves recalculating certain kinematic and thermodynamic parameters at these points directly. And then insert values for the densities at points 2 and 3 that will be iterated until the model converges in terms of enthalpy and pressure. Keeping the performance of the machine fixed at all times, which is not noticeably different in practice.

The simplification implies that certain losses are not conceived in the model, and is justified because it would increase the complexity enormously and performing tests for different input parameters obtaining different geometries would require powerful hardware for model execution.

The optimization of the model to improve the execution would allow the addition of these losses to increase the veracity of the tool and is pending for future projects prior to the "go-life" and the fabrication of the first prototype.

Model Simulations

The final tool composed by the coupling of the turbomachine model and the engine model will allow, as just mentioned, to solve the geometry of the compressor and also to extract the theoretical data expected for the engine once the assembly is put into operation.

So far, all the necessary equations have been formulated so that the model can be run for some input parameters for the centrifugal compressor. The next evolution made on this level of operation is to allow the model to vary these input parameters to find different solutions.

The literature cited offers certain ranges of values between which the optimum must be found. Taking into account these and developing others of our own, the following input parameter iteration system has been built to find the most suitable solution for the case study. It is recalled that the developed model differs from the methodology slightly as far as input parameters are concerned.

The working coefficient according to the literature should be between 0,5 and 0,6. From observation of the model results, it was quickly determined that the range of values that maximized the efficiency of the machine was at the upper limit of the proposed range. For this reason it was decided that the new range would be from 0,58 to 0,6 with incremental jumps of 0,01.

Similarly, the flow coefficient is recommended to be in the range of values between 0,2 and 0,3. The correction in this case, for the same reason, was made so that the value would increase in each iteration by 0,01 between 0,28 and 0,3.

The same applies to the degree of reaction, which according to the documentation was to be between 0,6 and 0,7. It was observed that the best solutions were in the upper range, between 0,68 and 0,7. This correction was imposed, and the incremental jump was determined to be 0,1 as in the previous cases.

The rotor hub diameter ratio is suggested to be between 0,01 and 0,11. A more accurate correction that eliminates non-optimal solutions is to correct this range and restrict the value to values greater than 0,09 and less than 0,11. Again, the incremental jump for each iteration is 0,1.

The input angle to the rotor was decided to remain fixed and equal to 0. This makes sense if maximum efficiency is to be sought at the design point, as is the case. This eliminates incidence losses in this regime.

And finally, the input added by the author to the method is the ratio of revolutions between the turbomachine and the vehicle engine. The range of iteration values for this parameter was narrowed following the recommendations offered for the design of automotive turbochargers. Knowing that the maximum engine revolutions are 6000 RPM, it was decided to limit it to between 10 and 20. This guarantees that the machine revolutions do not exceed 120000 RPM, which are considered extreme speeds for this type of machine. After reviewing the first results, as was done with the ranges for the previous input parameters, it was decided to narrow the range to between 14 and 18,5. With an incremental output of 1,5.

Decreasing the amplitude of the ranges allows maintaining an acceptable level of sharpness in terms of the incremental jumps of the ranges while increasing the speed of model execution.

Results

Selection and Design Results

The model, once finalized and debugged, was run by imposing reasonable boundary conditions which are explained below.

The atmospheric pressure of the air at the machine inlet was decided to be 0.95 bar. This is lower than the standard atmospheric pressure (1 bar), but is justified by the depression situation usually found between the air filter and the actual intake of the engine.

It was decided to use the air temperature of 25°C as an intermediate point between the maximum and minimum temperatures at which the vehicle is expected to operate normally, which are 40 °C and 10°C.

As already mentioned, the revolutions at the design point were chosen to be 4000 RPM, which is expected to be the maximum power and torque operating speed for the vehicle if these are maintained over a long period of time. Exceeding this RPM on a permanent basis poses a danger to the integrity of the engine.

Although not initially presented as input parameters, stator and rotor roughness were introduced as input during the explanation of the loss values in the previous chapter. It was decided that these should have a value of 5 µm. With this value one can be sure that the maximum admissible values are not exceeded and it is also a value achievable by the proposed manufacturing methods, which will be detailed later.

Finally, with the objective of not exceeding 200 HP in any case, after several simulations it was decided that the target power at the motor inlet would be 1,33 bar. This value guarantees that in no case will a power or torque with the potential to break the engine elements be reached, since there are on the market, as explained at the beginning of the project, models with a similar engine block that reach power levels slightly higher than the one just discussed.

With these boundary conditions and the iteration ranges of the input parameters defined, the model was run, obtaining 220 solutions.

Among all of them, those solutions that obtained a higher isentropic efficiency were chosen as valid. This efficiency measures the ease with which the machine transforms the power extracted from the motor shaft into energy provided for the optimum phase change of the fluid. In addition, among these solutions with a similar isentropic efficiency value, the one with the lowest compressor shaft speed was selected in order to safeguard the integrity of the unit.

The most relevant results of the selected solution are presented below.

The boundary conditions are:

Inlet Pressure	P1	0,95	bar
Inlet Temperature	T1	25	°C
Outlet Pressure	P3	1,33	bar
Engine Speed	n'	4000	RPM
Rotor selected roughness	KR	5	µm
Stator selected roughness	KS	5	µm

The input parameters that give the selected solution are:

Rotor / Engine Speed	RES	15,5	-
Work coefficient	ψ	0,59	-
Flow coefficient	ϕ	0,29	-
Degree of reaction	R	0,68	-
Rotor hub diameter ratio	δh	0,09	-
Inlet flow angle	$\alpha 1$	0	°

The efficiencies obtained are:

Isentropic efficiency	η_{is}	0,909	%
Rotor efficiency	η_R	0,875	%
Total to total efficiency	η_{TT}	0,908	%
Total to static efficiency	η_{TS}	0,838	%

The geometrical parameters that allow the part to be designed are:

Rotor inlet inner diameter	D1h	0,007	m
Rotor inlet outer diameter	D1t	0,036	m
Rotor outlet diameter	D2	0,073	m
Vaned diffuser stator inlet diameter	D2s	0,078	m
Outlet diameter	D3	0,118	m
Rotor axial length	La	0,027	m
Equivalent semi-axes a	a	0,026	m
Equivalent semi-axes b	b	0,026	m
Stator meridional length	Lmvaned	0,020	m
Rotor inlet width	b1	0,015	m
Rotor outlet width	b2	0,003	m
Vaned diffuser stator inlet width	b2s	0,003	m
Outlet width	b3	0,003	m
Rotor inlet relative angle	$\beta 1$	59	°
Rotor outlet relative angle	$\beta 2B$	65	°
Vaned diffuser stator inlet absolute angle	$\alpha 2s$	72	°
Stator outlet absolute angle	$\alpha 3$	48	°
Number of blades	NBR	27	-
Vaned diffuser number of blades	NBS	26	-
Blade thickness	tb	0,001	m
Clearances a	τa	0,0003	m
Clearances r	τr	0,0003	m
Clearances b	τb	0,0003	m

The parameters that allow the modeling of the vehicle's engine are:

Compression ratio	CR _{cyl}	10,6	-
Cylinder diameter	D _{cyl}	0,077	m
Cylinder stroke	S _{cyl}	0,086	m
Number of cylinders	N _{cyl}	4,000	m
95-octane gasoline specific energy	E95	46000	KJ/Kg
Air fuel ratio	AF _r	14,700	-
Volumetric efficiency	η_V	100	%
Indicated/Thermodynamic efficiency	η_l	40	%

The overall efficiency obtained in the engine is:

Global efficiency	η_G	34,6	%
-------------------	----------	------	---

And the power and torque values obtained at the design point are:

Brake Power	HP	109,591	HP
Torque	T	192,559	Nm

And the other two parameters of interest extracted from the engine part of the model:

Specific fuel consumption	SFC	0,226	Kg/KWh
Break mean effective pressure	BMEP	15,141	bar

For 1000 RPM, the model approximation provides the following parameters of interest:

Stator outlet pressure [for 1000 RPM]	p ₃	0,970	bar
Global efficiency [for 1000 RPM]	η_G	36,7	%
Brake Power [for 1000 RPM]	HP	23,397	HP
Torque [for 1000 RPM]	T	164,444	Nm
Specific fuel consumption [for 1000 RPM]	SFC	0,213	Kg/KWh
Break mean effective pressure [for 1000 RPM]	BMEP	12,930	bar
Rotor inlet angle [for 1000 RPM]	α_1	22,239	°

For 2000 RPM, the model approximation provides the following parameters of interest:

Stator outlet pressure [for 2000 RPM]	p ₃	1,032	bar
Global efficiency [for 2000 RPM]	η_G	36,0	%
Brake Power [for 2000 RPM]	HP	47,949	HP
Torque [for 2000 RPM]	T	168,501	Nm
Specific fuel consumption [for 2000 RPM]	SFC	0,217	Kg/KWh
Break mean effective pressure [for 2000 RPM]	BMEP	13,249	bar
Rotor inlet angle [for 2000 RPM]	α_1	17,776	°

For 3000 RPM, the model approximation provides the following parameters of interest:

Stator outlet pressure [for 3000 RPM]	p3	1,145	bar
Global efficiency [for 3000 RPM]	η_G	35,3	%
Brake Power [for 3000 RPM]	HP	75,669	HP
Torque [for 3000 RPM]	T	177,275	Nm
Specific fuel consumption [for 3000 RPM]	SFC	0,222	Kg/KWh
Break mean effective pressure [for 3000 RPM]	BMEP	13,939	bar
Rotor inlet angle [for 3000 RPM]	α_1	10,313	°

For 4000 RPM, the model approximation provides the following parameters of interest:

Stator outlet pressure [for 4000 RPM]	p3	1,327	bar
Global efficiency [for 4000 RPM]	η_G	34,6	%
Brake Power [for 4000 RPM]	HP	109,568	HP
Torque [for 4000 RPM]	T	192,517	Nm
Specific fuel consumption [for 4000 RPM]	SFC	0,226	Kg/KWh
Break mean effective pressure [for 4000 RPM]	BMEP	15,138	bar
Rotor inlet angle [for 4000 RPM]	α_1	0,018	°

For 5000 RPM, the model approximation provides the following parameters of interest:

Stator outlet pressure [for 5000 RPM]	p3	1,630	bar
Global efficiency [for 5000 RPM]	η_G	34,1	%
Brake Power [for 5000 RPM]	HP	155,787	HP
Torque [for 5000 RPM]	T	218,982	Nm
Specific fuel consumption [for 5000 RPM]	SFC	0,229	Kg/KWh
Break mean effective pressure [for 5000 RPM]	BMEP	17,219	bar
Rotor inlet angle [for 5000 RPM]	α_1	-12,637	°

For 6000 RPM, the model approximation provides the following parameters of interest:

Stator outlet pressure [for 6000 RPM]	p3	2,267	bar
Global efficiency [for 6000 RPM]	η_G	34,2	%
Brake Power [for 6000 RPM]	HP	236,191	HP
Torque [for 6000 RPM]	T	276,669	Nm
Specific fuel consumption [for 6000 RPM]	SFC	0,229	Kg/KWh
Break mean effective pressure [for 6000 RPM]	BMEP	21,755	bar
Rotor inlet angle [for 6000 RPM]	α_1	-27,751	°

The rest of the discarded solutions can be found in the .xslm file attached to this document.

This excel file with macros contains all the functional model that can be executed autonomously according to the instructions in one of its sheets.

Middle Results

The results so far presented are: boundary conditions, input parameters, geometrical results and motor performance results for the selected solution.

In addition to these, there are intermediate results, as shown in the chapter explaining the theoretical model, that can add value to this paper.

First, we will be able to plot the thermodynamic cycle of the machine on the enthalpy and entropy axes. This is done thanks to the calculation of the thermodynamic states of all the points of the machine, and can be seen below:

Point	Enthalpy - h [J/Kg]	Entropy - s [J/(Kg·K)]	pressure [bar]
1	424450,558	3899,03407	0,950
1t	426720,741	3899,03407	0,975
1tr	431355,130	3899,03407	1,029
2is	444906,295	3899,03407	1,197
2	446428,951	3903,80317	1,197
2tr	453714,591	3903,80317	1,295
2tris	453714,591	3899,03407	1,317
3is	454670,211	3899,03407	1,330
3is'	456239,301	3903,80317	1,330
3	456303,302	3903,99722	1,330
2t	458573,484	3903,80317	1,363
3t	458573,484	3903,99722	1,362

With this table, it is possible to represent the graph of the thermodynamic cycle, as shown in *Figure 12* below:

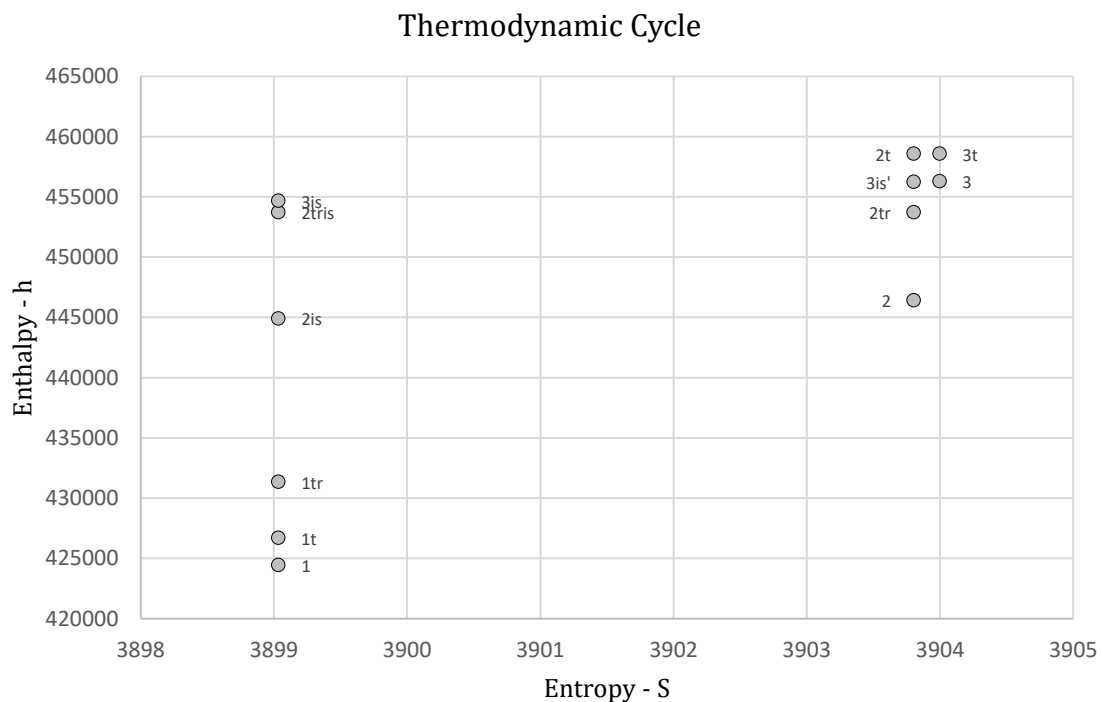


Figure 12: Thermodynamic Cycle of the Selected Solution

Similarly, the complete kinematic results for the selected solution can be found below.

At the rotor inlet:

Rotor inlet Blade speed [m/s]	u1	96,274
Rotor inlet relative meridional velocity [m/s]	w1u	96,274
Rotor inlet relative velocity [m/s]	w1	117,512
Rotor inlet absolute meridional velocity [m/s]	c1m	67,382
Rotor inlet absolute tangential velocity [m/s]	c1u	0,000
Rotor inlet absolute velocity [m/s]	c1	67,382

At the rotor outlet, which is the same to the vaneless stator inlet:

Rotor outlet Blade speed [m/s]	u2	232,353
Rotor outlet relative meridional velocity [m/s]	w2u	95,265
Rotor outlet relative velocity [m/s]	w2	120,712
Rotor outlet absolute meridional velocity [m/s]	c2m	74,135
Rotor outlet absolute tangential velocity [m/s]	c2u	137,088
Rotor outlet absolute velocity [m/s]	c2	155,849

Then, at the zone of transition from the vaneless stator to the vaned stator:

Vaned stator inlet absolute meridional velocity [m/s]	c2sm	41,919
Vaned stator inlet absolute tangential velocity [m/s]	c2su	129,013
Vaned stator inlet absolute velocity [m/s]	c2s	135,653

And finally, at the stator outlet

Vaned stator outlet absolute meridional velocity [m/s]	c3m	43,278
Vaned stator outlet absolute tangential velocity [m/s]	c3u	51,646
Vaned stator outlet absolute velocity [m/s]	c3	67,382

And with these values, it is easy to plot the velocity triangles at the points of interest. Figure 13 below shows the kinematic situation of the selected solution:

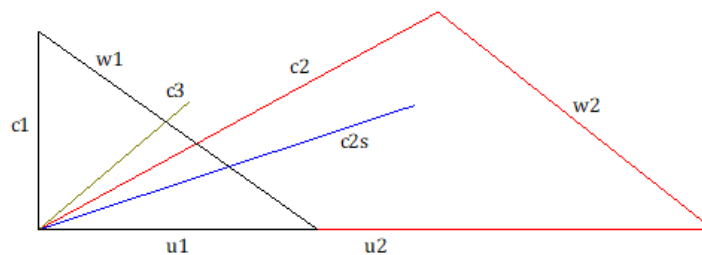


Figure 13: Triangles of Velocities of the Selected Solution

Design

The selected solution allows to know the geometric parameters necessary to determine the design of the parts of interest, which are the rotor and the stator of the turbomachine.

Once these geometries are designed, the rest of the parts that make up the assembly will be designed. The latter will have a lower level of detail and have been designed tentatively, which implies that there is a potential for improvement.

This chapter will explain and illustrate the design process of the parts and will have the following structure:

1. Impeller (Rotor)
2. Case (Stator)
3. Volute
4. Cover
5. Gearbox (Planetary system)
6. Connecting Elements
 - a. Bearings
 - b. Gaskets
 - c. Fastening hardware (screws and snap-fits)

As mentioned at the beginning of this document, the software used for the design process is [C] Solid Edge from Siemens. Thanks to this software, all geometries can be designed, no matter how complex they are, presenting great advantages over simpler tools.

It should be remembered that the geometries of the different parts are related following the order shown. An example of this would be to vary the height of the impeller, which would imply the automatic and consequent modification of the height of the volute and the length of the axis of revolution. This allows the same design model to be used for different input values, making the design process agile in the event of a change in any of the dimensional parameters.

The final geometries of these parts that make up the assembly in the order just described are described below. This is an illustrative presentation, since the detailed drawings can be found in Annex II of this document.

Impeller Design

From the geometrical parameters presented in the previous chapter, those that define the rotor geometry are:

Rotor inlet inner diameter	D1h	0,007	m
Rotor inlet outer diameter	D1t	0,036	m
Rotor outlet diameter	D2	0,073	m
Rotor axial length	La	0,027	m
Rotor inlet width	b1	0,015	m
Rotor outlet width	b2	0,003	m
Rotor inlet relative angle	β_1	59	°
Rotor outlet relative angle	β_{2B}	65	°
Number of blades	NBR	27→18	-
Blade thickness	tb	0,001	m

The geometry of the part once designed can be seen in *Figure 14* below:

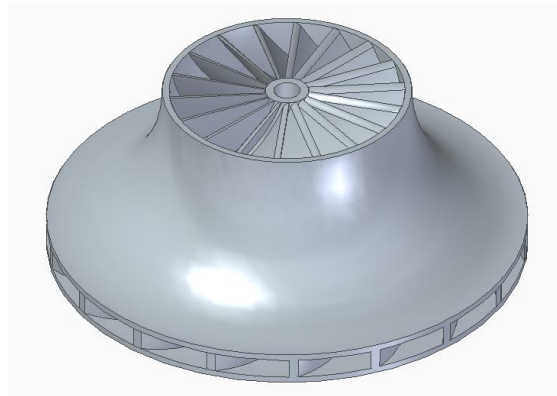


Figure 14: Impeller (1)

It was decided to reduce the number of blades, since the theoretical number seems very high compared to other solutions seen in the market. Although it improves the fluid guidance, it significantly increases the incidence losses, and since this is one of the parameters with greater freedom within the design theory, it was decided to modify it by taking it to its lower limit. The final number of blades in the rotor will therefore be 18.

The arrangement of these blades can be seen more clearly in *Figure 15* below:

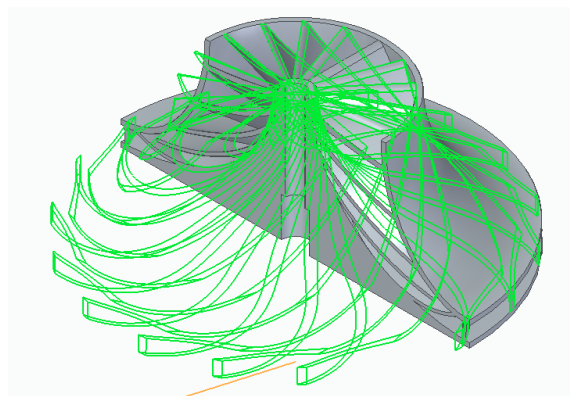


Figure 15: Impeller (2)

Case Design

This part has a double function, one of its faces serves as the stator and lower seal with the rotor, while the lower face will be responsible for containing the planetary gear system that connects the engine revolutions with the turbomachine.

The parameters that define the stator geometry are the following:

Vaneless stator inlet diameter	D2	0,073	m
Vaneless stator outlet / Vaned stator inlet diameter	D2S	0,078	m
Vaned stator outlet diameter	D3	0,118	m
Vaneless stator inlet width	b2	0,003	m
Vaneless stator outlet / Vaned stator inlet width	b2s	0,003	m
Vaned stator outlet width	b3	0,003	m
Vaned stator inlet angle	β_{2s}	72	°
Vaned stator outlet angle	β_3	48	°
Number of blades	NBS	26→18	-
Blade thickness	tb	0,001	m

The following *Figure 16* shows the face that makes contact with the fluid and forms the geometry of the stator:

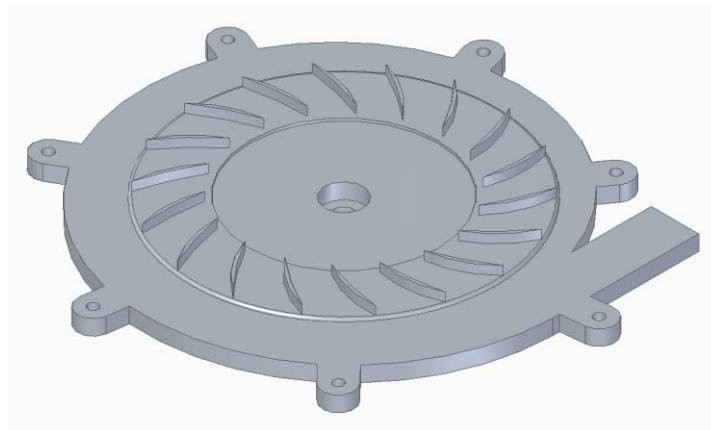


Figure 16: Case (1)

And in the following *Figure 17*, the face that will be part of the gearbox can be seen in detail:

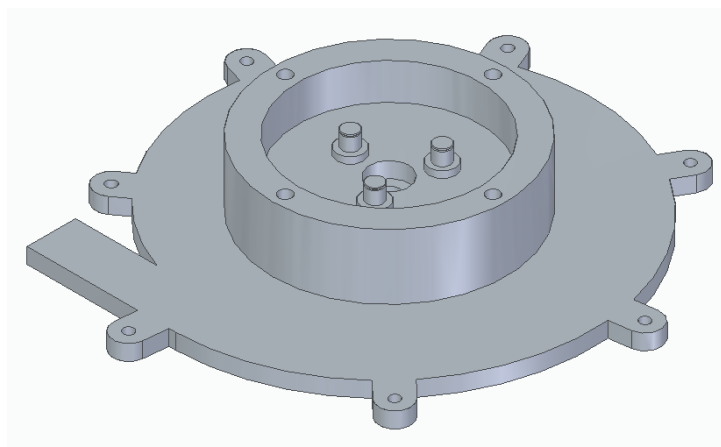


Figure 17: Case (2)

Volute

The volute was designed using the extrusion method with variable areas at 4 points in different planes. Each of these 4 areas was dimensioned taking into account the volumetric flow that the machine has at its point 3. Therefore, these areas increase their surface in a proportional way to the increase of flow per degree of rotation. The result can be seen in the following *Figure 18* and *Figure 19*:

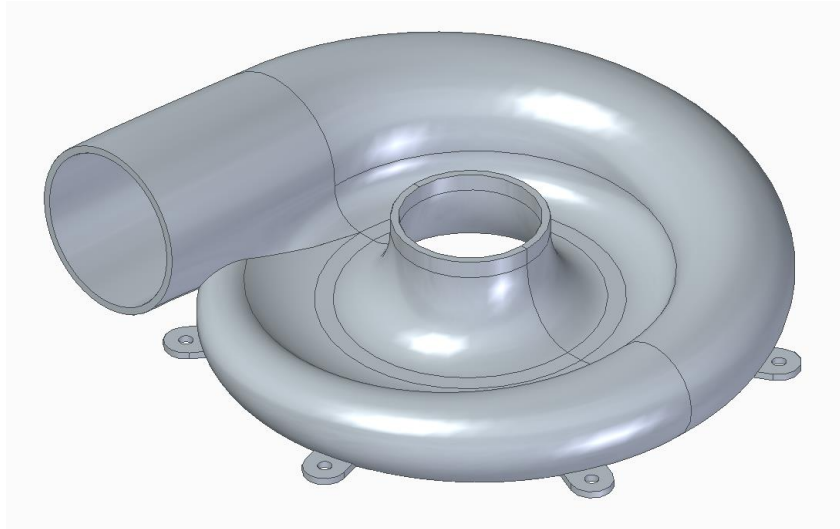


Figure 18: Volute (1)



Figure 19: Volute (2)

Cover

This part serves as a cover for the planetary gear system. In the following *Figure 20* you can see the design made:

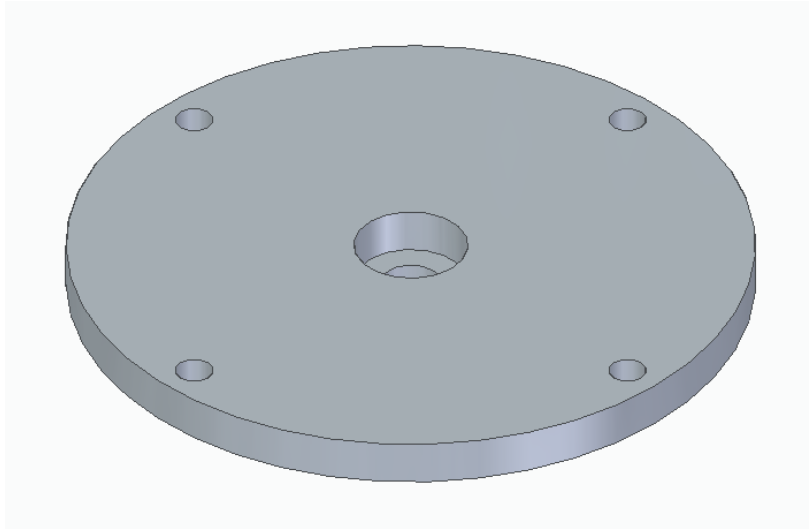


Figure 20: Cover (1)

This will be the face that will make the seal of the gearbox, while the outer face can be seen in the following *Figure 21*:

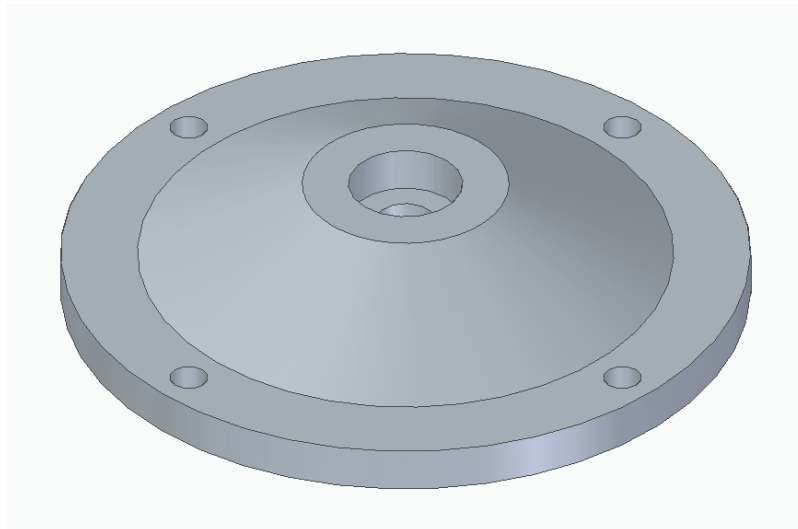


Figure 21: Cover (2)

Gearbox

The planetary system consists of 3 types of gears that must comply with the transmission ratio imposed by the model.

Although, the ratio may differ slightly, since the diameter chosen for the pulley will ultimately allow the ratio to be adjusted. This is why it was decided to establish a ratio that would facilitate the design, which is 10.

It is important to mention that the transmission ratio must be established between the largest and smallest gears, being the intermediate ones not relevant to conform the ratio. The latter will serve to transmit the rotation and must be adapted to the geometries of the former.

The parameters defining the gear design are shown below.

They were tentatively calculated following two main objectives:

1. That the dimensions were in accordance with the dimensions of the parts designed through the model.
2. To withstand dynamic and mechanical stresses oversized a priori.

Gear Parameters:

	Pinion to Gear	Mid-Gear to Gear
Desired Gear Ratio	5	2
(a) Pressure Angle	20,00 °	20,00 °
Module	0,50 mm	0,50 mm
(r) Root Fillet	0,10 mm	0,10 mm
Gear Accuracy	1	1
Total Unit Correction	0	0
Roughness Factor	1	1
Application Factor	1,2	1,2
Pinion Mounting Constant	0,8	0,8

Calculations:

	Pinion	Mid-Gear	Gear
No. of Teeth	20	40	100
(DM) Mounting Hole Diameter	-	-	-
(b) Face Width	8,00 mm	8,00 mm	8,00 mm
Power	6000,000 W	6000,000 W	6000,000 W
Speed	33480000 deg/s	16740000 deg/s	6696000 deg/s
Efficiency	0,92		
Size Factor for Contact	1	1	1
Size Factor for Bending	1	1	1

The design of the gears was carried out thanks to the tool for the design of standardized parts found in [C] Solid Edge. The parameters that have been presented allow us to extract the geometries of the parts directly.

In the following *Figure 22* and *Figure 23* can be seen, respectively, the set formed by the largest gear (Gear) and the smallest one (Pinion) in charge of keeping the speed ratio; and the set formed by all the gears. Both are shown in the primary form, as they are extracted from the software without modifications:

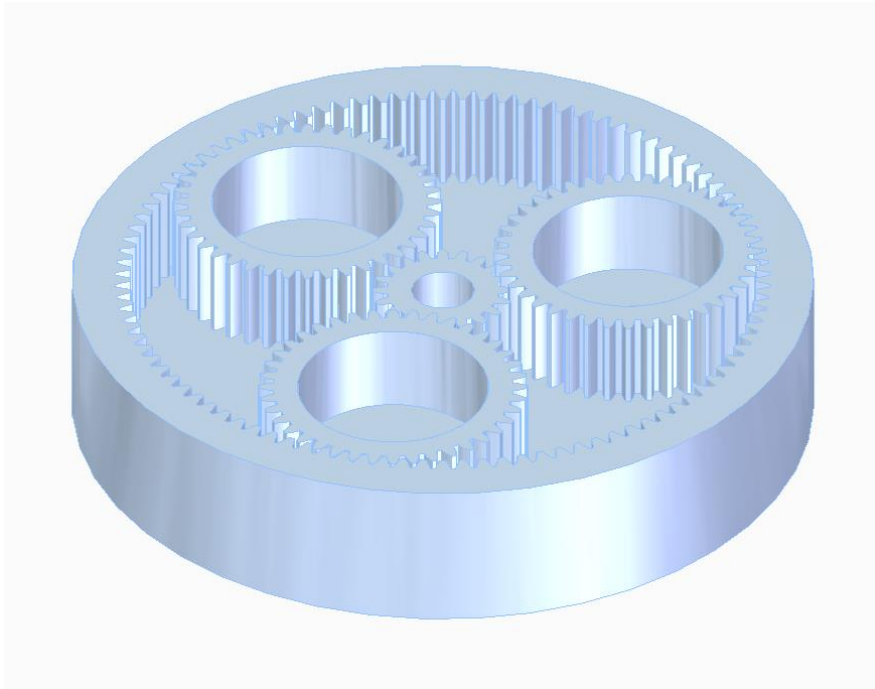


Figure 22: Gearbox (1)

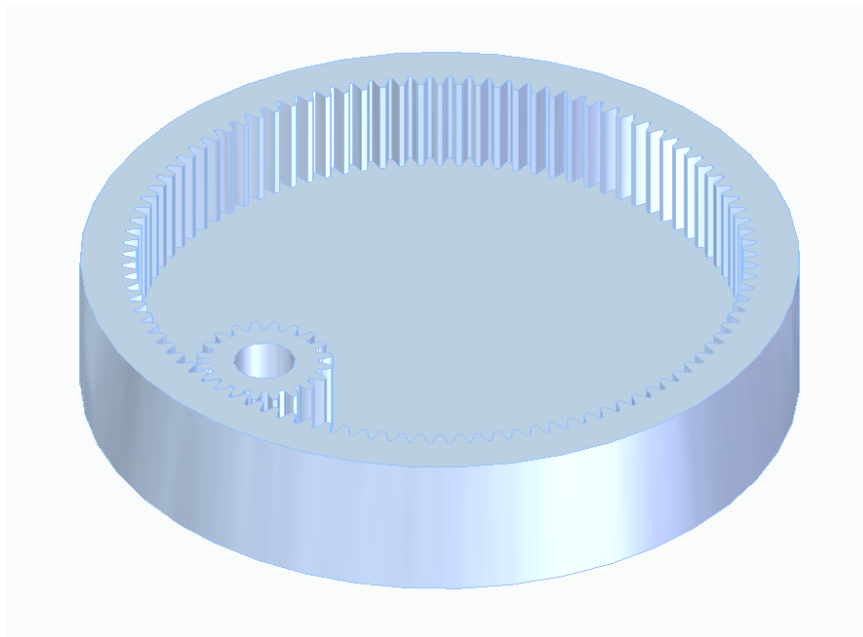


Figure 23: Gearbox (2)

It was decided to make the geometry of these parts more complex in order to fulfill different functions. The pinion was combined with the shaft of the turbomachine to form a single part capable of driving the impeller and fixing it to the shaft. The intermediate gear was modified so that it could be fixed axially to the 3 rotation shafts arranged in the case, taking into account the need to mount bearings on it. Finally, the largest part, as with the pinion, was modified to have a solid shaft capable of transmitting the rotation and being fixed to the traction pulley.

The following *Figure 24* shows the assembly after the above-mentioned modifications:

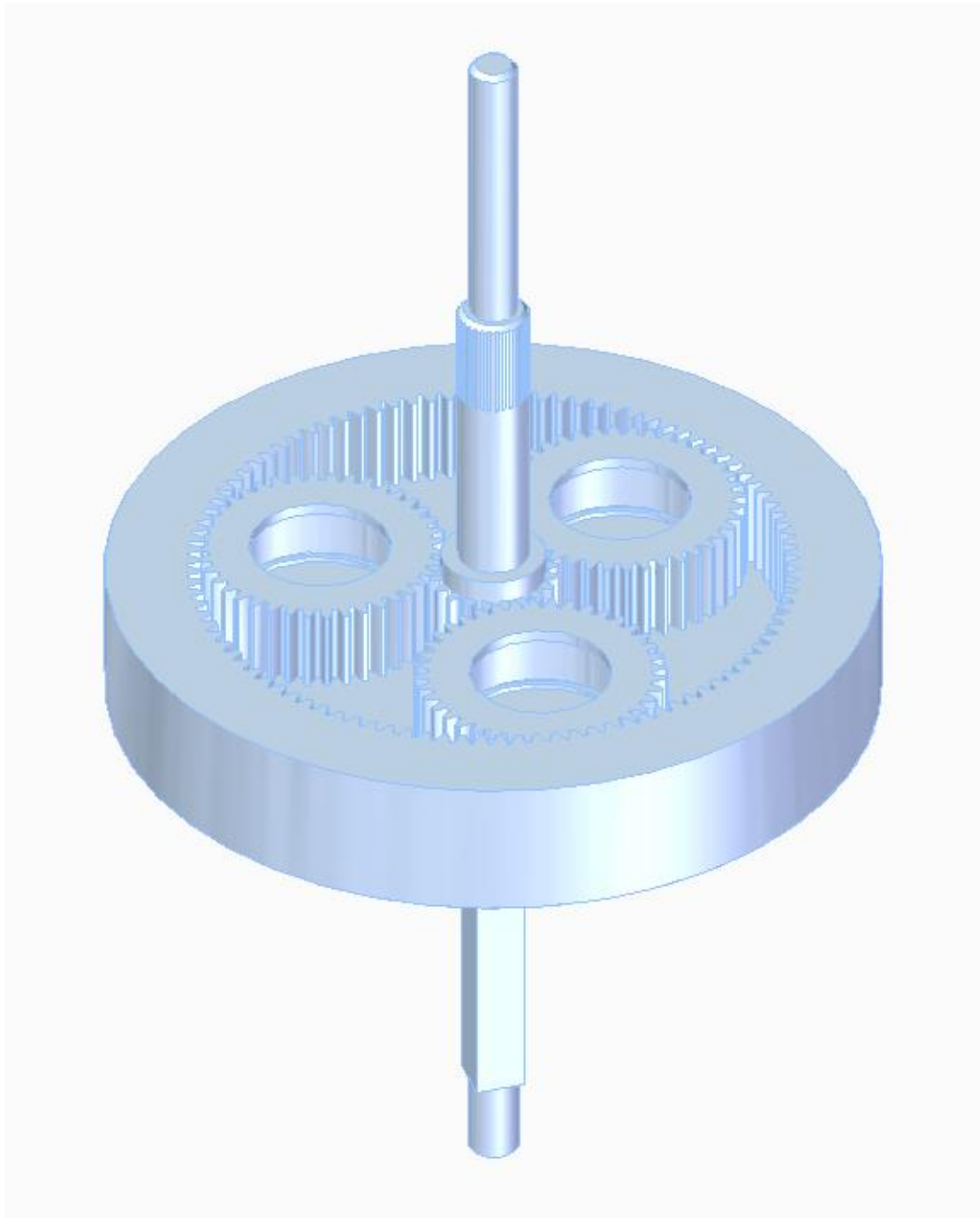


Figure 24: Gearbox (3)

Connecting Elements

Bearings:

This part is replicating a standardized one, and was designed using its code: 15X6X5 mm



Figure 25: Bearing

Gaskets:

The following pair of gaskets were designed to cover 2 main functions:

1. To compensate the manufacturing deviations, since in the event of a significant deviation, these are cheap parts that are easy to manufacture and would allow adjusting the parts depending on whether play or tightening is required.
2. To avoid friction between parts that are fixed and parts that rotate when the machine is in operation, especially when these are mounted on bearings.

In the following *Figure 26* and *Figure 27* the mentioned parts can be observed, being the first one the one that mounts between the inner diameter of the bearing and the shaft, and the second one the one that mounts between the outer diameter of the bearing and the bore:

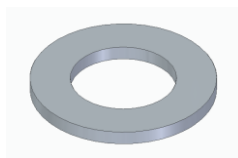


Figure 26: Inner Gasket

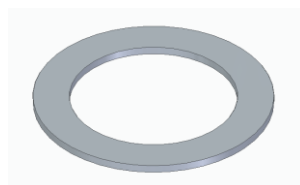


Figure 27: Outer Gasket

Fastening hardware:

Next, all the pieces that are used as a union to attach the rest of the pieces of the assembly are shown.

In *Figure 28* below, the screw used to fix the cover to the case (where the threaded hole for it is located) can be seen.

Also, in *Figure 29*, it is possible to see the snap-fit that joins the Volute to the Case. This type of joints are trending now a days. They are inexpensive, quick to assemble and easy to replace while keeping the joint secure.

The joints employed to fix the elements to the bearing in the axial direction can be seen in *Figure 30* and *Figure 31*. They are called snap-rings and can be inner or outer ones.

Finally, in *Figure 32*, the nut that secures the impeller to the pinion shaft can be seen.

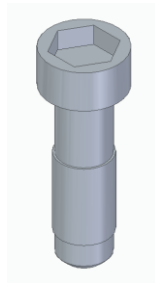


Figure 28: Case Screw

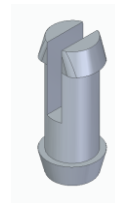


Figure 29: Volute Snap-fit



Figure 30: Outer Snap-ring

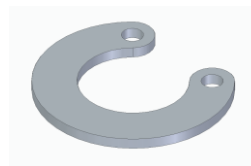


Figure 31: Inner Snap-Ring



Figure 32: Impeller Nut

Assembly

In this final section of the chapter dedicated to explain the design of the parts, the images of the final assembly and the corresponding parts list are presented.

First, as can be seen in *Figure 33* below, the plan of the exploded assembly is shown:

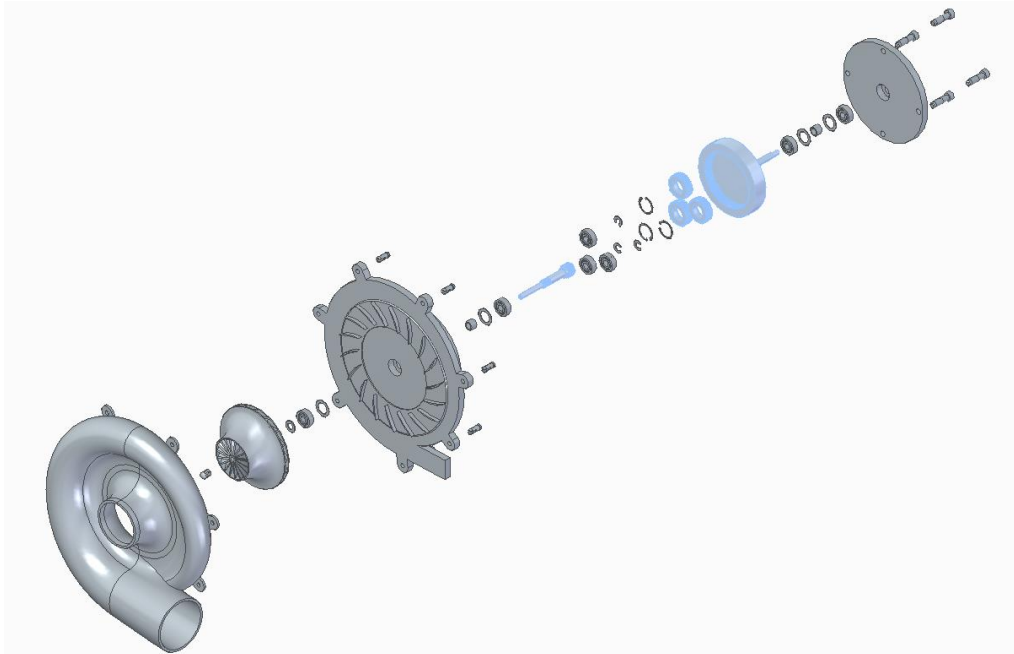


Figure 33: Compressor Assembly (1)

The list of parts required for the manufacture and assembly of the compressor is as follows. This list shows the type of materials proposed for the manufacture of each part when it is not considered standard:

#	Part Name	Q.	Drawing	Nature	Proposed Material
1	Impeller	1	1.10.20	original design	Aluminum or Titanium
2	Case	1	1.10.30	original design	Aluminum or Steel
3	Volute	1	1.10.40	original design	Aluminum, Plastic or Resin
4	Cover	1	1.10.50	original design	Aluminum or Steel
5	Gear	1	1.10.60	original design	Steel
6	Midgear	3	1.10.70	original design	Steel
7	Pinion	1	1.10.80	original design	Steel
8	Bearing	7	-	standard part	-
9	Inner gasket	1	-	standard part	-
10	Outer gasket	4	-	standard part	-
11	Spacer	2	-	standard part	-
12	Case screw	4	-	standard part	-
13	Snap-fit	7	-	standard part	-
14	Outer snap-ring	3	-	standard part	-
15	Inner snap-ring	4	-	standard part	-
16	Impeller nut	1	-	standard part	-

The numbers are referred to the Assembly Drawing (1.10.10) attached in Annex II.

Figure 34 below shows the assembled and mounted unit with a frontal plane cut that shows the location of all the components:

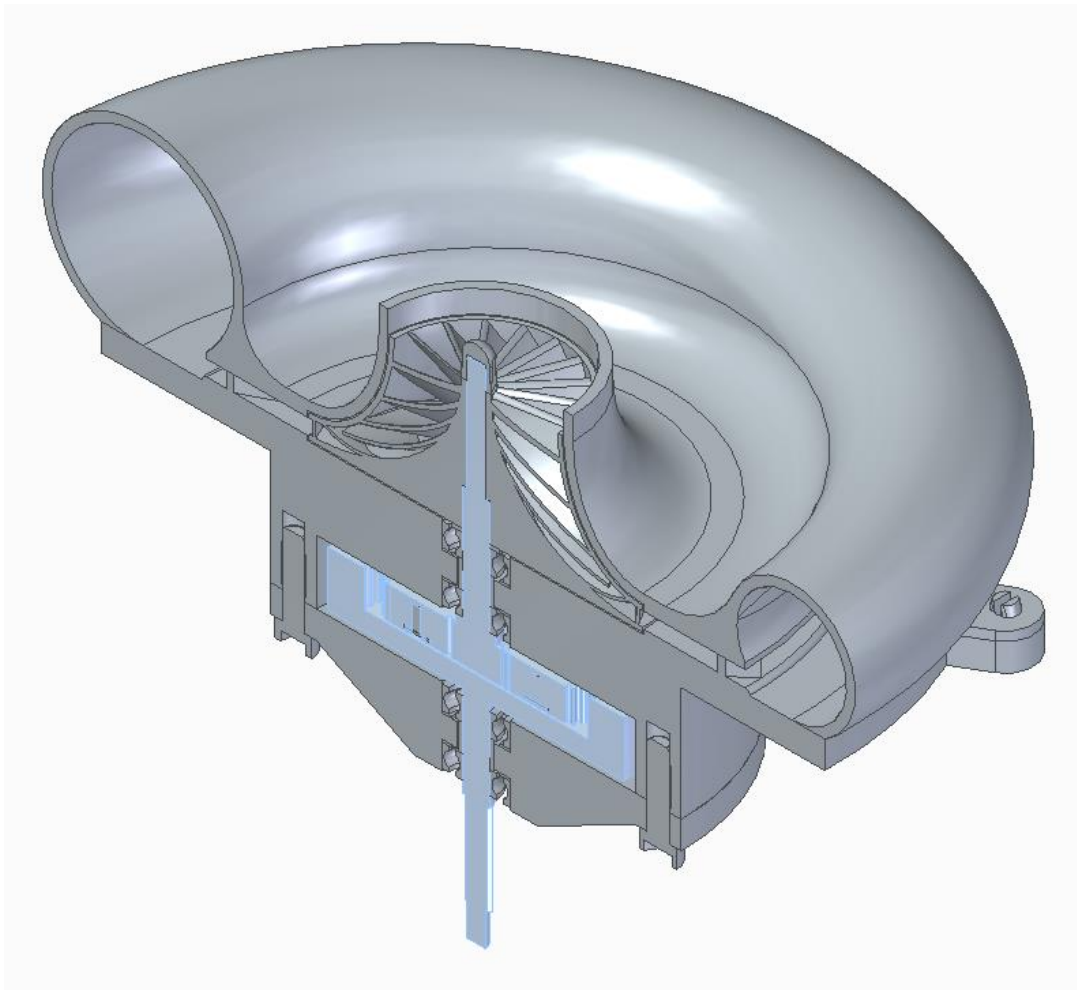


Figure 34: Compressor Assembly (2)

Economic Feasibility

This exercise will be of little precision, but may serve as a first approach to the real cost of prototype development.

First of all, as has been repeatedly mentioned, the fabrication of certain components will be done by additive technologies. Some other parts will be manufactured by material removal/abrasive methods. And others will be available on the market as standardized common parts.

In this way, it is intended to list each part with a cost range in order to subsequently account for the total manufacturing cost of a unit (as a minimum valid product).

#	Part Name	Q.	Manufacturing Method	Cost	
				Lower Bound	Upper Bound
1	Impeller	1	Additive (metals)	50 €/h x 5 h = 250 €	100 €/h x 10 h = 1000 €
2	Case	1	CNC (aluminum)	20€/h x 3h = 60 €	30€/h x 4h = 120 €
3	Volute	1	Additive (resins)	5 €/h x 10 h = 50 €	7 €/h x 15 h = 105 €
4	Cover	1	CNC (aluminum)	20€/h x 1h = 20 €	30€/h x 2h = 60 €
5	Gear	1	CNC (steel)	25€/h x 2h = 50 €	35€/h x 3h = 105 €
6	Midgear	3	CNC (steel)	25€/h x 1h = 25 €	35€/h x 2h = 70 €
7	Pinion	1	CNC (steel)	25€/h x 2h = 50 €	35€/h x 3h = 105 €
8	Bearing	7	Market	1,00 €	2,00 €
9	Inner gasket	1	Market	0,25 €	0,50 €
10	Outer gasket	4	Market	0,25 €	0,50 €
11	Spacer	2	Market	0,25 €	0,50 €
12	Case screw	4	Market	0,50 €	1,00 €
13	Snap-fit	7	Market	0,25 €	0,50 €
14	Outer snap-ring	3	Market	0,75 €	1,50 €
15	Inner snap-ring	4	Market	0,75 €	1,50 €
16	Impeller nut	1	Market	0,50 €	1,00 €

Although these costs have been deducted through experience and observation in the market, they are considered valid to obtain a first accumulation of the total price. It has been decided to make the approximation by hours (including all the costs included because of the use of market comparison examples).

Therefore, the lower limit, according to the above values is:

$$250€ + 60€ + 50€ + 20€ + 50€ + 3 \cdot 25€ + 50€ + 7 \cdot 1€ + 0,25€ + 4 \cdot 0,25€ + \\ + 2 \cdot 0,25€ + 4 \cdot 0,50€ + 7 \cdot 0,25€ + 3 \cdot 0,75€ + 4 \cdot 0,75€ + 0,50€ = \mathbf{573,25€}$$

And the upper bound would be:

$$1000€ + 120€ + 105€ + 60€ + 105€ + 3 \cdot 70€ + 105€ + 7 \cdot 2€ + 0,50€ + 4 \cdot 0,50€ + \\ + 2 \cdot 0,50€ + 4 \cdot 1,00€ + 7 \cdot 0,50€ + 3 \cdot 1,50€ + 4 \cdot 1,50€ + 1,50€ = \mathbf{1742,00€}$$

These economic limits constitute the first approximation of costs associated with the manufacturing of the project and are considered valid to evaluate the development of future projects in relation to this one.

Conclusions

The document ends with this chapter of conclusions drawn from the development of the work.

This master's thesis sought, from the very first moment it was proposed, to carry out a rigorous design process. To do so, the author tried to discretize the work in the different parts already mentioned in the introduction, and to apply in each of them the knowledge acquired during his training, adapting it to the nature of each part. Therefore, conclusions will be drawn from each of these parts separately.

In the first part, the analytical capacity has been put into play through the reading and in depth study of the book that has been used as main documentation. This bibliography presents a high engineering level and it can be concluded that it is the fundamental basis on which this project is based. In addition, it is the first point of connection between the theoretical design process and the empirical reality expressed by the authors cited in it.

Secondly, the calculation model was built. This required knowledge of turbomachinery as well as applied experience in computational optimization. The model turned out to be fully functional and adaptable to different operating conditions, as initially intended. It became a great tool for understanding the operating principles of centrifugal compressors, as any variable can be changed and performance results would vary accordingly.

The third part of the project was the 3D modeling process. In this part it was necessary to design using complex geometries that could be adapted to the results obtained in the model. Again, the modeling was done in a parametric and related way, so that the digital designs can be reused for other operating conditions or different vehicle models.

Finally, in the chapter prior to the current one, a small study of the economic feasibility was carried out. And it is now concluded that the estimated costs justify the continuity of this project for the author.

With respect to the second part, it is important to highlight that the calculation model allows a glimpse of the effect that the machine would have on the vehicle if it were operating according to the theoretical results. These can be contrasted with the results obtained by modeling the engine in atmospheric conditions under the same assumed conditions.

The power and torque values as a function of engine revolutions obtained for the engine in atmospheric operation, the overloaded engine in the absence of the turbomachinery load, the engine carrying the load of the compressor (net calculations) are given in the following table:

n [RPM]	Atmospheric		Supercharged without load		Supercharged with load	
	Power [HP]	Torque [Nm]	Power [HP]	Torque [Nm]	Power [HP]	Torque [Nm]
1000	11,120	78,151	23,415	164,566	23,376	164,290
2000	23,801	83,639	48,078	168,952	47,748	167,793
3000	37,501	87,855	76,052	178,171	74,844	175,342
4000	62,266	109,406	110,271	193,753	107,033	188,065
5000	105,496	148,291	156,167	219,517	148,571	208,840
6000	117,407	137,528	228,979	268,220	211,110	247,290

This allows us to conclude that theoretically a remarkable improvement in torque and power would be achieved throughout the whole range of revolutions, as can be seen in the following *Figure 35* and *Figure 36*:

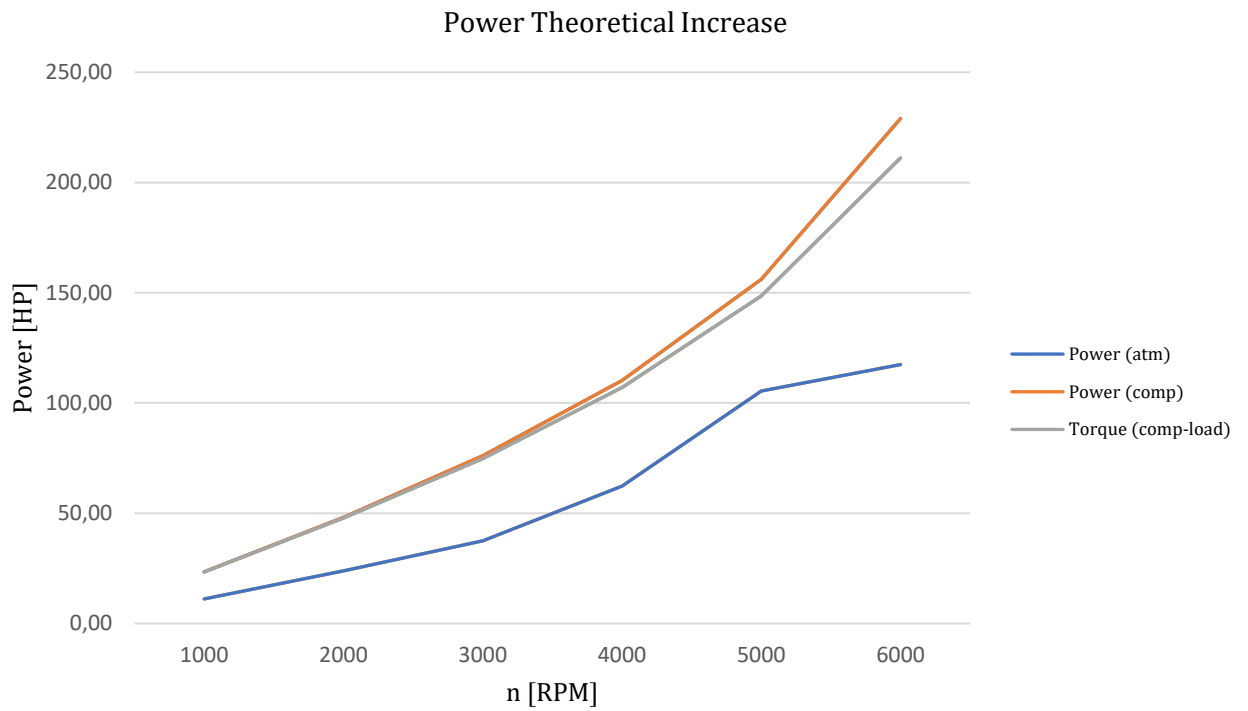


Figure 35: Power Theoretical Increase

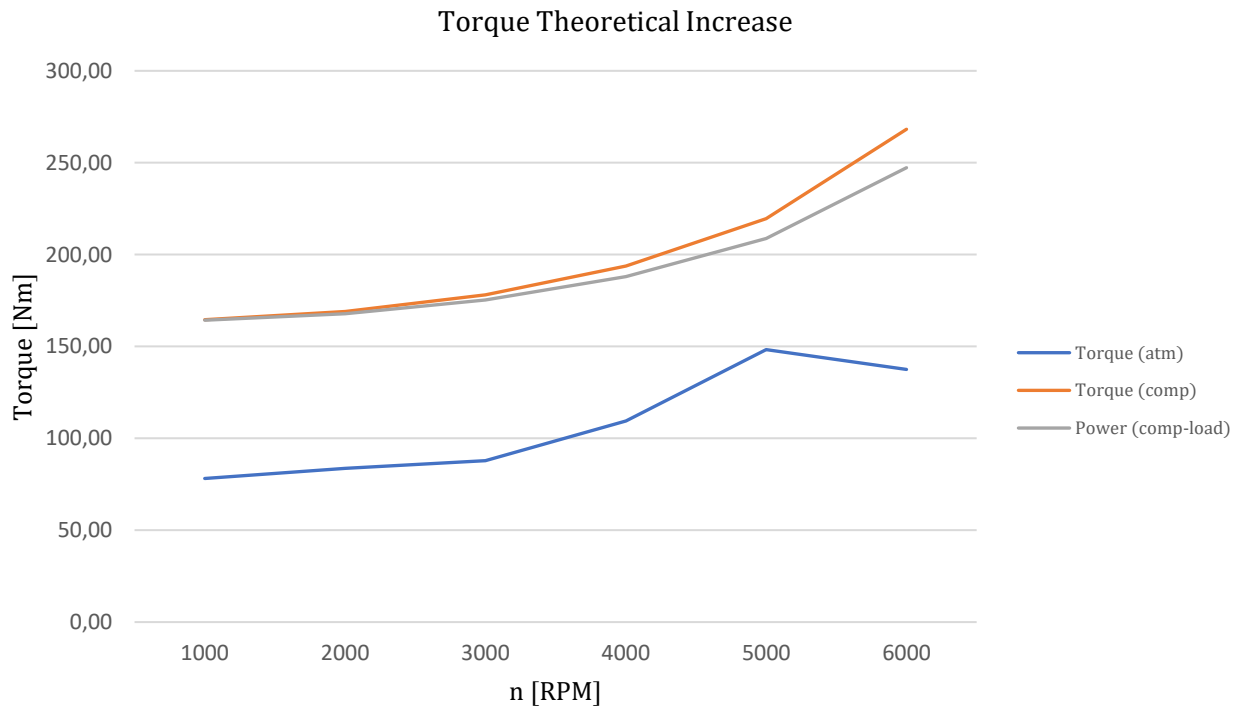


Figure 36: Torque Theoretical Increase

With these, the next steps or projects to be carried out are proposed:

- Optimization and improvement of the calculation model to make it more agile as well as giving more options to the user (i.e. covered vs uncovered impeller configurations).
- Finite element analysis of the different parts to check the structural integrity in operation given specific materials.
- Fluid analysis with specific software to fully understand the distribution of the properties through the different parts of the machine.
- Accurate manufacturing cost analysis through consultation with manufacturers in the market.
- 3D polymer printing fabrication of a non-functional prototype to check the correct assembly of the components and the potential need to modify manufacturing tolerances.
- Manufacture of a functional prototype to be tested under the desired operating conditions and to evaluate the installation in the vehicle.

Finally, a render of the designed machine is presented in *Figure 35* to show the product that is expected to be manufactured and perhaps inspire readers to join and continue with this project or develop their own:



Figure 37: Render of the Expected MVP

Work cited and Tools Needed

The following documentation was used for the development of the project:

[1] “Turbomachinery Fundamentals: selection and preliminary design” - Marco Gambini y Michela Vellini

[2] Technical data sheet of the car:

<https://www.km77.com/coches/mini/mini/2001/estandar/cooper-s/cooper-s/informacion/mini-cooper-s-motor-potente-y-gradable>

[3] Improved vehicle performance:

https://www.revlimit.gr/index.php?option=com_content&view=article&id=169:mini-cooper-s-r53-stage-1,2-2-en&catid=708&lang=en&Itemid=172

[4] Turbo compressor calculator:

<https://strikeengine.com/turbo-size-calculator-find-cfm-pressure-ratio/>

[5] Standard temperatures at compressor outlet:

<https://www.motor.es/que-es/intercooler#:~:text=El%20aire%20sale%20del%20compresor,la%20potencia%20del%20motor%20disminuyen.>

Similarly, to complete the project, the following software was required:

[A] Microsoft – Excel

[B] CoolProp – CoolProp Excel Plugin

[C] Siemens – Solid Edge

Annex I: Alignment with SDGs

Although the main objective of the project was to increase the peak power and torque values of the vehicle for which the turbomachine was designed, it was mentioned in the introduction of this document that other parameters would be taken into account when selecting the optimal solution.

These parameters contemplated, mainly, the improvement of the efficiency with which the engine generated power from the fuel.

As was done in the conclusions section with power and torque, a comparative table is shown below to help understand the improvement in vehicle efficiency with respect to the starting conditions:

n [RPM]	Atmospheric		Supercharged without load		Supercharged with load	
	η_G [%]	SFC [Kg/KWh]	η_G [%]	SFC [Kg/KWh]	η_G [%]	SFC [Kg/KWh]
1000	33,60%	0,233	36,68%	0,213	36,68%	0,214
2000	32,69%	0,239	36,01%	0,217	36,01%	0,219
3000	31,48%	0,249	35,29%	0,222	35,29%	0,225
4000	31,36%	0,250	34,62%	0,226	34,62%	0,233
5000	31,88%	0,245	34,13%	0,229	34,13%	0,241
6000	29,86%	0,262	34,07%	0,230	34,07%	0,249

It can be seen in *Figure 38* below that the efficiency of the vehicle improves slightly by improving its mechanical performance (parameter that was introduced in the section explaining the engine model) throughout the whole engine speed range:

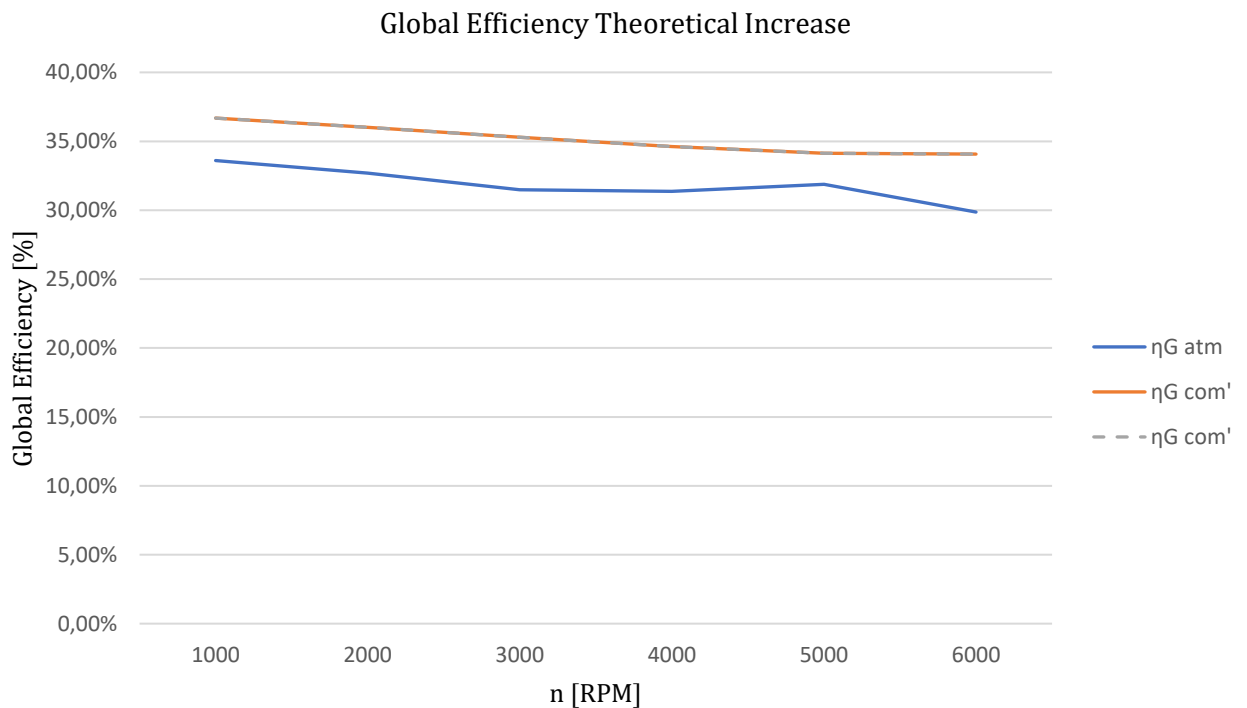


Figure 38: Global Efficiency Theoretical Increase

Similarly, if the fuel quantities are computed as a function of the power generated, a remarkable improvement can be observed, even when the power needed to run the compressor is included in the calculations. *Figure 39* below shows the Specific Fuel Consumption throughout the engine speed range, a parameter widely used in the automotive industry:

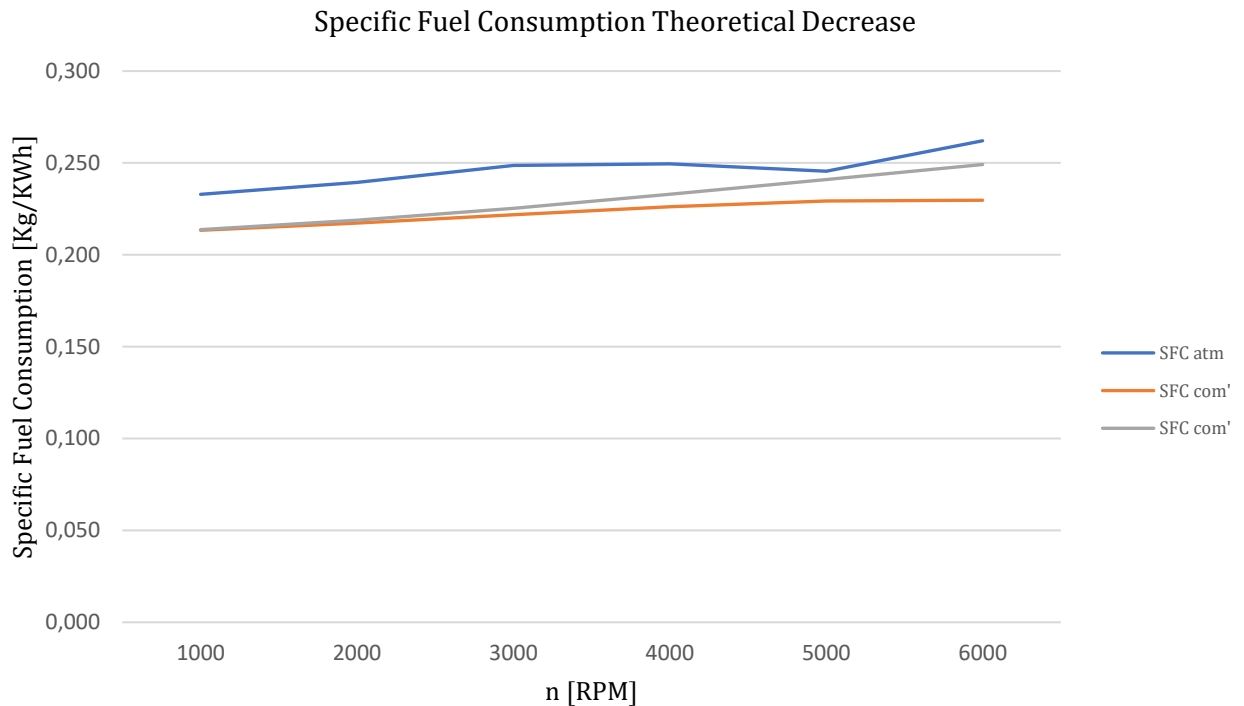


Figure 39: Specific Fuel Consumption Theoretical Decrease

It is because of this improvement in efficiency that the project can be considered to be aligned with the SDGs of the 2030 agenda. The following are the goals that are considered to be covered and the reason why they are so considered:

SDG 7: Affordable and Clean Energy

It is clear that an improvement in motor efficiency has a direct impact on the energy consumed for a similar use. This is why the development of this product is considered to be steering in the direction of a world in which machinery makes a more sustainable use of energy.

SDG 9: Industry, Innovation and Infrastructure

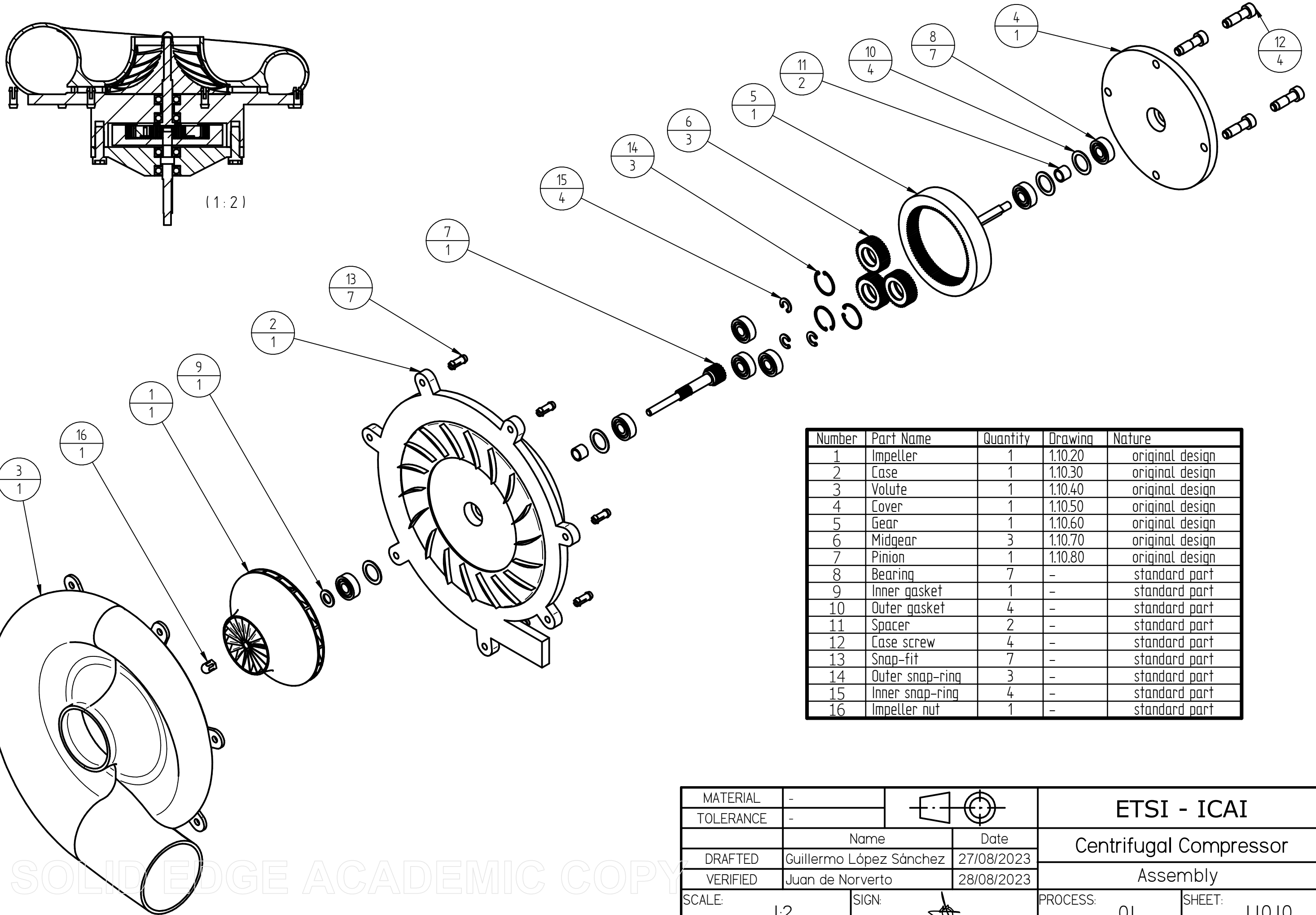
Similarly, this project is considered to be innovative and seeks to develop a product rarely seen in the automotive sector. In a utopian case, the research and development of the compressor of interest could be a disruption in this industry, which is highly relevant in terms of sustainability due to its size.

SDG 12: Responsible Consumption and Production

Finally, it has been repeatedly mentioned that additive manufacturing methods are being pursued for the first MVPs, that will not only allow the development of complex geometries and adjust each part to the needs of operation, but will also allow to make an optimal usage of the manufacturing material, a feature that makes these technologies a great sustainable alternative.

Annex II: Drawings

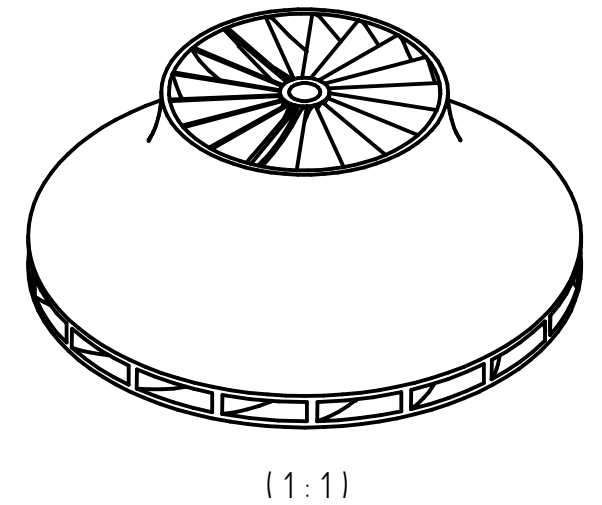
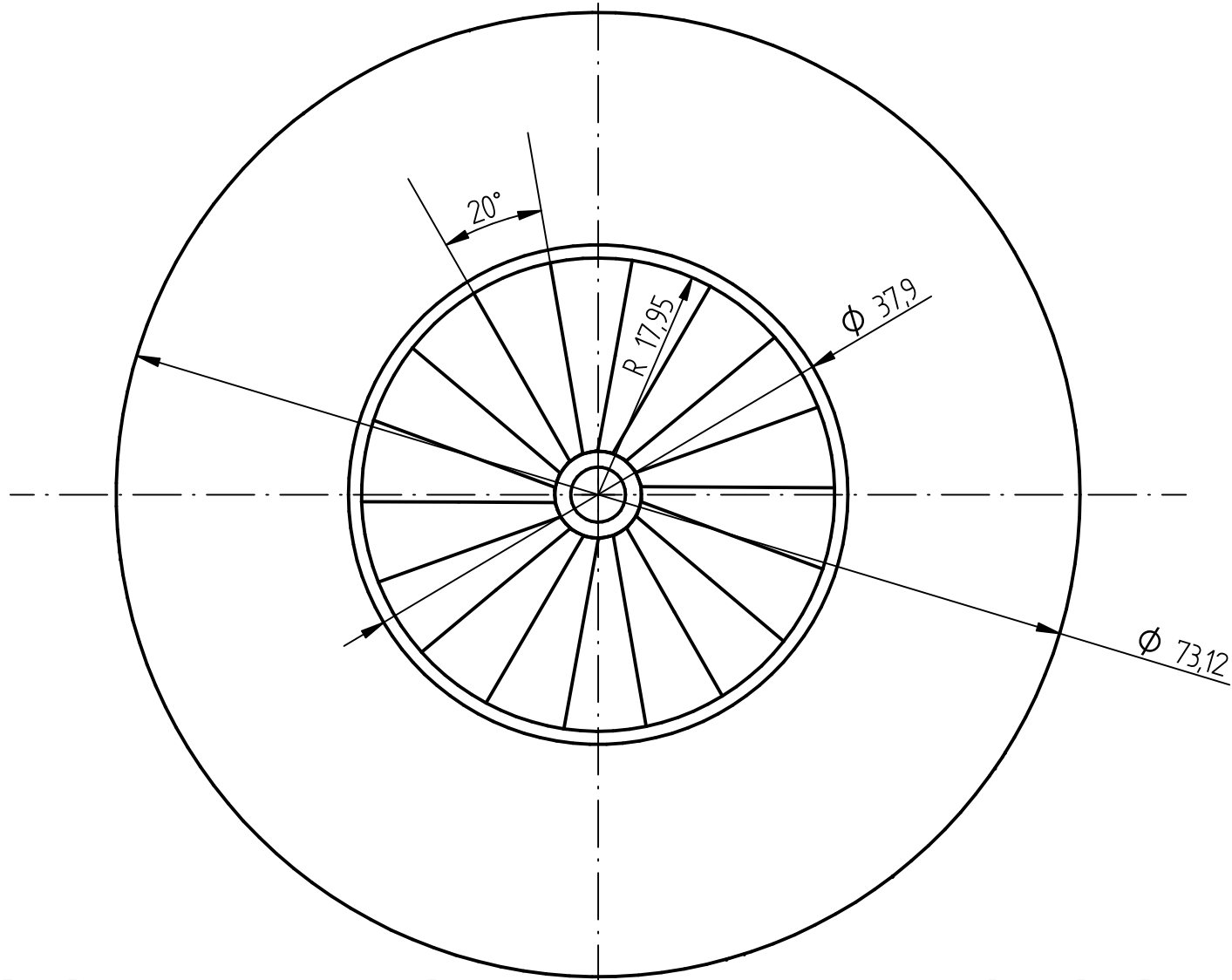
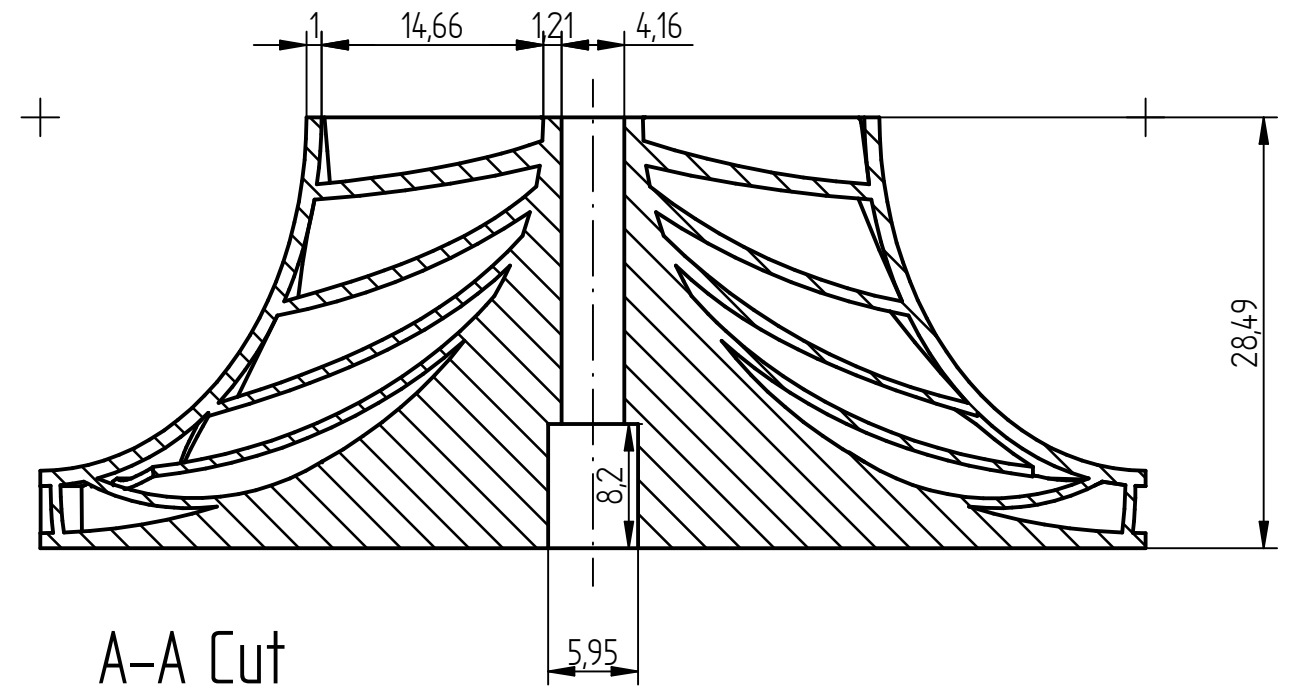
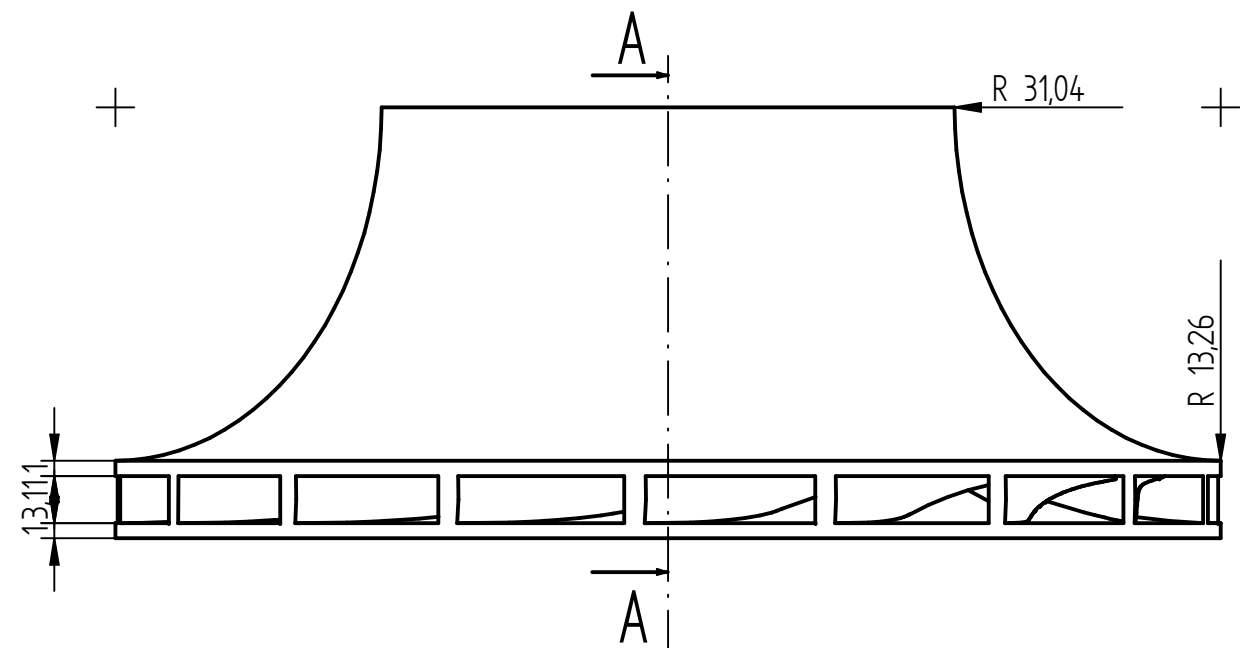
Technical drawings of the designed parts are attached in the following pages.



Number	Part Name	Quantity	Drawing	Nature
1	Impeller	1	1.10.20	original design
2	Case	1	1.10.30	original design
3	Volute	1	1.10.40	original design
4	Cover	1	1.10.50	original design
5	Gear	1	1.10.60	original design
6	Midgear	3	1.10.70	original design
7	Pinion	1	1.10.80	original design
8	Bearing	7	-	standard part
9	Inner gasket	1	-	standard part
10	Outer gasket	4	-	standard part
11	Spacer	2	-	standard part
12	Case screw	4	-	standard part
13	Snap-fit	7	-	standard part
14	Outer snap-ring	3	-	standard part
15	Inner snap-ring	4	-	standard part
16	Impeller nut	1	-	standard part

MATERIAL	-		ETSI - ICAI Centrifugal Compressor Assembly		
TOLERANCE	-				
	Name	Date			
DRAFTED	Guillermo López Sánchez	27/08/2023			
VERIFIED	Juan de Norverto	28/08/2023			
SCALE:	1:2	SIGN:		PROCESS: 01	SHEET: 1.10.10

SOLID EDGE ACADEMIC COPY

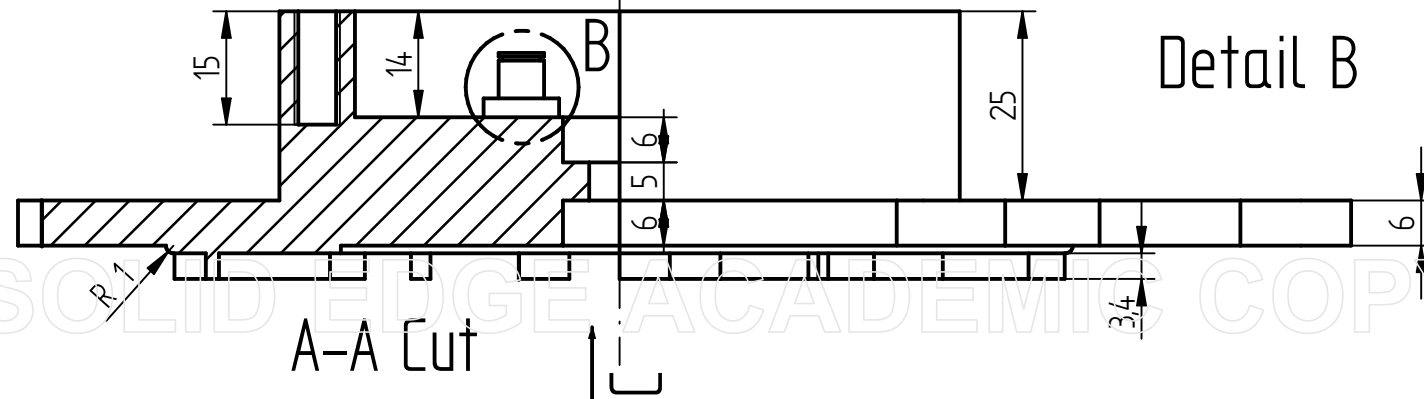
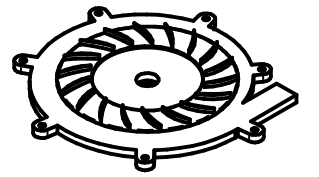
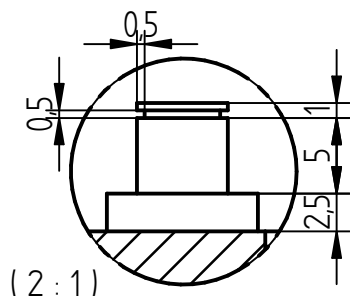
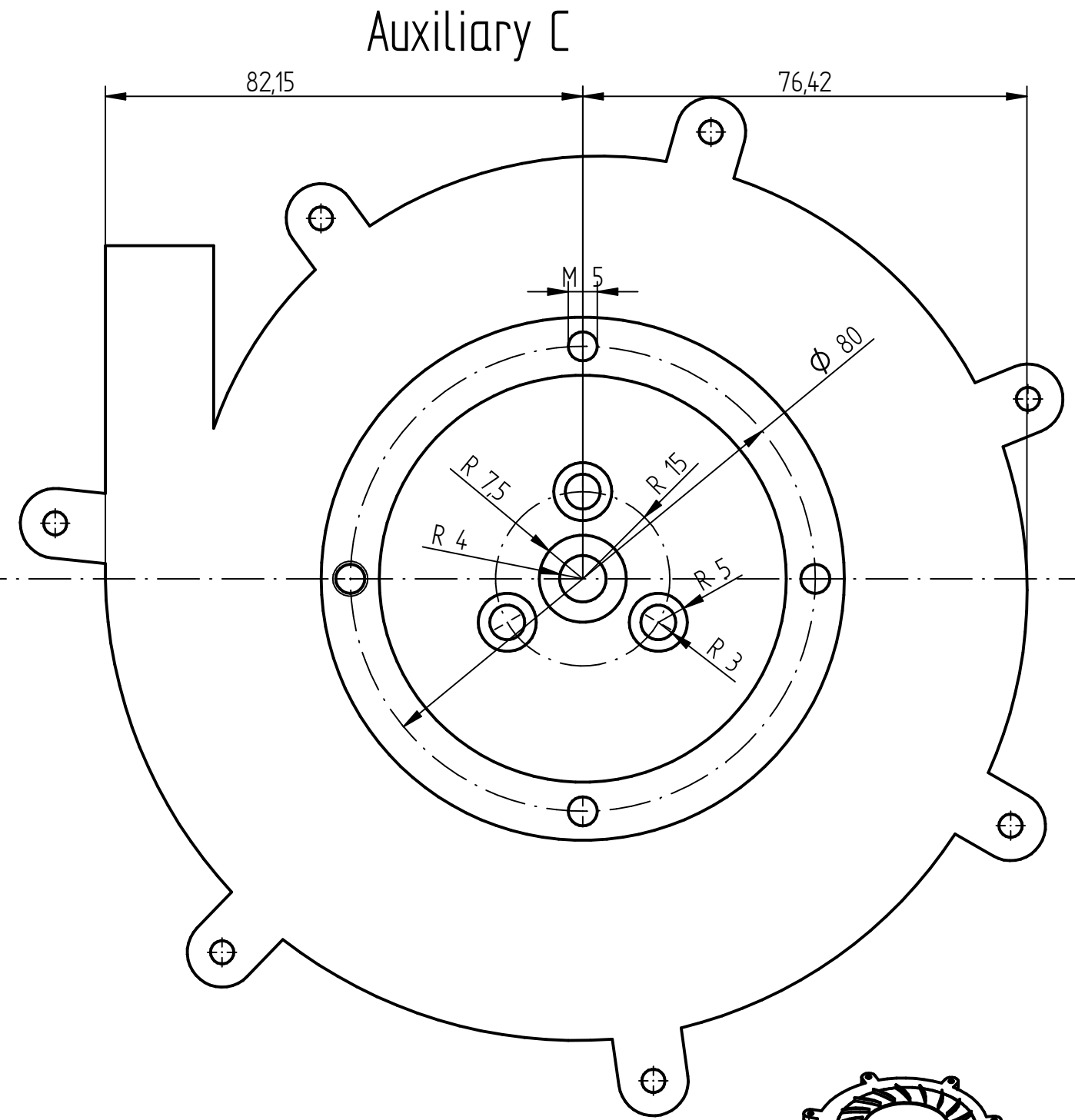
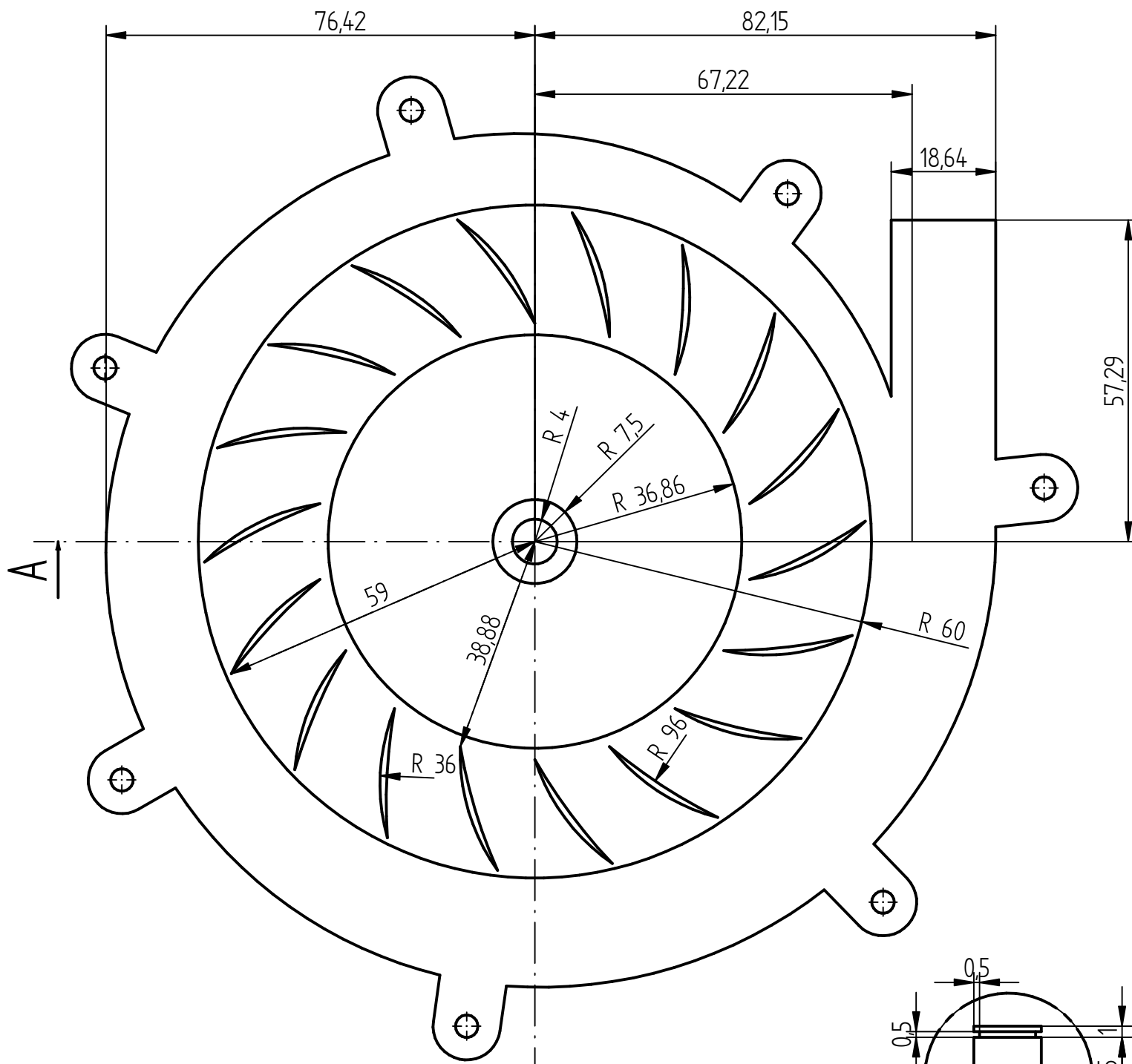


Note: the geometry of the blades is considered complex and will be defined in the digital design file attached to the technical manufacturing document.

5 ✓

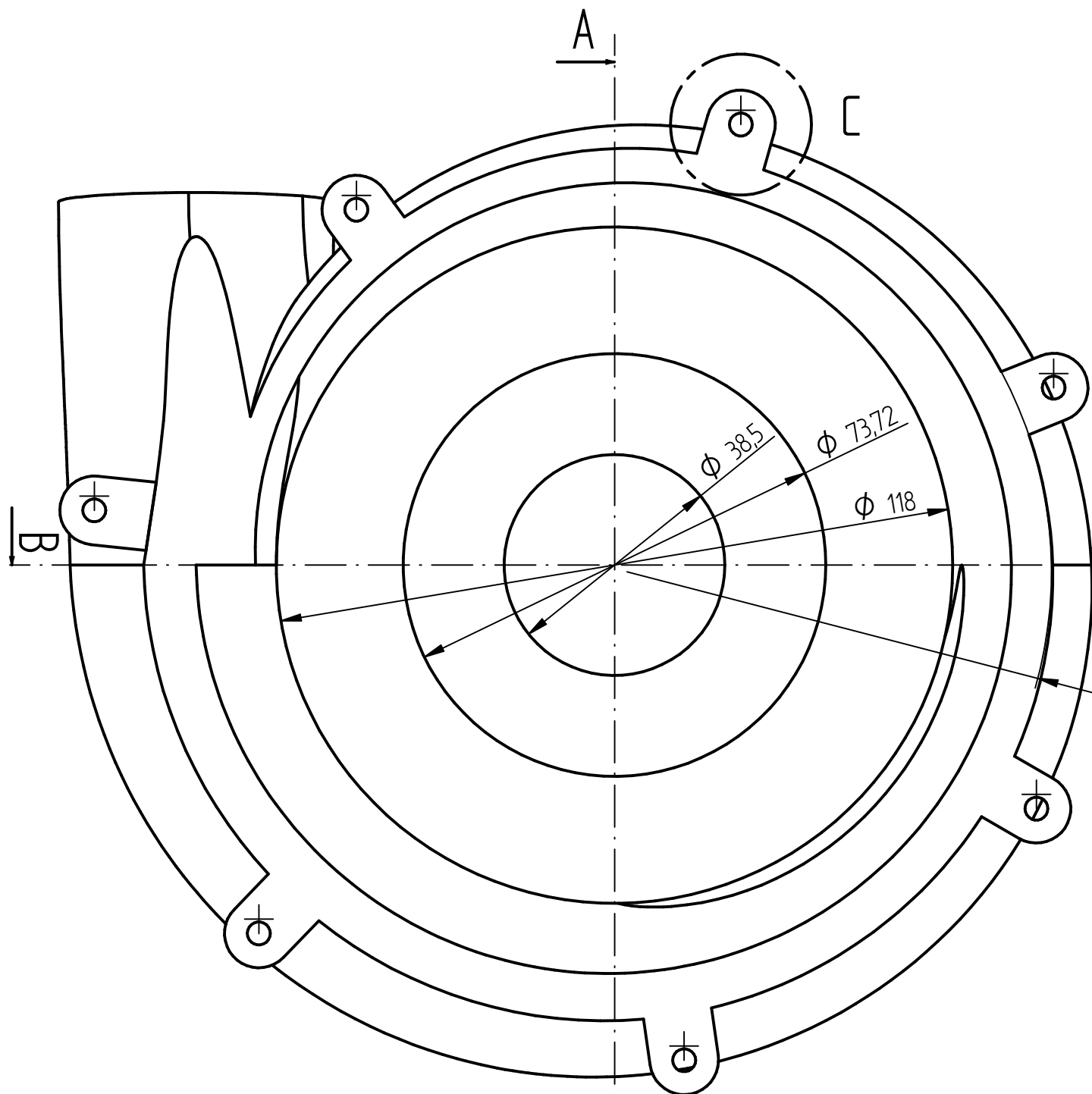
MATERIAL	-		ETSI - ICAI Centrifugal Compressor Impeller	
TOLERANCE	UNE EN 22768 fK			
	Name	Date		
DRAFTED	Guillermo López Sánchez	27/08/2023		
VERIFIED	Juan de Norverto	28/08/2023		
SCALE:	2:1	SIGN:	PROCESS:	SHEET:
			01	1.10.20

SOLID EDGE ACADEMIC COPY

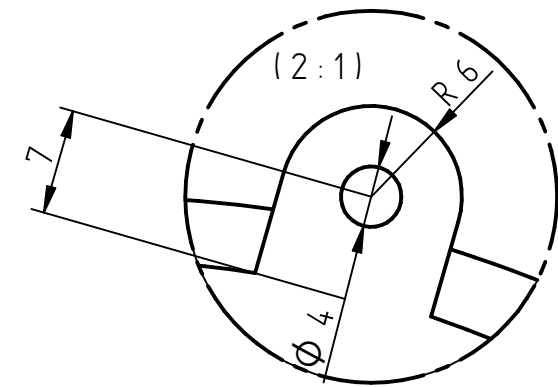
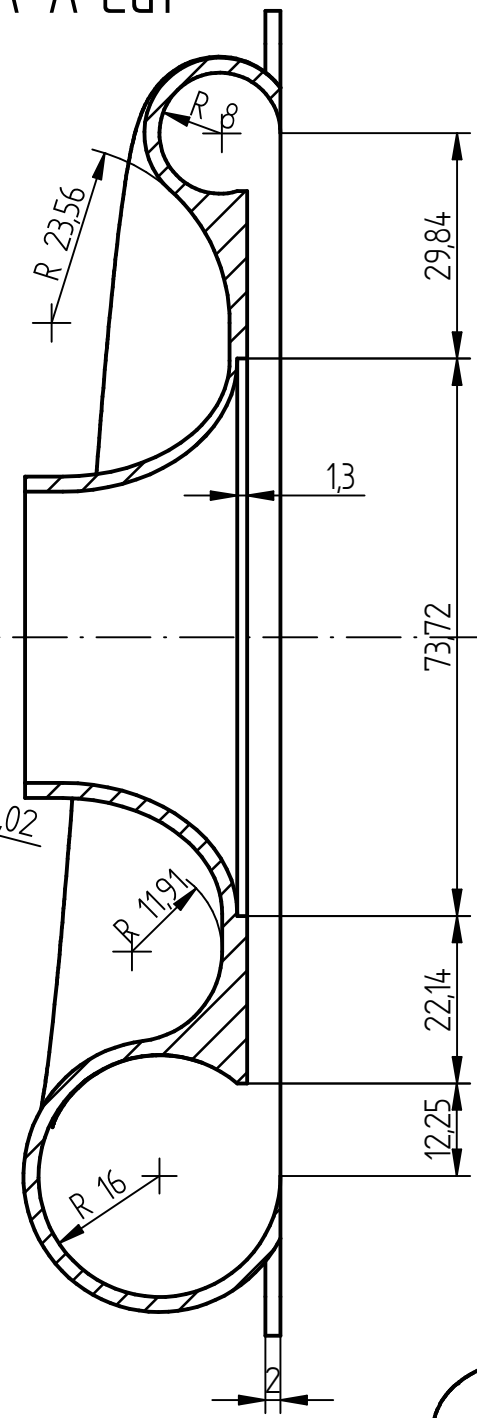


5 ✓

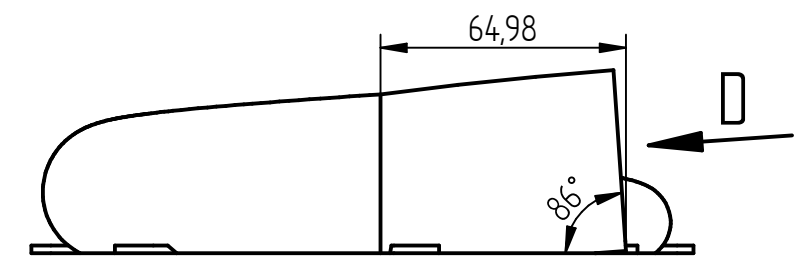
MATERIAL	-		ETSI - ICAI	
TOLERANCE	UNE EN 22768 fK		Centrifugal Compressor	
	Name	Date	Case	
DRAFTED	Guillermo López Sánchez	27/08/2023		
VERIFIED	Juan de Norverto	28/08/2023		
SCALE:	1:1	SIGN:	PROCESS:	SHEET:
			01	1.10.30



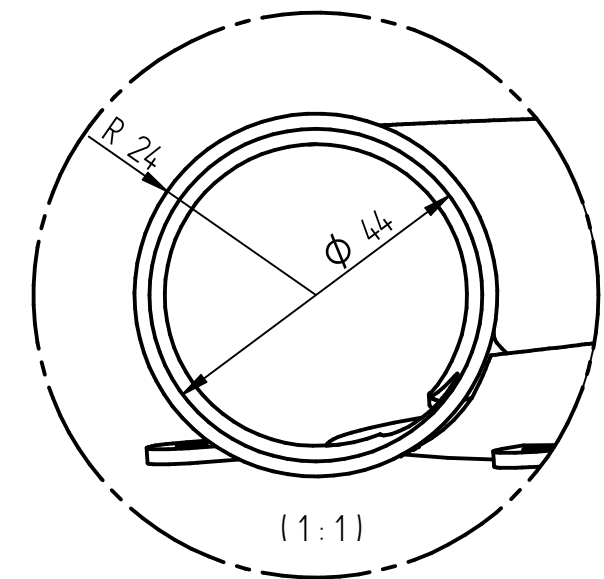
A-A Cut



Detail C

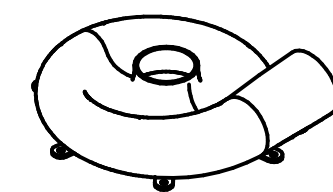
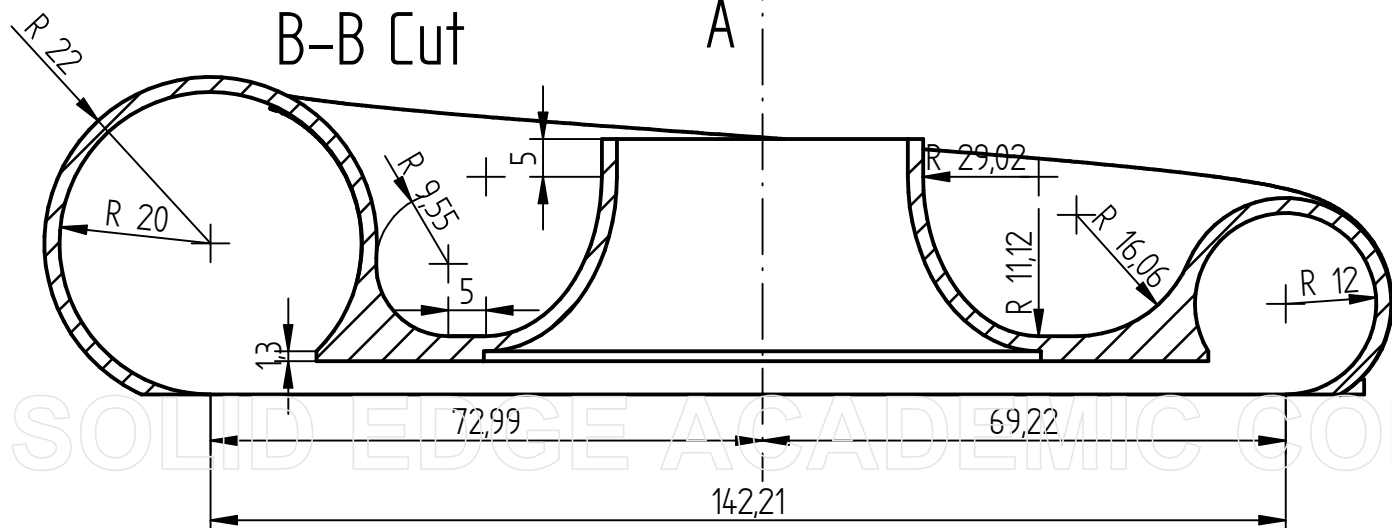


(1:2)



Auxiliary Detail D

B-B Cut

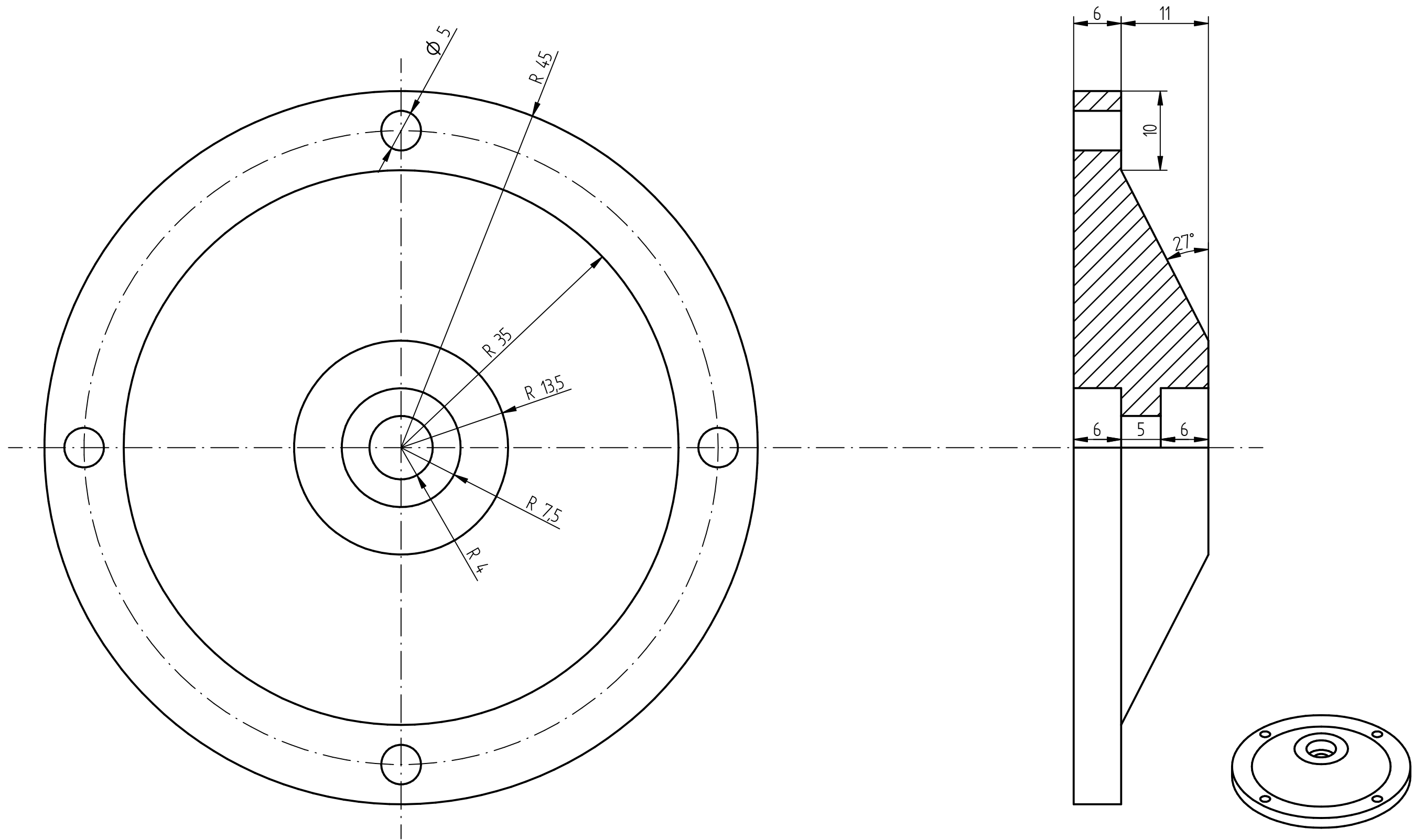


(1:5)

5 ✓

MATERIAL	-		ETSI - ICAI	
TOLERANCE	UNE EN 22768 fK			
	Name	Date	Centrifugal Compressor Volute	
DRAFTED	Guillermo López Sánchez	27/08/2023		
VERIFIED	Juan de Norverto	28/08/2023		
SCALE:	1:1	SIGN:	PROCESS:	01
			SHEET:	1.10.40

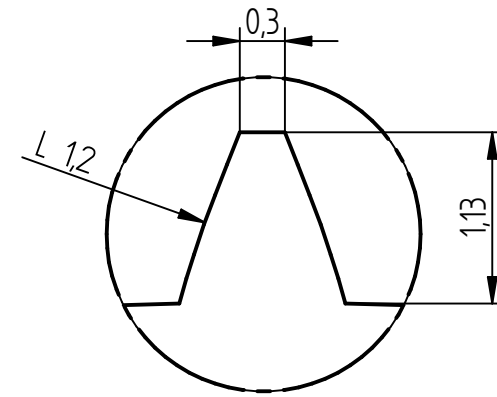
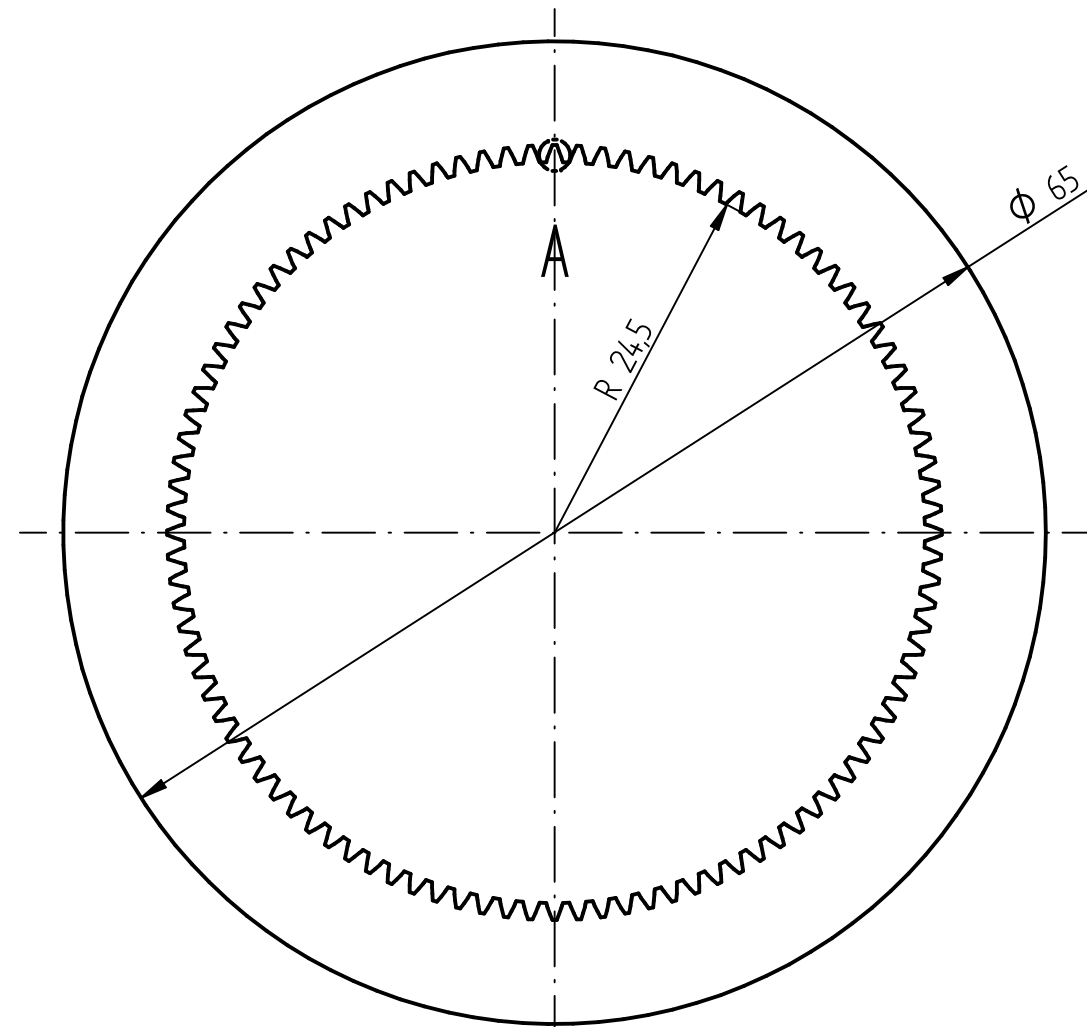
SOLID EDGE ACADEMIC COPY



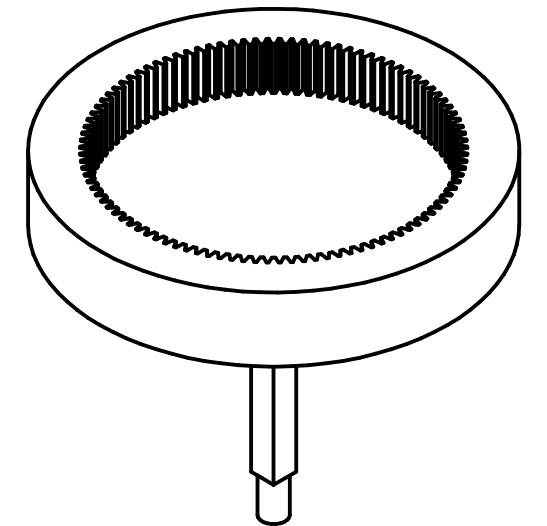
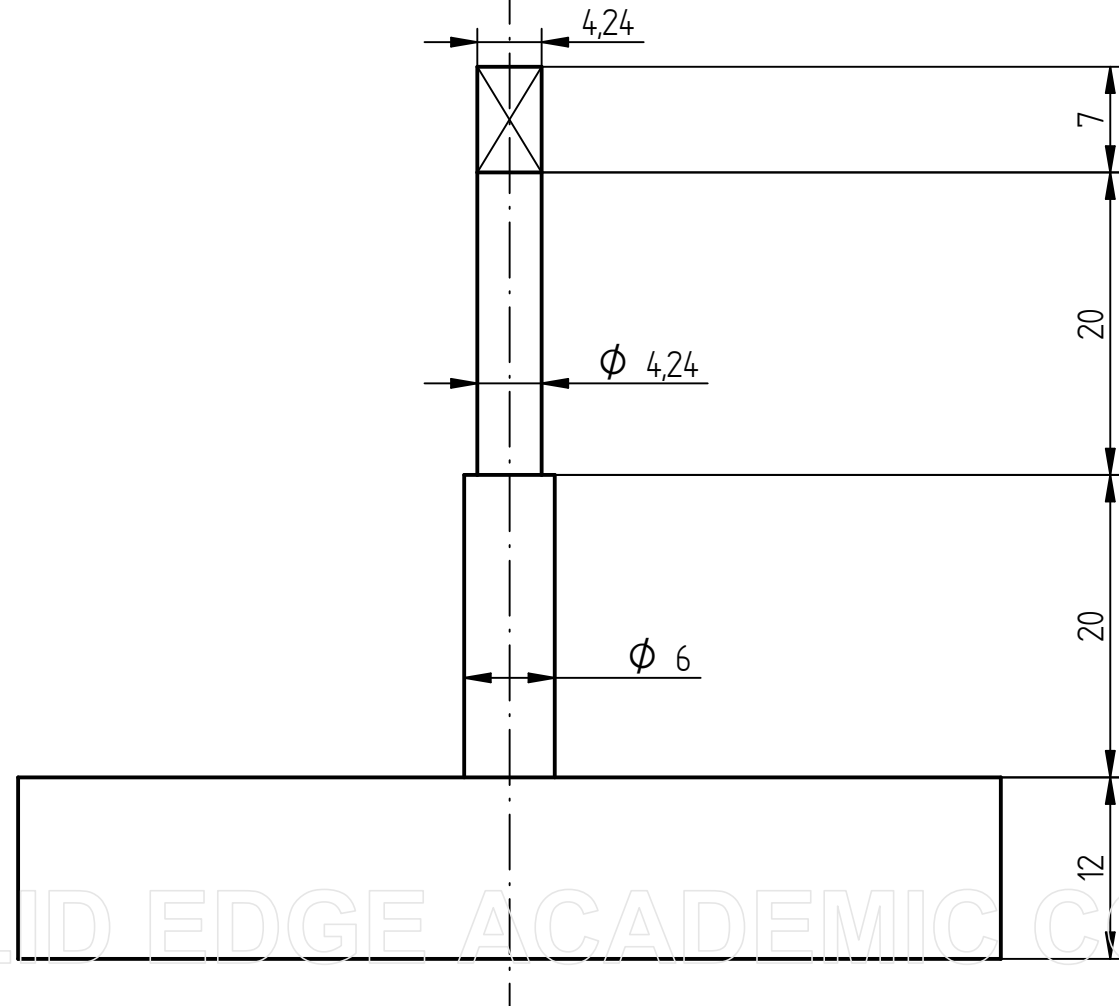
5 ✓

MATERIAL	-		ETSI - ICAI Centrifugal Compressor Cover	
TOLERANCE	UNE EN 22768 fK			
	Name	Date		
DRAFTED	Guillermo López Sánchez	27/08/2023		
VERIFIED	Juan de Norverto	28/08/2023		
SCALE:	1:1	SIGN:	PROCESS:	SHEET:
			01	1.10.50

SOLID EDGE ACADEMIC COPY



DETALLE A

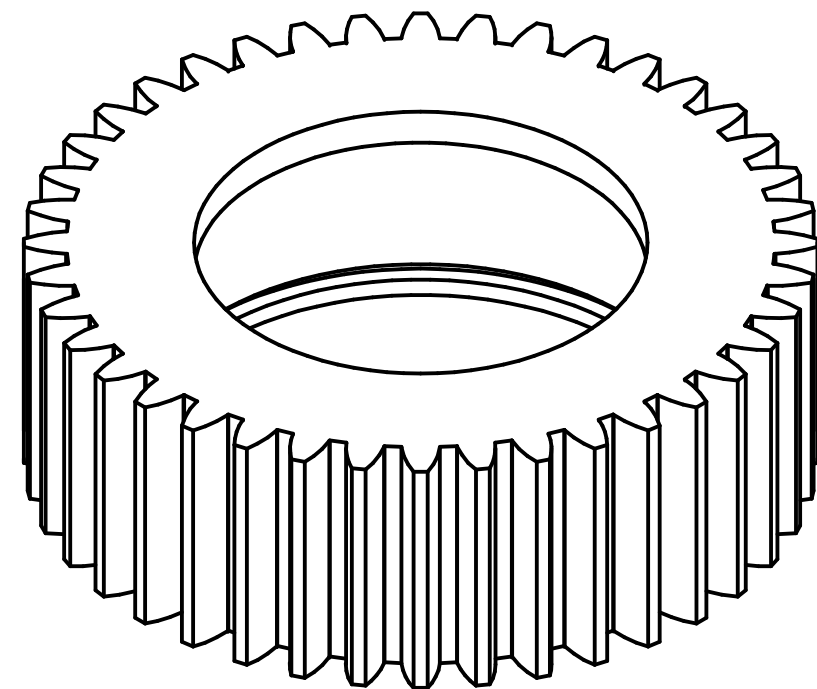
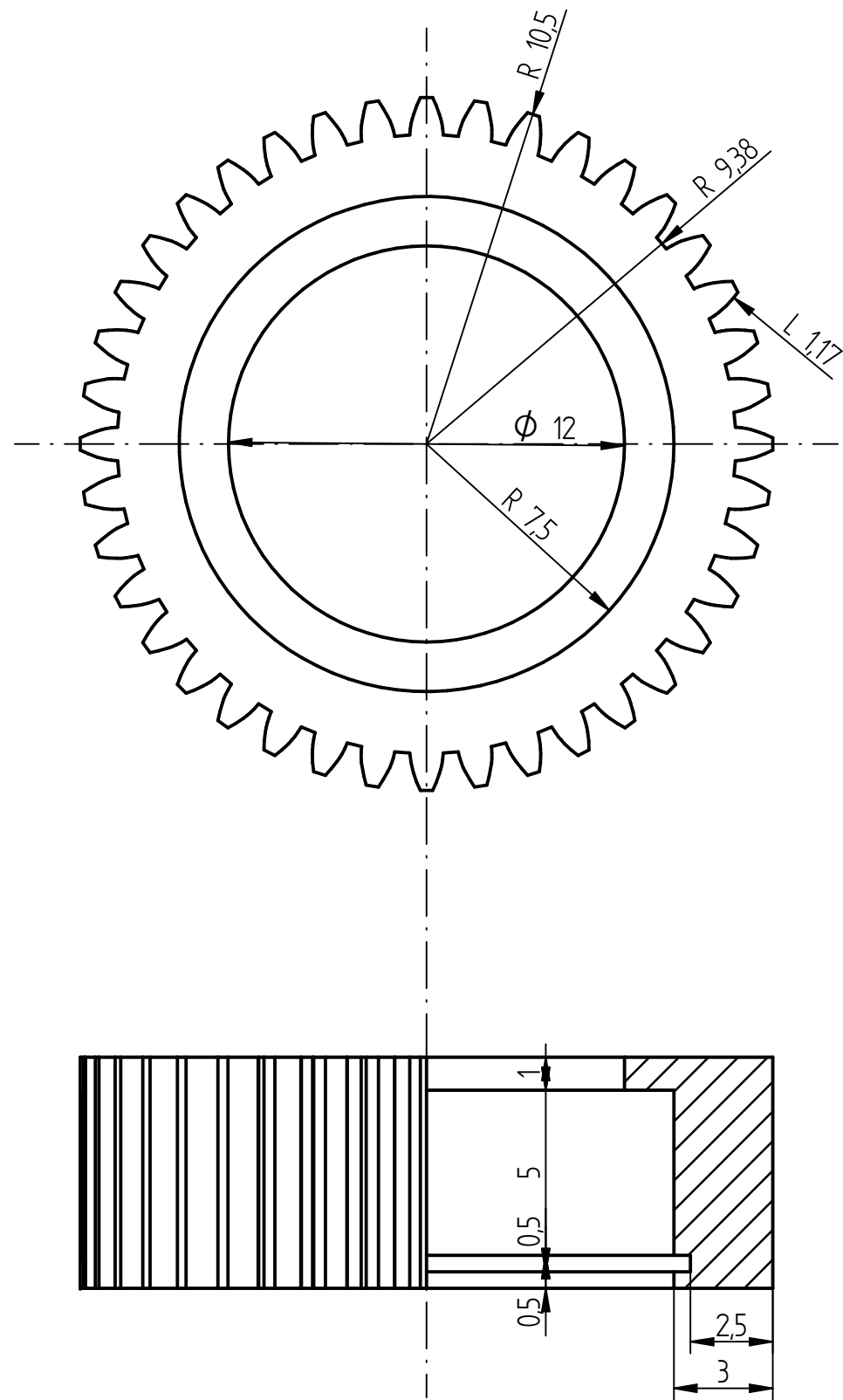


(1:1)

5 ✓

MATERIAL	-		ETSI - ICAI	
TOLERANCE	UNE EN 22768 fK		Centrifugal Compressor	
	Name	Date	Gear	
DRAFTED	Guillermo López Sánchez	27/08/2023		
VERIFIED	Juan de Norverto	28/08/2023		
SCALE:	2:1	SIGN:	PROCESS: 01	SHEET: I.10.60

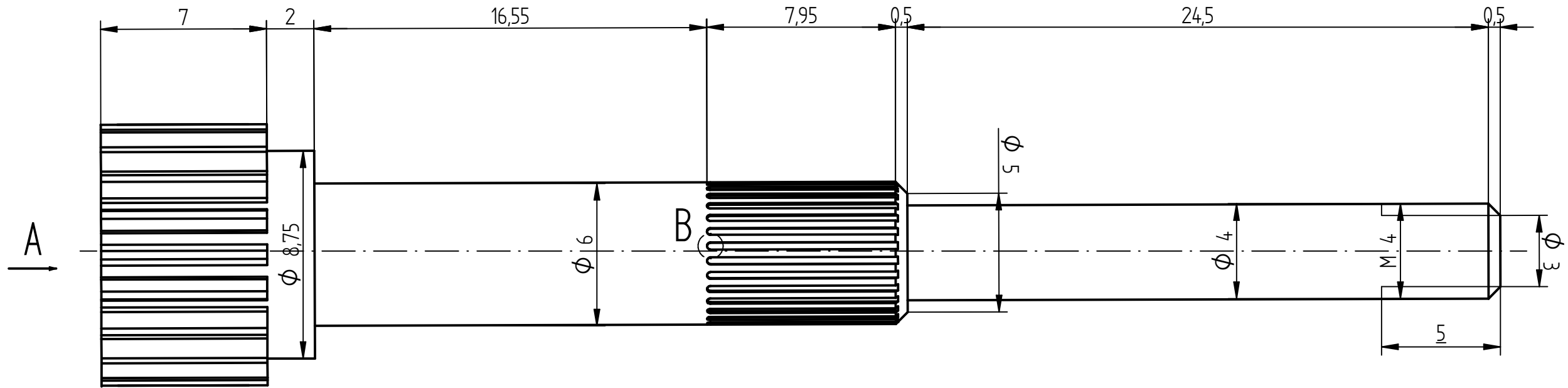
SOLID EDGE ACADEMIC COPY



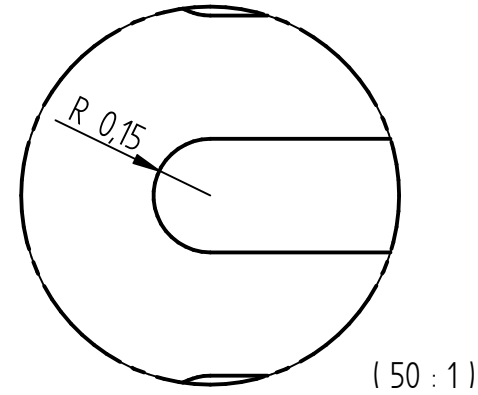
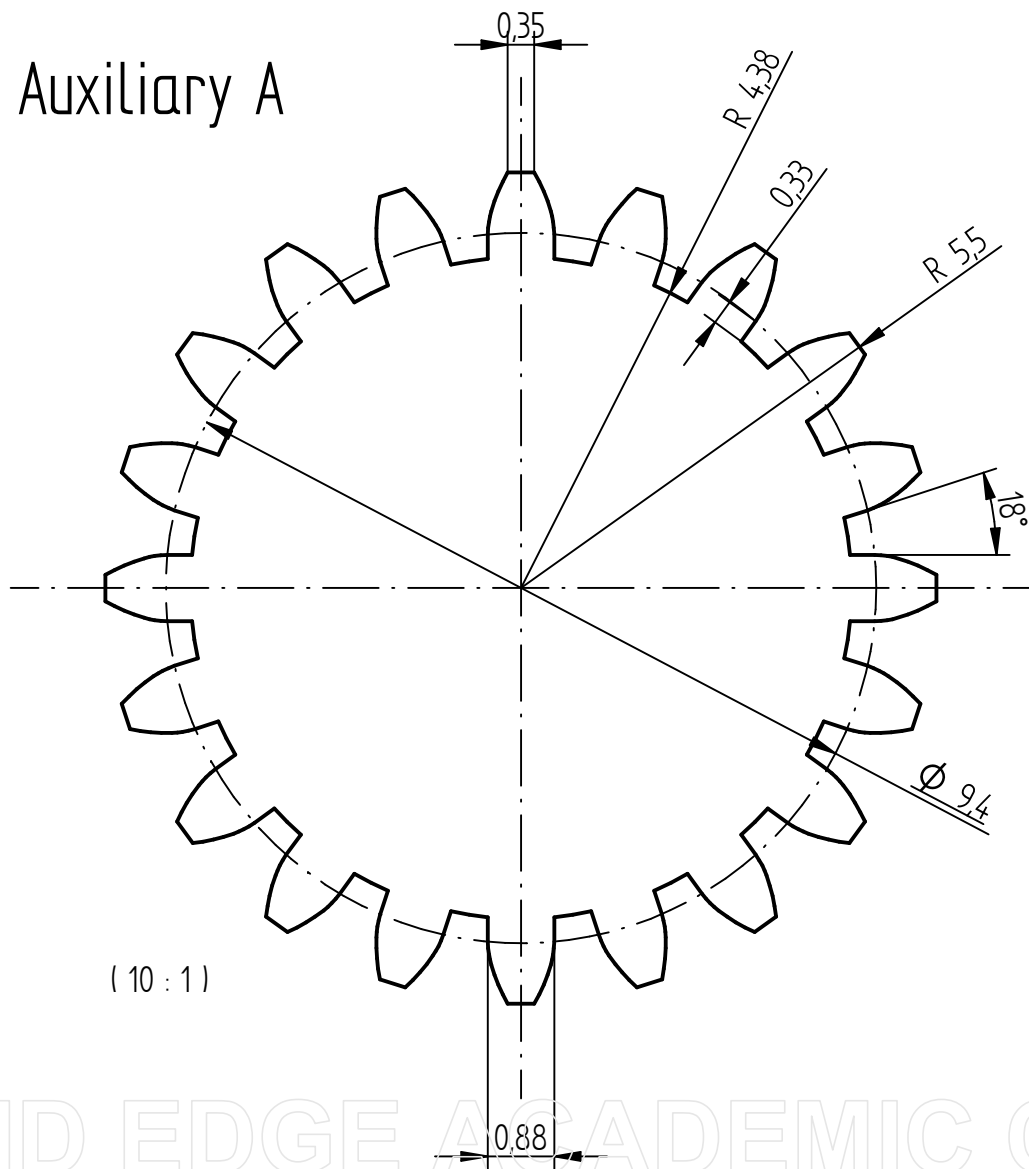
5 ✓

MATERIAL	-		ETSI - ICAI			
TOLERANCE	UNE EN 22768 fK					
	Name	Date	Centrifugal Compressor Midgear			
DRAFTED	Guillermo López Sánchez	27/08/2023				
VERIFIED	Juan de Norverto	28/08/2023				
SCALE:	5:1	SIGN:	PROCESS:	01	SHEET:	I.10.70

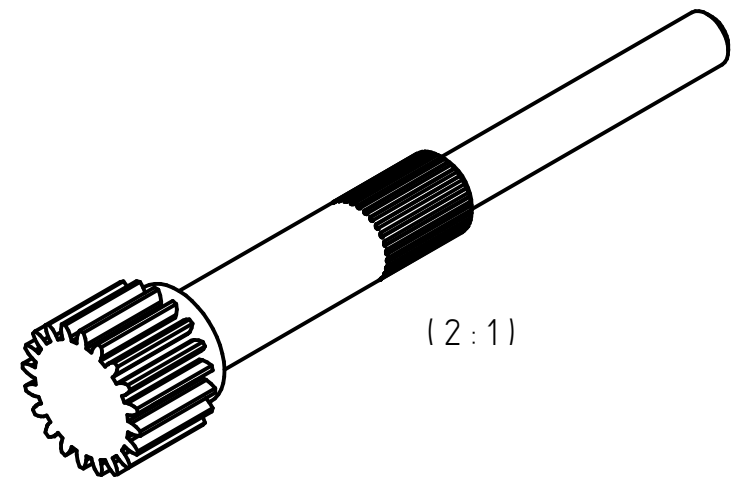
SOLID EDGE ACADEMIC COPY



Auxiliary A



Detail B



MATERIAL	-		ETSI - ICAI Centrifugal Compressor Pinion	
TOLERANCE	UNE EN 22768 fK			
	Name	Date		
DRAFTED	Guillermo López Sánchez	27/08/2023		
VERIFIED	Juan de Norverto	28/08/2023		
SCALE:	5:1	SIGN:	PROCESS:	SHEET:
			01	I.10.80

SOLID EDGE ACADEMIC COPY